

N71-16595
C.2

NASA CONTRACTOR REPORT

NASA CR-61340

DEVELOPMENT, FABRICATION, TESTING, AND DELIVERY OF ADVANCED FILAMENTARY COMPOSITE NONDESTRUCTIVE TEST STANDARDS

By W. M. Pless, B. L. Weil, and W. H. Lewis
Lockheed - Georgia Company
Marietta, Georgia

November 1970

Final Report

*should be
CR-61340*

N71-16595 (NASA-CR-103011) DEVELOPMENT, FABRICATION, TESTING, AND DELIVERY OF ADVANCED FILAMENTARY COMPOSITE NONDESTRUCTIVE TEST STANDARDS. Final report: W.M. Pless, et al (Lockheed-Georgia . . . pp. 110 G3/18 CSCL 11D

Unclas

1 OF 2
N71 16595

Pr
N
M

N71-16595

NASA CONTRACTOR
REPORT

NASA CR-61340

**CASE FILE
COPY**

DEVELOPMENT, FABRICATION, TESTING, AND
DELIVERY OF ADVANCED FILAMENTARY
COMPOSITE NONDESTRUCTIVE
TEST STANDARDS

By W. M. Pless, B. L. Weil, and W. H. Lewis
Lockheed - Georgia Company
Marietta, Georgia

November 1970

Final Report

Prepared for

NASA-GEORGE C. MARSHALL SPACE FLIGHT CENTER
Marshall Space Flight Center, Alabama 35812

1. REPORT NO. CR-61340		2. GOVERNMENT ACCESSION NO.		3. RECIPIENT'S CATALOG NO.	
4. TITLE AND SUBTITLE DEVELOPMENT, FABRICATION, TESTING, AND DELIVERY OF ADVANCED FILAMENTARY COMPOSITE NONDESTRUCTIVE TEST STANDARDS (Final Report)				5. REPORT DATE November 1970	
				6. PERFORMING ORGANIZATION CODE	
7. AUTHOR(S) W. M. Pless, B. L. Weil, and W. H. Lewis				8. PERFORMING ORGANIZATION REPORT # ER-10883	
9. PERFORMING ORGANIZATION NAME AND ADDRESS Lockheed-Georgia Company Marietta, Georgia				10. WORK UNIT NO.	
				11. CONTRACT OR GRANT NO. NAS 8-25679	
12. SPONSORING AGENCY NAME AND ADDRESS National Aeronautics and Space Administration Washington, D. C. 20546				13. TYPE OF REPORT & PERIOD COVERED Contractor Report	
				14. SPONSORING AGENCY CODE	
15. SUPPLEMENTARY NOTES Work performed for Quality and Reliability Assurance Laboratory George C. Marshall Space Flight Center					
16. ABSTRACT Detailed designs of the test standards, including configuration, placement of defects/ variations, and fabrication methods are presented together with the NDT development and results. Destructive tests were conducted on additional test panels, where necessary to verify the defective condition of the standards. A single nondestructive test method did not reveal all possible defects in a composite structure. Two or more methods were used in a complementary fashion to characterize these materials adequately. Generally, radiography and ultrasonic C-scan techniques reveal most defects that may be present in a single structure.					
17. KEY WORDS			18. DISTRIBUTION STATEMENT Unclassified - unlimited <i>James C. Bates</i>		
19. SECURITY CLASSIF. (of this report) Unclassified		20. SECURITY CLASSIF. (of this page) Unclassified		21. NO. OF PAGES 109	22. PRICE \$3.00

FOREWORD

Under Contract NAS8-25679, the Lockheed-Georgia Company designed, fabricated, and tested advanced composite standards which represent, as naturally as possible, the potential variations which can occur when these materials are processed into a finished structure. This final report presents the detailed designs, complete fabrication procedures, and nondestructive evaluations of the test standards as specified under Phases I and II of the program. For internal control purposes, this report has been designated as Lockheed-Georgia Report ER-10883.

This program was conducted in the Materials Development Laboratory of Lockheed-Georgia which is under the surveillance of Mr. J. F. Cotton, Manager of the Laboratory; Dr. E. E. Underwood, Associate Director of Research, Materials Sciences; and Dr. J. F. Sutton, Director of Research. Mr. W. H. Lewis was the Program Manager and Messrs. B. L. Weil, W. M. Pless, and G. W. Burton were principal investigators.

The authors wish to acknowledge the important contributions made to this program by Messrs. G. W. Burton, S. C. Porter, and R. W. Nagy of the Lockheed-Georgia Materials Development Laboratory, who fabricated and cured the composite standards; the Lockheed-Georgia Quality Assurance Branch, who was responsible for all X-radiographic services; and D. S. Harmer of the Georgia Institute of Technology, who contributed his services in performing neutron radiography of several of the standards.

TABLE OF CONTENTS

<u>Section</u>	<u>Title</u>	<u>Page</u>
I	INTRODUCTION	1
II	DESIGN AND FABRICATION	3
	Design of Standards	3
	Fabrication of Standards	3
III	NONDESTRUCTIVE EVALUATION	9
	Ultrasonic Evaluation	9
	Ultrasonic Results	12
	Radiographic Evaluation	15
	X-Radiographic Results	16
	Neutron Radiography	18
	Neutron Radiography Results	19
	Infrared Evaluation	20
	Summary of Nondestructive Evaluation	20
	FIGURES	23
	BIBLIOGRAPHY OF SELECTED WORKS	95
	APPENDIX	A-1

I - INTRODUCTION

The appearance of high-strength, high-modulus, low-density filaments during the late 1950's ushered in an exciting new development of advanced composite materials. These materials have undergone rapid transition from the laboratory to their present applications in advanced aerospace structures. Fiber-reinforced materials (boron and graphite in plastic matrices) promise dramatic improvement in strength, stiffness, and weight. However, current applications are not using the full potential of these materials because satisfactory levels of engineering reliability and confidence have not been established. Usage will continue to be severely restricted until material properties can be determined during fabrication and verified throughout the service life. The answer to this problem lies in the development and extensive use of improved non-destructive evaluation procedures and test equipment, which will require preparation of test standards so that the material characteristics and discontinuities can be determined as a function of equipment response.

Advanced composite materials, by their nature, can incorporate many variations not found in homogeneous metallic materials. Such variables as the number and orientation of plies, duration of cure, heating rates, and accidental inclusion of foreign matter during layup can undermine the integrity of a finished structure. The test standards developed during this program present, as naturally as possible, the inconsistencies which can occur when fiber composites are fabricated under typical production conditions.

II - DESIGN AND FABRICATION

Design of Standards

Test standards serve as valuable inspection tools as long as they closely represent the possible configurations of the finished article. The test article is judged defective or defect-free by means of comparative evaluation with the appropriate test standards. Evaluating service-life potential calls for consideration far beyond the detection of cracks and voids. The test standards are designed to contain typical errors of process and fabrication peculiar to the chosen materials and processes so that the internal conditions of the standards represent the most probable conditions to be found in production hardware. The type of defect present, and its size, orientation, and location with reference to the available inspection surface are designed to represent the fabrication variable; they are not optimized with respect to the capability of state-of-the-art NDT equipment. This means that design emphasis was placed on creating known defects in the panels which were not necessarily detectable through current NDT techniques. Therefore, destructive tests were conducted on four additional test panels where it was considered necessary to verify the defective condition of the standards.

Detailed designs of the test standards, including configuration, placement of defects/variations, and fabrication methods are presented in Figures A-1 through A-7.

Fabrication of Standards

The fabrication of NDT standards was accomplished using typical production equipment which is part of the facilities of the Lockheed-Georgia Materials Development Laboratory. The test standard panels were 11-1/4 inches square, with stepped thicknesses spaced 2-1/4 inches apart. Step thickness increments are 0.010 inch from 0.020 to 0.060 inch. The definition of the steps was assured by using a machined caul plate placed face-to-face with the laminate during cure.

The boron/epoxy material was purchased in tape form, approximately 3 inches wide. The graphite/epoxy material was purchased in 12- by 38-inch sheet form with a specified configuration of 4 tows per inch to yield an approximate cured thickness of 5 mils per ply. Figure A-1 shows an exploded view of a typical laminate.

The flat panels were molded in a clamshell autoclave at 85 psig for 60 minutes at 350(±10°)F. Closed silicone-rubber dams and controlled bleeding techniques were used to control size and thickness. The honeycomb sandwich panels consist of heat-resistant phenolic (HRP) core, 3.0#/ft³ density, and thicknesses of 1/2" (3/16" cell) and 1" (1/4" cell). The face-sheet panels for both sides of the standards containing honeycomb core were individually laminated and bonded to the core in a secondary bonding operation to avoid altering the condition of the laminate established during cure. This technique duplicates the methods presently used to manufacture composite structures from fiber materials. The honeycomb panels were edged sealed with polysulfide and epoxy compounds so that water would not enter the core during subsequent test and evaluation.

Controlled-temperature molding was used to provide flat laminates of the above-specified materials with titanium sheet metal 0.014 inch thick. Laminates were bonded to the metal in a secondary bonding operation, using HySol 9614 cured at 150°F for 2 hours.

The internal defects were placed into the laminates between the first and fourth ply (see Figure A-1) at the time of layup of each configuration. All other defects were incorporated during the cure process or prior to the secondary bonding operation. The following defects were created in the panels:

	<u>Number of Panels</u>	
	<u>Boron</u>	<u>Graphite</u>
Density/porosity, resin variation	3	3
Cure variation, inclusions	3	3
Bias variation	3	3
Fiber spacing, overlap, broken fibers	3	3
Delaminations, voids, crushed area in honeycomb core	3	3

Because of the fabrication processes, the limited size of the panels, and the number of defects incorporated, all panels do not have defect-free areas. Honeycomb panels were fabricated with a defect-free laminate on the far side of the core.

Density/Porosity and Resin Variations

An unsuccessful attempt was made to produce typical density/porosity variations (as shown in Figure A-2) by strip-heating blankets to raise the temperature of the ends of the panel quickly to a point beyond cure temperature. This process applied in the past with similar resins (American Cyanamid BP 919) produced foaming in the resin and created a porous, low-density area. Doubts about the success of this process dictated that phenolic microballoons be inserted during layup to ensure porosity. Figure 1 shows the microballoons between the second and third layer with no porosity and normal density throughout the remainder of the laminate. Resin-rich and resin-poor areas depicted in Figure A-2 were achieved through a controlled bleeding technique using Mylar and Armalon separately on halves of the laminate. Analysis performed on a boron-epoxy destructive test panel (No. 104) and a graphite-epoxy test coupon showed the following:

TABLE I
PERCENT RESIN CONTENT
Narmco Epoxy Resin

	<u>5505 (Boron)</u>	<u>5205 (Graphite)</u>
As-Received Raw Material	33.8	40.2
Nominal Laminate	23.5	30.4
Resin Rich	25.2	33.1
Resin Poor	21.3	27.2

NOTE: The resin content can vary $\pm 3\%$ on the prepreg tape. A similar variation can be expected in the laminate, assuming a dense laminate with low void content.

Cure Variations and Inclusions

Cure variations that significantly affect the strength of the high-modulus materials are states of undercure. Overcure or post-curing would do little to change the strength characteristics. Undercure is most commonly produced through uneven heating in the autoclave.

The process data for Narmco epoxy resins 5505 and 5205 call for a cure of 1 hour at 350°F. Experience with these resins had been directed toward the processing of samples for design allowable data. Consequently, there was no experience with undercuring these resins. The undercured panels in this program were processed at 310°F for 30 minutes, which was expected to produce a definitely undercured state. However, the Barcol hardness tests show an average of 70 for undercured areas and 75 for cured areas, indicating that considerable curing of the panels had taken place. Extensive mechanical tests were not planned for cure variation. Consequently, there was not sufficient material remaining to make samples for testing interlaminar shear strength and transverse flexural strength to determine the degree of degradation of properties by the change in process conditions. However, in fabrication of similar laminate systems, it is unlikely that a cure below 310°F for 30 minutes would ever be scheduled. Any process quality control procedure would certainly spot the departure from specification and indicate appropriate action. Therefore, no further work to evaluate undercure was undertaken.

Cure variations (as shown in Figure A-3) were produced by arresting cure after 30 minutes when the instrumented end of the laminate nearer the autoclave heat source showed that an undercure temperature of 310°F had been reached. The laminate was removed from the autoclave, and half of it was wrapped with a heating tape and was held at 350°F for 60 minutes. During this cure cycle a heat sink of aluminum sheet was secured to the undercured half of the panel in an attempt to maintain typical undercure properties.

The most potential inclusion, as a result of careless layup, is represented in Figure A-3; this shows an entire strip of prepreg backing left in the laminate.

Fiber Variations

The most common defective condition with respect to fiber spacing arises not through irregular spacing in the raw material but in improper placement of adjoining plies at a butt joint to create a strength-affecting gap. This spacing problem is more serious with larger, more rigid boron fibers than with the soft, slender graphite fibers. Fiber spacing defects and overlaps were produced in the panels (as shown in Figure A-4) by improper placement of adjoining plies at butt joints. Broken fibers, common to boron, usually occur across an entire tape; therefore, entire tapes were manually slit. Broken

fibers are atypical of graphite, and were not incorporated in the panels. Instead, a void half the size of the void used for fiber spacing defects was placed in the laminate.

Figure A-5 illustrates a 0° , $0(\pm 90)^\circ$, and $0(\pm 45)^\circ$ bias in the orientation of the boron or graphite fiber material. One orientation variation of 10° was considered sufficient to create a typical standard for each bias. The panel must be rotated to represent the desired bias orientation.

Delaminations, Voids, and Damaged Core

Delamination defects (depicted in Figures A-6 and A-7) were produced by inserting Tedlar/Amalox discs approximately 0.0015 inch thick. The extent of actual delamination (Figure 2) is shown in a cross-section photomicrograph of a portion of a destructive test panel. Gross delamination from overaged material was produced by staging the material in an oven for four hours at 275°F , to simulate effects from material left out of refrigeration for over 60 days. Figure 3 shows delamination in a cross-section photomicrograph made from a portion of a (No. 525) destructive test panel. Prior to final layup, a section of core with the crushed areas was photographed and is presented in Figure 4.

III - NONDESTRUCTIVE EVALUATION

A single nondestructive test method does not suffice to reveal all possible defects in a composite structure. Two or more methods must be used in a complementary fashion to characterize these materials adequately. Generally, radiography and ultrasonic C-scan techniques will reveal most, but not necessarily all, defects that may be present in a single structure. Other methods such as infrared and microwave may add more information, but the revelation of some defects may have to await further developments and refinements in NDT technology.

One problem is caused by the inherent variability in the heterogeneous composite structure, which becomes superimposed on the recorded signal and may mask the presence of a defect. Although this problem remains to be solved, various signal enhancement approaches can help to clarify such NDT information.

In light of the above considerations, three nondestructive test methods were chosen to evaluate the graphite and boron standards designed and fabricated during this program: ultrasonic C-scan, radiography, and infrared methods. Discussions of the techniques and their results follow.

Ultrasonic Evaluation

The ultrasonic method was applied in two basic techniques, both using longitudinal waves and water-immersion: pulse-echo and through-transmission. The through-transmission technique was the only one suitable to evaluate the honeycomb standards. While either technique could be used with the flat panels, the pulse-echo technique was used because of the potential enhancement due to two-way travel through the panel. However, the pulse-echo wave could not penetrate the two-way thickness of the honeycomb panels.

The ultrasonic techniques were not necessarily optimally developed for any panel, but were developed to a point of adequacy for portraying the particular defects. Optimizing the techniques for each defect type in each panel would be a major undertaking due to the need for determining the optimum values of all the pertinent system and material/defect parameters. System parameters include (1) frequency, diameter of

search unit (S/U), focused or unfocused; (2) search unit-to-reflector plate distance for pulse echo; (3) transmitting S/U to receiving S/U distance for through-transmission; (4) sensitivity; (5) reject setting; (6) recording voltage range for signal excursions (contrast) and maximum voltage; and (7) pulsing frequency. Material parameters include (1) thickness, (2) filament material, (3) structure, (4) complexity, (5) adhesive layer bond quality, and (6) defect type.

The basic ultrasonic techniques are portrayed in the line drawings in Figure 5.

A Sperry UM721 reflectoscope was used in conjunction with a special-function cabinet containing a Sperry Fast Transigate, a Transigraph, and a Type S recording amplifier. Either a 10N or a HFN pulser/receiver unit was used in the UM721 console. Other major equipment includes an Automation Industries Research Tank containing variable scanning and indexing controls, a variable-angle search unit manipulator, a thermo-sensitive Alfax facsimile recorder, and an assortment of focused and unfocused search units. (See Table II.)

The standards were immersed in water in the research tank while being scanned and they were held in position by a specially made fixture. The high buoyancy of the honeycomb panels required a heavy holding fixture to keep them immersed and stationary while scanning. It was necessary to spray the standards lightly with a mild soap solution before immersion to prevent the formation of bubbles particularly on the underside of the standards.

The flat panels were scanned in the pulse-echo mode using a 10 mHz sharp-focus 0.375-inch-diameter search unit (57A2789). Unfocused 5 mHz and 2.25 mHz were tried on some of the flat panels, but the results were inferior to the results of the focused 10 mHz unit. A flat, smooth aluminum panel was used as the reflector plate with a 1/4-inch separation between panel and plate. The sharp-focus 10 mHz search unit was focused on the surface of the aluminum reflector plate.

The honeycomb panels were scanned in the through-transmission mode, using a pair of 5 mHz (pulsed at 2.25 mHz) or 2.25 mHz search units for both transmitter and receiver. Penetration of

TABLE II
ULTRASONIC SEARCH UNITS USED TO
EVALUATE THE COMPOSITE STANDARDS

a. Pulse Echo

1. 10 MHz sharp focus SIL 57A2789, 0.375 in. dia.

b. Through-Transmission

1. 10 MHz sharp focus SIL 57A2789, 0.375 in. dia. and 10 MHz sharp focus SIL 57A2753, 0.187 in. dia.
2. 5 MHz flat SIL 57A3619, 0.375, 2 each, with plastic-tape diaphragm over face of receiving transducer.
3. 2.25 MHz flat SIL 57A3615, 0.375 in. dia., 2 each, with plastic tape diaphragm over face of receiving crystal.

10 MHz ultrasound was not sufficient to be used on the honeycomb standards. For 5 MHz or 2.25 MHz operation, the receiving search unit was masked with a plastic tape diaphragm with a 0.2-inch-diameter hole for better clarity of detail. The aligned search units were separated by 2.0 inches.

The voltage limits and sensitivity on the transigraph were set to provide good overall recording contrast over each panel. An alternate approach (not attempted) is to obtain optimum contrast between defective and defect-free regions in the panel. However, the former approach usually provided satisfactory results similar to that attainable in the latter approach. An upper limit of 30 volts and a lower limit of 10 volts were generally chosen, corresponding to signals at full-scale deflection (on the display) and 25 percent deflection, respectively.

The signals that emerge from the filamentary composite, and then recorded, have been modulated by the inherent structural variations in the material. This presents the problem of discriminating between defects and good material on the recording. The signals from the honeycomb composite includes modulations from variations in two filament/epoxy face-sheets, the thickness variations and bond quality of two adhesive layers, and the patterned structure of the honeycomb core material. Hence, small defect indications may be lost in a maze of indications from structural details.

Ultrasonic Results

Evaluation of the flat panels required setting the UM 721 sensitivity control at different levels for the plain and the titanium substrate areas. Various panel thicknesses on either area also require different sensitivity levels for optimum contrast for a given thickness, although in this program, most panels were scanned at a fixed sensitivity set up on the medium thickness of the panel.

Results of ultrasonic C-scan evaluations of the panels are discussed below in terms of defect type.

Density/Porosity and Resin Variations

The C-scan recordings of the flat graphite Panel 101 and flat boron Panel 104 shown in Figures 6 and 7, respectively, show a difference between the bare (without titanium)

portions of the panels having porosity and having no porosity (porosity is due to the presence of microballoons only). This is evidenced by a darker shading for the non-porous areas. Only a slight difference can be seen between the low and the high resin-to-fiber ratio, the former being darker in shade. However, these differences can be made more discriminating by optimizing the sensitivity, reject, and contrast controls of the UM721 and the Transigraph. Significant differences between these defective conditions did not appear in areas containing the titanium substrate with the particular NDT set-up used.

The C-scan recordings of the honeycomb Panels 102, 103, 105, and 106 are shown in Figures 8, 9, 10, and 11, respectively. In all of the C-scans, considerable difference is shown between the porous (microballoons), over-cured regions and the non-porous regions, regardless of the resin-to-fiber (r-f) ratio. Significant differences did not appear between the porous low r-f area and high r-f areas for the setup used.

Cure Variations - Inclusions

C-scan recordings of the flat graphite Panel 207 and the flat boron Panel 210 are shown in Figures 12 and 13, respectively. The backing inclusion (misplaced in the boron panel) is easily detectable, as this does not permit transmission of the ultrasound at any frequency attempted (10 mHz, 5.0 mHz, and 2.25 mHz). The backing is detectable under titanium substrate in the graphite panel. There is slight, but inconsistent, evidence that the undercure portion of the panels permits less transmission than the properly cured portion.

The backing inclusion is readily seen also in the C-scan recordings of honeycomb Panels 208, 209, 211, and 212 shown in Figures 14, 15, 16, and 17, respectively. Indications of the undercure condition do not appear in these recordings but would be in the lower half of the recordings (except for Panel 212, Figure 17, which was scanned on the opposite side with respect to the other panels) had the technique been sensitive to this particular defect.

Bias Variations

Figures 18 and 19 show the C-scan recordings of the flat graphite Panel 313 and the flat boron Panel 316, respectively. These recordings easily reveal the $\pm 45^\circ$ alignment of the fibers. Evidence of the 10° misalignment in the second ply is noticeable in the 0.020-inch thick section in the upper half of the figure, but in thicker sections, the

recording features are dominated by the orientation of subsequent plies which tend to obscure the 10° misalignment.

Figures 20, 21, 22, and 23 show the C-scan recordings of honeycomb Panels 314, 315, 317, and 318. The only features recognizable in the recordings are those of the honeycomb core, in all panels. Filament features cannot be seen superimposed on the core detail; thus, the second ply misalignment cannot be observed in the C-scans.

Broken Fibers, Overlaps, Fiber Spacing

The C-scan recording of the flat graphite Panel 419 is shown in Figure 24. The 1/4-inch by 6-inch slots in the third ply of this panel are observable in all thickness ranges in both plain and substrated areas. The overlaps in the second ply appear as lighter areas in the recording, while the fiber spacing voids in the second ply appear as darker areas. Except for the 6-inch slits, results are similar for the boron Panel 422 shown in Figure 25, although with somewhat less definition. Resolution of narrow slits across the boron fibers in this panel appear to be beyond the capability of the instrumentation (operating at 10 MHz with a focused transducer).

The C-scan recordings for the honeycomb Panels 420, 421, 423, and 424 are in Figures 26, 27, 28, and 29, respectively. None of the slots, overlaps, fiber spacings, and slits are apparent in these recordings as the signal-to-noise ratio (with respect to the defect signals) is quite low for the setup used. This is due to the complexity of these panels. The thickness steps are generally observable in all the panels.

Delaminations/Disbond - Plain and Titanium

Figure 30 and 31 show C-scan recordings of Panels 525 and 526, respectively. The flat graphite Panel 525 presented considerable variations to the ultrasonic signal, but all defects are revealed, including the 1/4-inch and 1/2-inch armalon/tehdlar inserts (for disbonds between 2nd and 3rd plies), the 1/2-inch inserts between the laminate and titanium (adhesive disbond), and the general disbond produced by incorporating pre-aged material into the panel. Results for the flat boron Panel 526 are similar, but with considerably less variations.

Delaminations/Disbonds - Honeycomb

Figures 32 and 33 show the C-scan recordings for two No. 527 panels (1/2-inch honeycomb with graphite facesheets). Figure 32 is a C-scan of the original No. 527(A) panel with all intended defects but also with many unintentional disbonds which limit the usefulness of the panel. As a result of the obviously poor quality in the original panel, a second Panel 527(B) was fabricated, but the laminate/honeycomb disbond inserts and the crushed core were inadvertently left out of this panel. The C-scan of this second panel (Figure 33) shows only the 1/4-inch interlaminar disbonds and the general disbond area produced by the preaged material. A new panel was constructed to conform to the design for Panel No. 527C. This panel includes all of the designed artificial defects and includes no unintentional disbonds. The ultrasonic C-scan of this panel is shown in Figure 71 which reveals the presence of all intentional defects and no unintentional disbond areas.

Figures 34, 35, and 36 show the C-scan recordings for honeycomb Panels 528, 529, and 530. The far-side and near-side core-to-laminate disbonds and the crushed core are easily visible in these recordings. The 1/4-inch interlaminar disbonds between 2nd and 3rd plies are easily observable in the 1/2-inch-thick Panel 529, but are only partially observable in the 1-inch-thick Panels 528 and 530. The honeycomb core and adhesive layer tend to cause overlapping of the structural images on the recordings, distorting feature boundaries and causing the defects to appear smaller than their actual size. The small representation of some of the 1/2-inch near-side disbonds suggests that a near-side disbond as small as 1/4 inch may be completely obscured by the tendency for features to become overlapped. This tendency can probably be alleviated by using a search unit of smaller diameter and increasing the operating frequency. The preaged area on the lower fourth of each panel does not appear on the recordings for Panels 528, 529, and 530, but does appear on the recording for Panel 527. The behavior of the preaged material in forming good or bad bonds with adjacent material during the curing process was unpredictable.

Radiographic Evaluation

The composite standards were radiographed to reveal the finer detail of the honeycomb core and filament characteristics. X-ray and neutron radiography were used in this program. However, neutron radiography was used only on a trial basis and was applied to Panel 211 (boron/honeycomb) and to a Lockheed panel similar to Panel 102 (graphite/honeycomb)

X-Ray Radiography

All panels were X-rayed in the Lockheed-Georgia production radiographic facilities. A conventional X-ray technique was followed using a Norelco MG150 X-ray machine operating at 50 kilovolts and 4 milliamperes to obtain the exposures. A Norelco type 150/BE tube having a focal spot size of 2.5 millimeters was installed in the X-ray machine. The radiographs were made at a film-focal-distance of 60 inches on Ansco Type B film. The graphite (flat and honeycomb) panels were exposed for 45 seconds, and the boron (flat and honeycomb) panels were exposed for 25 seconds. The exposed film was developed automatically in a Kodak Industrial X-omat Processor.

Because of the similarity of density of the graphite fibers and epoxy matrix, radiographs showing individual fibers could not be produced for the graphite standards. Only gross fiber characteristics due to bunching tendencies can be seen readily. When a titanium substrate is present, it is even more difficult to observe the composite features. The density of the boron fibers, on the other hand, is sufficiently different from the epoxy, phenolic core and titanium to produce good contrast in the radiographs. Filament characteristics in the boron standards can be seen quite easily, particularly in the flat panels. The radiographs for the boron honeycomb panels are very "busy" due to the individual components, and the fibers in the face sheet closest to the film dominate the radiographs as far as overall fiber features are concerned. Results of the X-radiographic evaluation are discussed below in terms of defect type. The figures giving the X-radiographic results were produced from reduced positive photographs of the radiographs in which some of the defect detail present in the original radiographs is no longer present.

X-Radiographic Results

Density/Porosity and Resin Variations

The density, porosity, and resin variations are not discernible in the radiographs for either the graphite or boron panels. Revealing these types of defects in filament composites may be nearly impossible for ordinary production and radiographic techniques. Fiber bunching and thickness variations are distinguishable in the graphite flat Panel 101 (Figure 37), but only the core features are visible in honeycomb Panels 102 and 103 (Figures 38 and 39). Individual filaments as well as thickness variations and honeycomb core are distinguishable in the radiographs of the boron panels (Figures 40, 41, 42).

Cure Variations – Inclusions

In the radiograph for the graphite flat Panel 207 (Figure 43) the backing inclusion is discernible as a change in shade, but the undercure area is not distinguishable. Thickness steps and fiber bunching are distinguishable in the bare portions of the panel. In the radiographs for the graphite honeycomb Panels 208 and 209 in Figures 44 and 45, respectively, only the core walls are discernible.

In Figure 46, the radiograph for the flat boron Panel 210, does not reveal the backing or undercure areas, although the filaments and thickness steps are visible. These comments also apply to the radiographs of Panels 211 and 212 shown in Figures 47 and 48. Panel 212 has sealant infusion in the left upper and lower corners.

Bias Variations

The radiograph for the flat graphite Panel 313, in Figure 49, shows the gross fiber bunching in $\pm 45^\circ$ orientations, but the 10° misalignment of the second ply is not discernible. Thickness variations are visible in the bare areas. The face sheets are not sufficiently visible in the radiograph for graphite/honeycomb Panel 314 in Figure 50 to show orientations, although thickness variations are faintly visible. Fiber orientations are not visible in the Panel 315 radiograph in Figure 51. Core features are dominant in both these panels.

In Figure 52, the radiograph for Panel 316 does show the 10° misalignment of the second ply amidst the $\pm 45^\circ$ orientation of the other plies in all thickness ranges. All thickness steps are visible. The 10° misalignment and $\pm 45^\circ$ fiber orientations are visible in the radiographs for Panels 317 and 318 in Figures 53 and 54, respectively. The 10° misalignment is not readily visible in the 0.050-inch and 0.060-inch thickness steps of either panel, however.

Broken Fibers, Overlaps and Spacing

In Figure 55, the radiograph for Panel 419 reveals all defects including the fiber gaps (1/4-inch slots), overlaps, and spacing in the plain area. In honeycomb Panels 420 and 421 shown in Figures 56 and 57, respectively, the 1/4-inch slots are visible only in the 0.020-inch thickness step of Panel 421 and are not discernible in other thickness ranges or in Panel 420. The second-ply voids and overlaps are visible in both panels. The radiograph for Panel 420 shows sealant infusion in the core near the center edge of the 0.020-thickness step.

The radiograph for the flat boron Panel 422 in Figure 58 shows the slits, void, and overlap in the plain area. Slits are also visible in the substrate area. For honeycomb Panels 423 and 424 (Figures 59 and 60), voids and overlaps are visible, but the slits are not discernible in either panel. These slits may be revealed if the defective face sheet is placed nearest the film during radiographic exposure.

Delaminations/Disbonds - Plain and Titanium

In the radiograph of Panel 525 shown in Figure 61, the 1/4-inch and 1/2-inch armalon/tehdar inserts in the second and third plies are visible in each thickness range. The pre-aged second and third plies appear as slightly lighter shading in the lower half of the panel. In the boron Panel 526 radiograph (Figure 62), the inserts are not discernible. Thickness steps and filaments are visible. Since exposure times sufficient to reveal filament characteristics are not enough to expose the armalon and tehdar inserts, they are not visible in the radiographs.

Delaminations/Disbonds - Honeycomb

The radiographs for graphite honeycomb Panel 528 are shown in Figure 63. The crushed core, armalon/tehdar inserts for far- and near-side disbonds and second-ply disbonds are visible in Panel 528. Figures 64 and 65 show the radiographs for the two 527 panels. In Figure 64, only the 1/4-inch inserts between second and third plies are visible, and the other intentional defects are not discernible. In Figure 65, all defects are discernible. The pre-aged area in either panel is not discernible. A print of the radiograph for Panel No. 427C is shown in Figure 72. Only the crushed core defects are visible in the reproduction.

The radiographs for the boron honeycomb Panels 529 and 530 are shown in Figures 66 and 67, respectively. The pre-aged area and the inserts are not visible in either radiograph. The crushed core areas are discernible only in Panel 529. Filaments, core, and thickness steps are observable in both panels.

Neutron Radiography

Two honeycomb panels were subjected to a neutron radiographic process on a trial basis, using the 1000-kilowatt Georgia Tech Research Reactor as the neutron source. This facility is owned and operated by the School of Nuclear Engineering of the

Georgia Institute of Technology in Atlanta, Georgia, and has been used heavily in biomedical applications. Panels given the neutron exposure included a density/porosity and resin variation panel (#102L - graphite) and a cure variation/inclusion panel (#211 - boron).

The reactor uses a highly enriched uranium-235 source moderated and cooled with heavy water (D_2O). The facility consists of a beam port exiting into a large shielded room (originally designed for thermal-neutron cancer therapy). Neutrons enter the room through a circular 4-inch-diameter port with a remote-controlled shutter. Bismuth blocks are used to decrease the gamma-ray components of the neutrons. A diagram of the facility is shown in Figure 68.

In making the exposures, the panels were placed in the neutron beam at a distance of 128.5 inches from the port. The beam had a diameter of 0.5 inch at the port, powered by the 1-megawatt reactor. An oscillating aluminum/cadmium anti-scatter grid was used between the panel and detector foil to reduce the number of scattered neutrons intercepted by the foil. This improves resolution and sharpness of the image. The detecting foil itself is a dysprosium sheet about 0.010 inch thick. The images were exposed on NS54T film for 60 minutes. Some experimentation with the system parameters was necessary to convert from a biomedical-oriented setup to one suitable for evaluating the composite panels.

Neutron Radiography Results

Since these tests were done on a very limited basis, the potential usefulness in evaluating boron and graphite materials with epoxy matrices has not been fully determined. The absorption coefficients of neutrons for various materials differ radically from coefficients of X-rays for the same materials. For instance, boron and lead are quite transparent to neutrons but not to X-rays. Hydrocarbons are somewhat opaque to neutrons but transparent to X-rays. Therefore, there is a potential for neutron radiography to serve a useful role in evaluating composite materials, serving to complement X-ray and other NDT techniques.

Figures 69 and 70 are positive prints of neutron radiographs made on boron/honeycomb Panels 211 and the Lockheed graphite/honeycomb panel.

Figure 69 represents an area near a corner of the boron Panel 211, showing the 0.040-, 0.050- and 0.060-inch thickness steps. A dark horizontal band about 2 inches below the top coincides with the undercure area on the panel. Figure 70 presents a high degree of resolution in showing core features in Lockheed Panel 102L, a graphite/honeycomb composite. The dark streaks in this print are due to imperfections in the anti-scatter grid.

Infrared Evaluation

One promising method for evaluating filamentary composites of the type fabricated under this program is infrared NDT. The infrared system available at Lockheed-Georgia is called the Traversing Infrared Inspection System (TIRIS) and uses the Bofors T-101 infrared camera as the main component. The heat is supplied by two electrically heated air blowers, which is applied to the panel before scanning with an adjustable lead time. The Bofors display unit is equipped with a Polaroid scope camera for recording size and shape of detected voids. Operation is monitored on an auxiliary 8" x 10" CRT display. The system is calibrated by means of a specially designed black body fitted with a digital thermometer, which is used as a gray scale.

This system can be used to evaluate bonded assemblies up to 80 inches by 202 inches, and it is particularly suited for metallic materials. A honeycomb panel similar to Panel 102 (graphite face sheets 0.020 to 0.060 inch thick, 1/2-inch honeycomb core containing density, porosity and resin variations) was submitted for preliminary evaluation with TIRIS. Unfortunately, the best results strongly indicated that the system in its present arrangement is not suitable for evaluating specimens of this type and of such small size as fabricated under this program. Problems of heat dissipation associated with the relatively small panel rendered the evaluation ineffective. Plans to submit additional panels for evaluation by TIRIS were thwarted by a breakdown in the equipment. Thus, infrared evaluation of the composite standards is inconclusive.

Summary of Nondestructive Evaluation

The results of the ultrasonic C-scan and the X-ray radiographic evaluations are summarized in Table III. This table lists the intentional defects which were fabricated into each panel and whether the defect was detected with the ultrasonic technique, the X-ray technique, or with both techniques. An "0" denotes that the defect was not discernible by either technique with the parameters used.

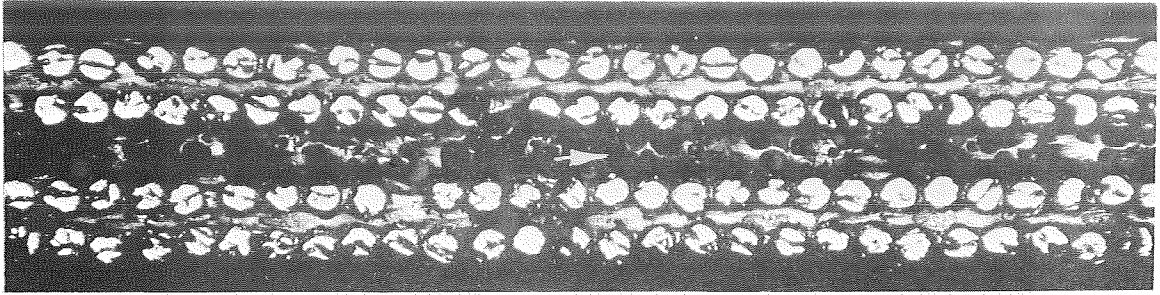
TABLE III
SUMMARY OF PANEL DEFECTS AND THE NDT TECHNIQUES WITH WHICH THEY WERE DETECTED

Panel Number	Porosity	Resin Variation	Inclusion	Undercure	Broken Fibers	Overlap	Spacing Void	Bias Misalignment	Delamination	Disbond-Titanium	Crushed Core	Disbond-Honeycomb	Pre-Aged Area	Remarks
101 102 103 104 105 106	I I I I I I	I 0 0 I 0 0												Except in substrated areas.
207 208 209 210 211 212			III I I I I	0 0 0 0 0										
313 314 315 316 317 318								I 0 0 III III						10° misalignment visible in 0.020" step Misalignment not visible in the 0.050" & 0.060" steps
419 420 421 422 423 424					III 0 II II 0 0	III II II III II	III II III II							1/4" slot visible only in 0.020" step
525 526 527 528 529 530									III I III III	III I		III III III	III I 0	Pre-aged area only slightly visible with X-ray Delaminations partially revealed by U/S Delaminations partially revealed by U/S

I - Detected with ultrasonic C-scan tech.
II - Detected with X-ray technique

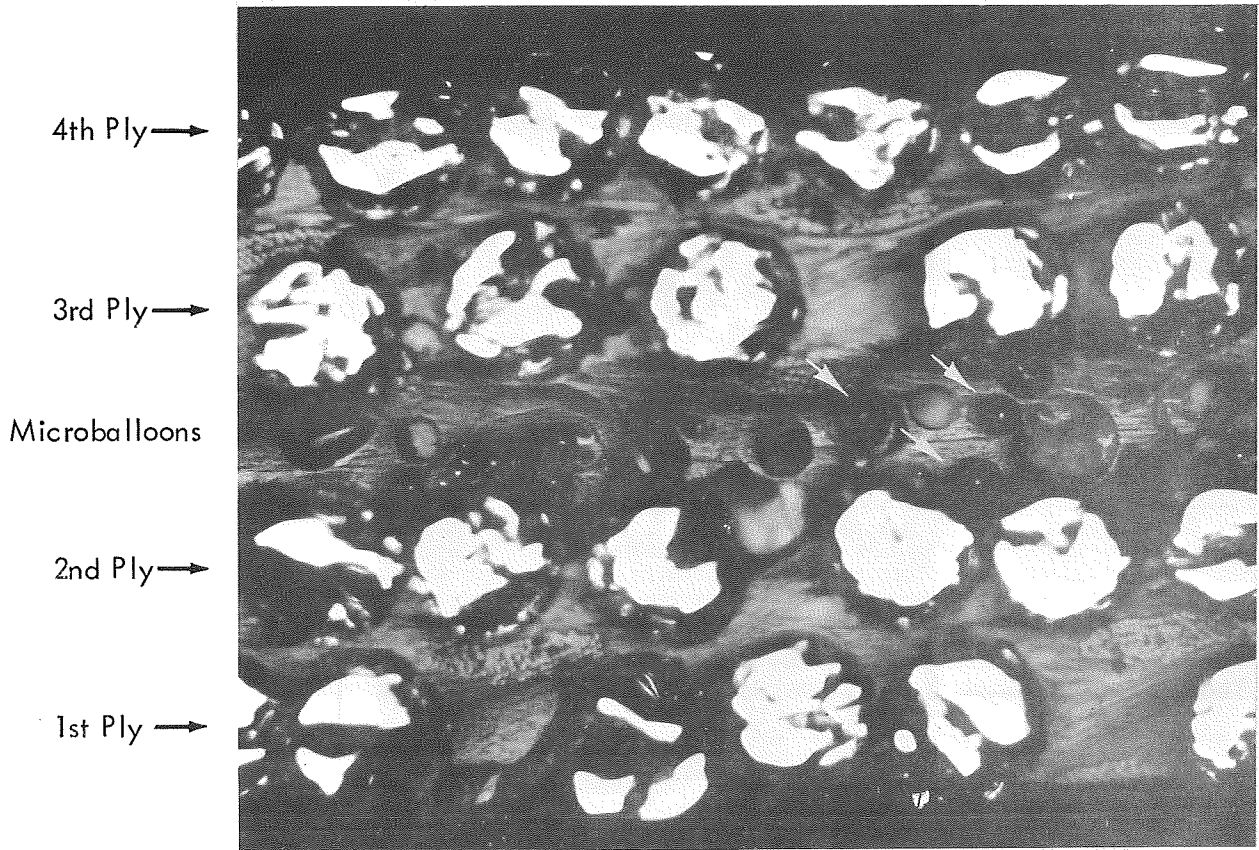
III - Detected with both ultrasonic and X-ray tech.
0 - Not detected by either method

LAMINATE OF FOUR PLYS OF BORON/EPOXY
APPROXIMATELY 0.020 INCH THICK



Magnification: 50X

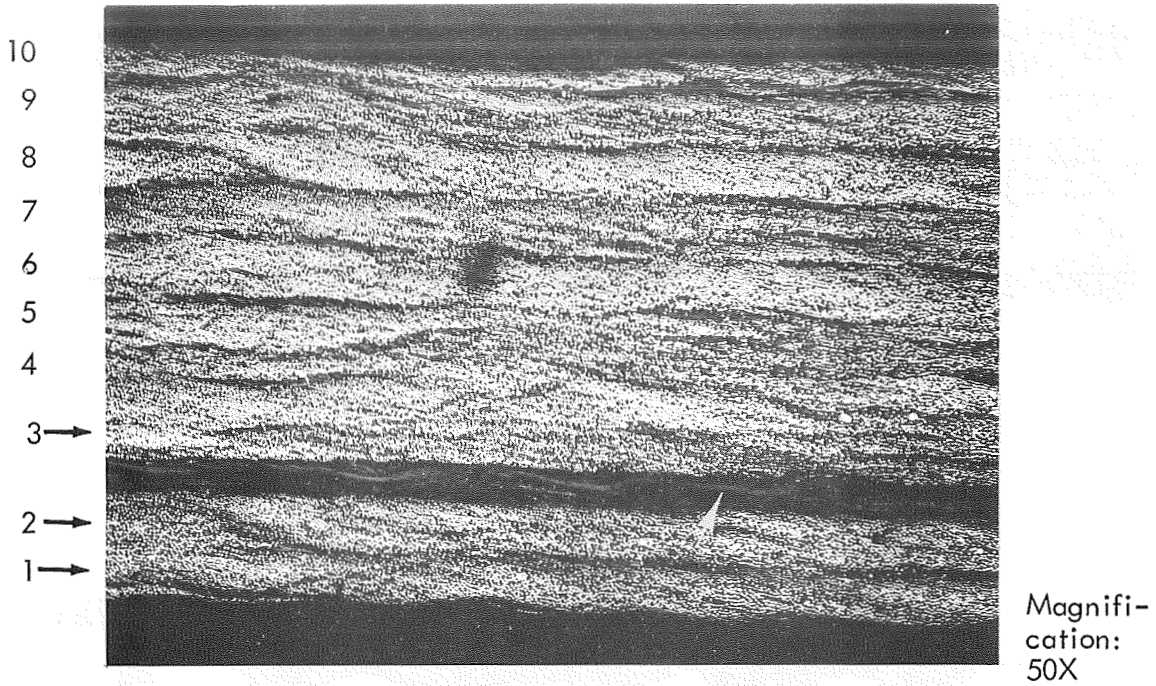
Arrow Points to Zone Shown Magnified
Below - Contains Microballoons to
Simulate Resin Porosity



Magnification: 200X

FIGURE 1. PHOTOMICROGRAPH OF CROSS-SECTION OF
FOUR-PLY SEGMENT OF BORON-EPOXY
DESTRUCTIVE TEST PANEL NO. 104

TEN PLYS OF GRAPHITE/EPOXY APPROXIMATELY 0.050 INCH THICK



Arrow Points to Zone Shown Magnified Below - Contains Delamination Produced by Insert.

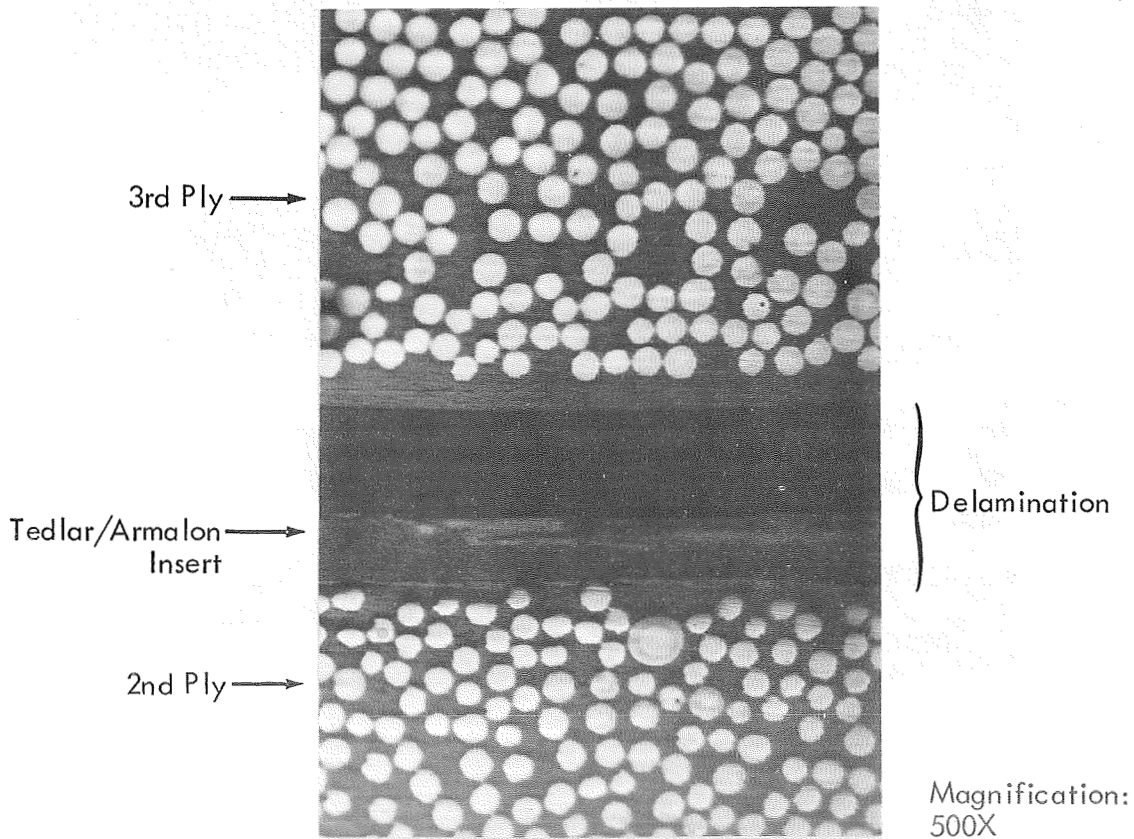


FIGURE 2. PHOTOMICROGRAPH OF CROSS SECTION OF TEN-PLY SEGMENT OF GRAPHITE/EPOXY DESTRUCTIVE TEST PANEL NO. 525

LAMINATE OF TEN PLYS OF GRAPHITE/EPOXY
APPROXIMATELY 0.050 INCH THICK

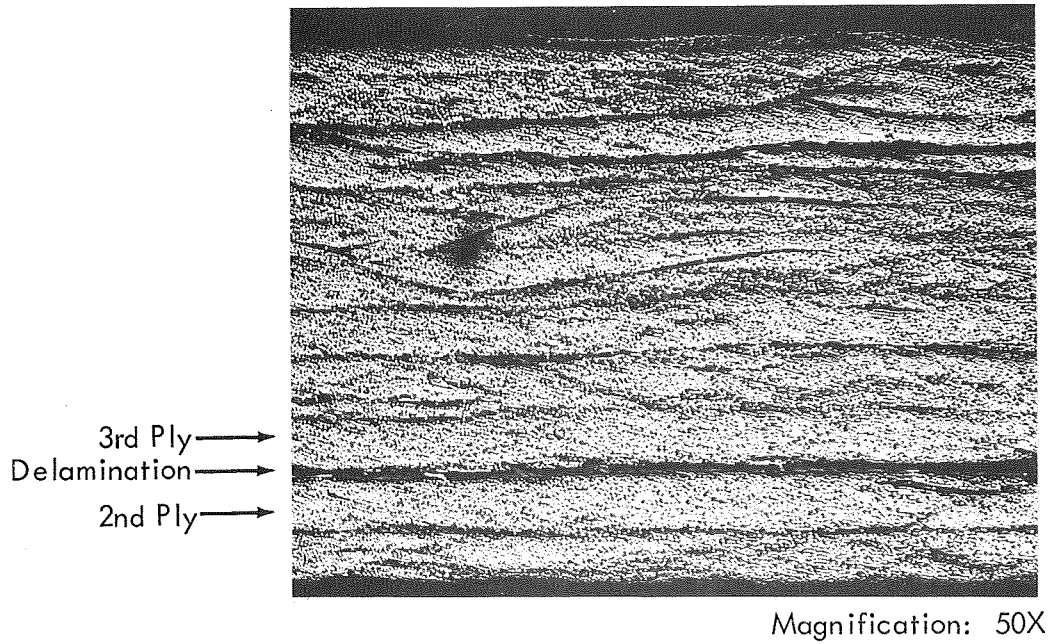


FIGURE 3. PHOTOMICROGRAPH OF CROSS SECTION OF TEN-PLY SEGMENT OF GRAPHITE/EPOXY DESTRUCTIVE TEST PANEL NO. 525

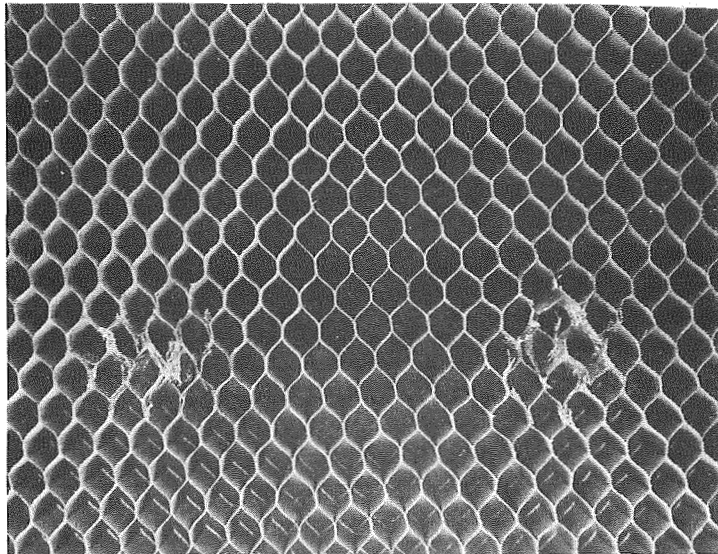
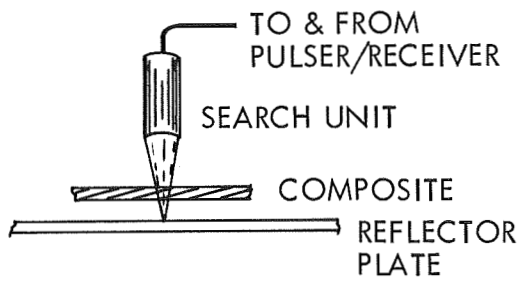


FIGURE 4. HONEYCOMB CORE WITH TYPICAL 3/4-INCH DIAMETER
CRUSHED AREAS USED IN PANEL NO.'s 527 THRU 530

PULSE-ECHO TECHNIQUE



THROUGH-TRANSMISSION TECHNIQUE

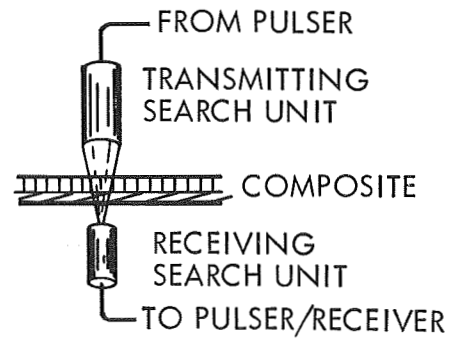


FIGURE 5. LINE DRAWINGS ILLUSTRATING THE ULTRASONIC PULSE-ECHO AND THROUGH-TRANSMISSION TECHNIQUES USED IN EVALUATING THE COMPOSITE STANDARD PANELS

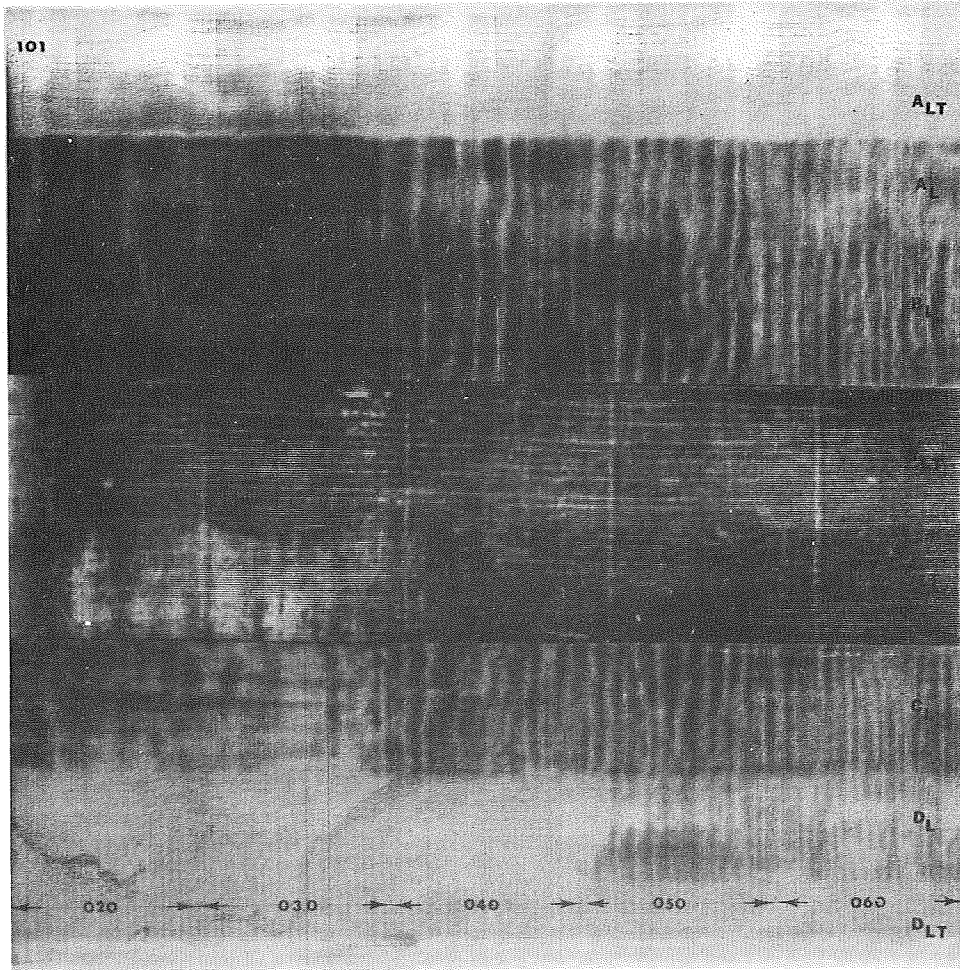


FIGURE 6. ULTRASONIC C-SCAN RECORDING AT 10 MHz OF THE FLAT GRAPHITE PANEL 101 SHOWING POROUS CONDITIONS IN AREAS A_L AND D_L

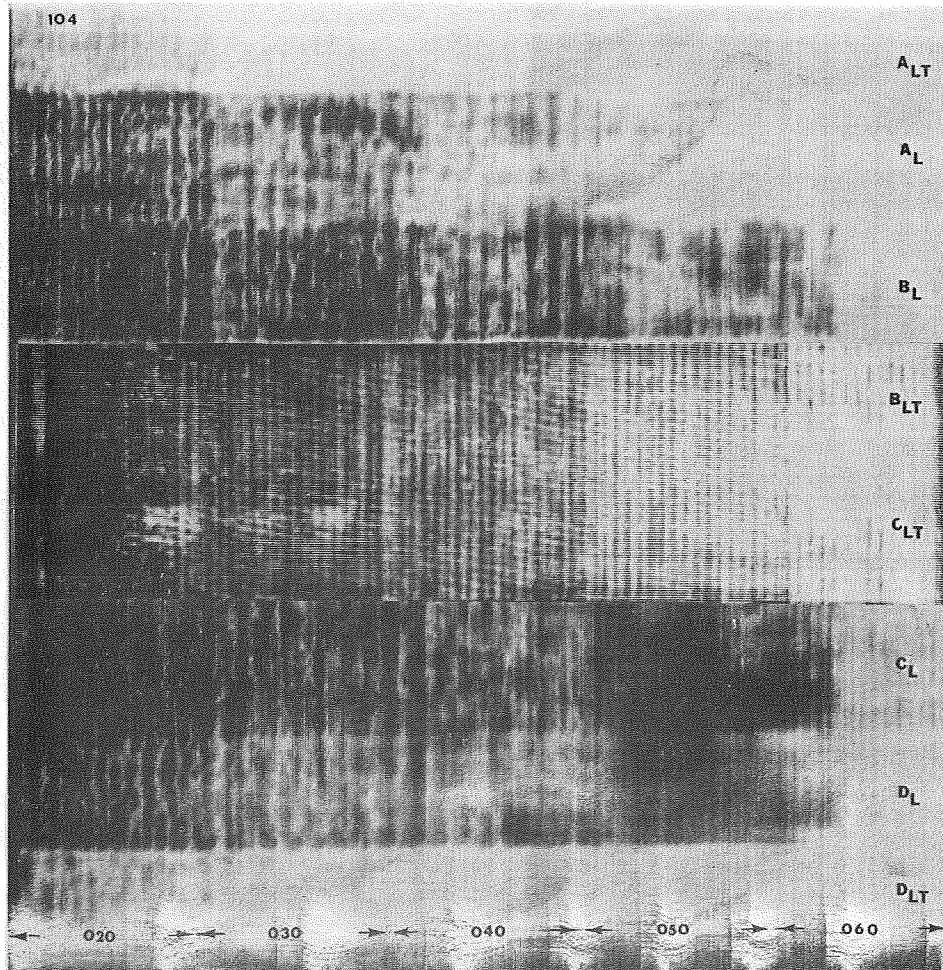


FIGURE 7. ULTRASONIC C-SCAN RECORDING AT 10 mHz OF THE FLAT BORON PANEL 104 SHOWING POROUS CONDITIONS IN A_L AND D_L

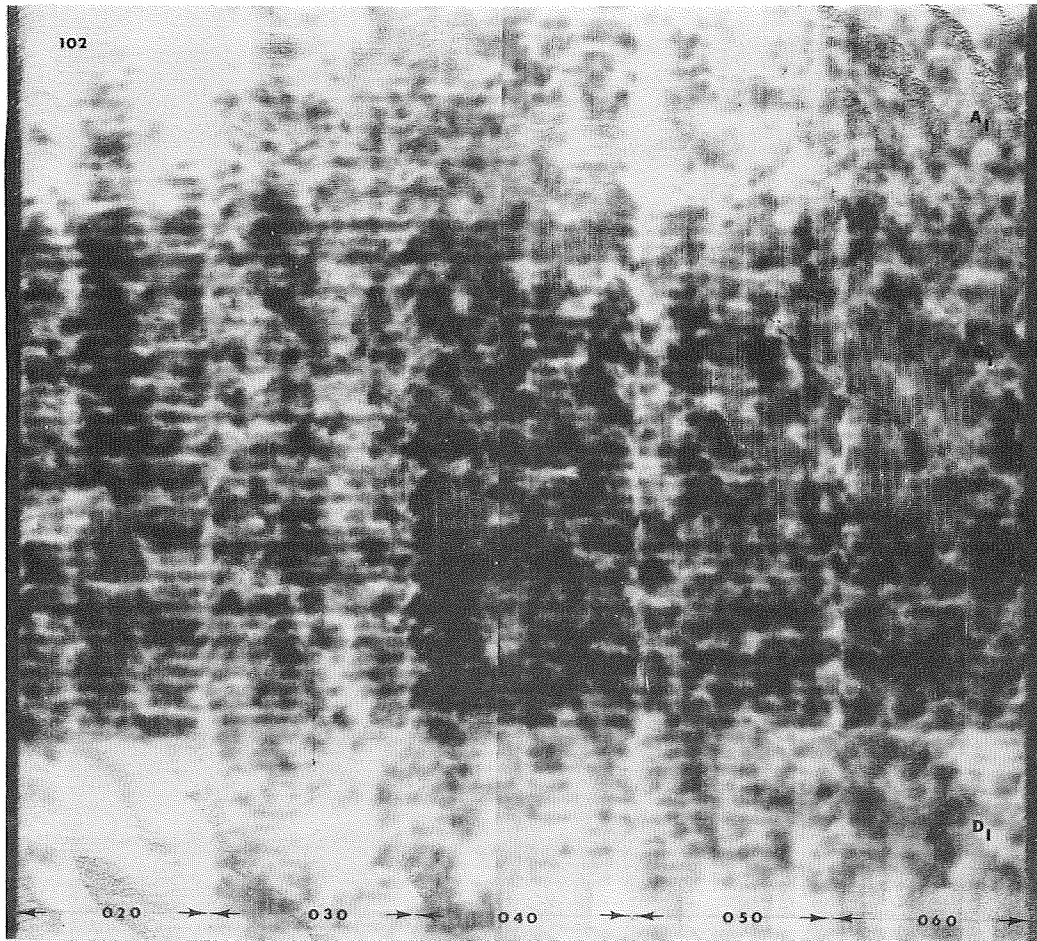


FIGURE 8. ULTRASONIC C-SCAN RECORDINGS AT 2.25 MHz OF THE 1/2-INCH GRAPHITE HONEYCOMB PANEL 102 SHOWING POROUS CONDITIONS IN AREAS A AND D

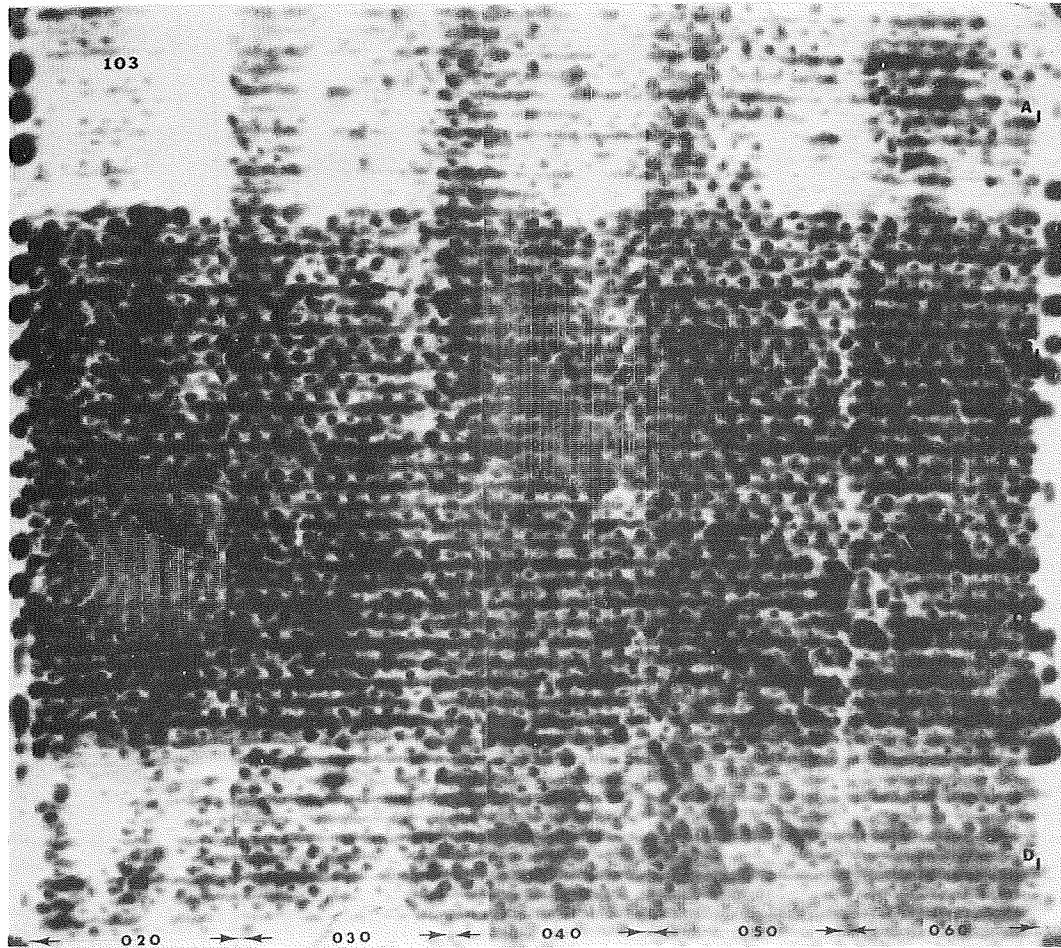


FIGURE 9. ULTRASONIC C-SCAN RECORDINGS AT 2.25 MHz OF THE 1-INCH GRAPHITE/HONEYCOMB PANEL 103 SHOWING POROUS CONDITIONS IN AREAS A AND D

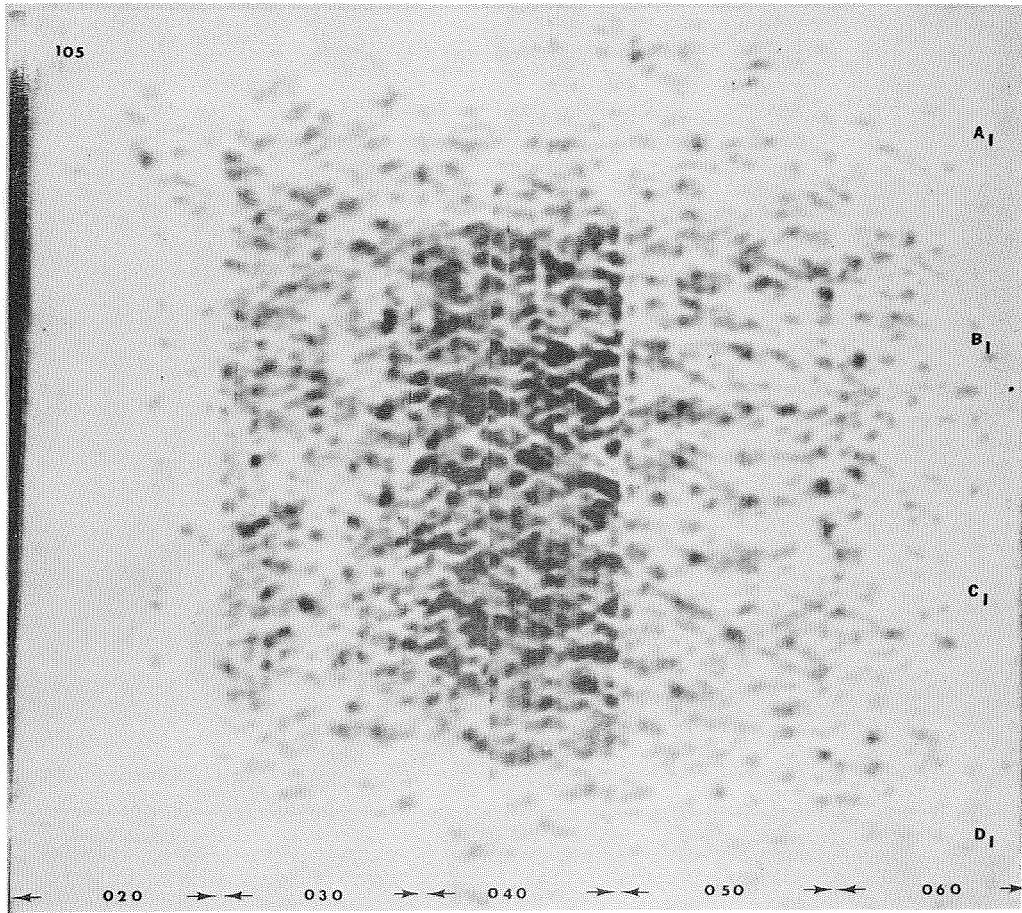


FIGURE 10. ULTRASONIC C-SCAN RECORDING AT 2.25 MHz OF THE 1/2-INCH BORON/HONEYCOMB PANEL 105 SHOWING POROUS CONDITIONS IN AREAS A AND D

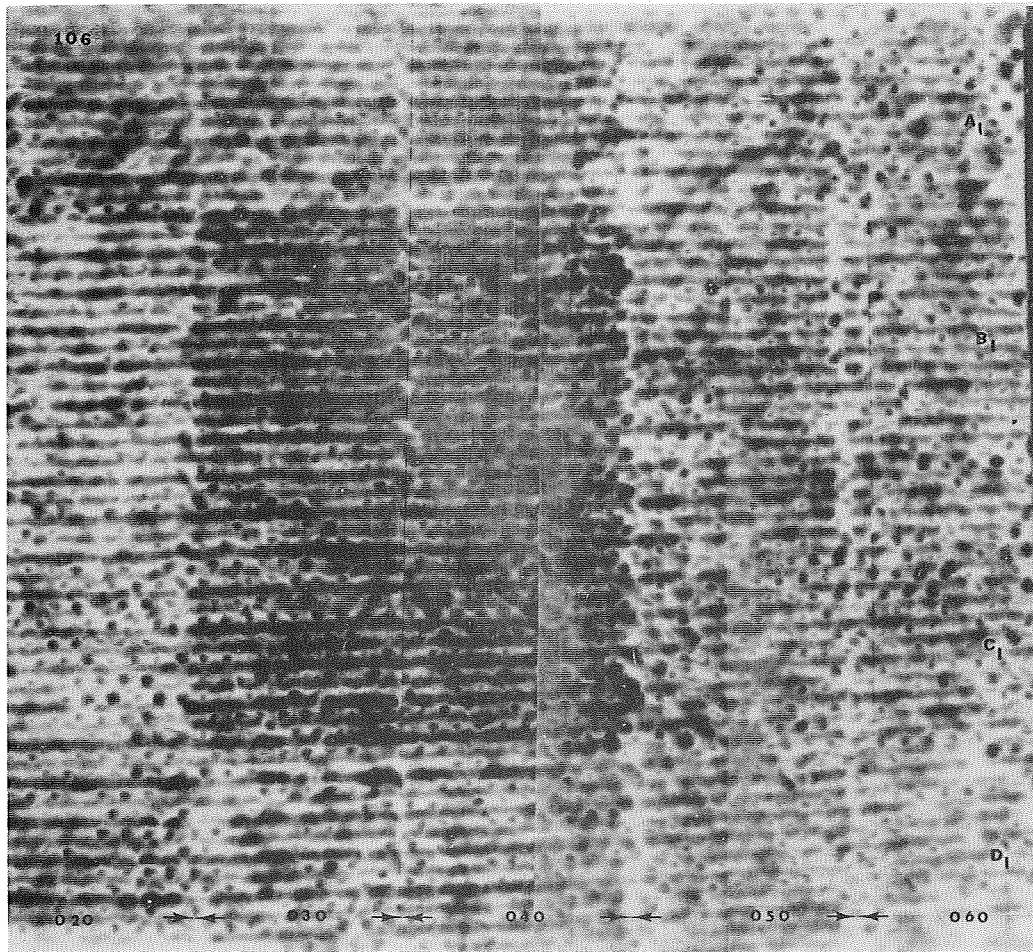


FIGURE 11. ULTRASONIC C-SCAN RECORDING AT 2.25 MHz OF THE 1-INCH BORON/HONEYCOMB PANEL 106 SHOWING POROUS CONDITIONS IN AREAS A AND D

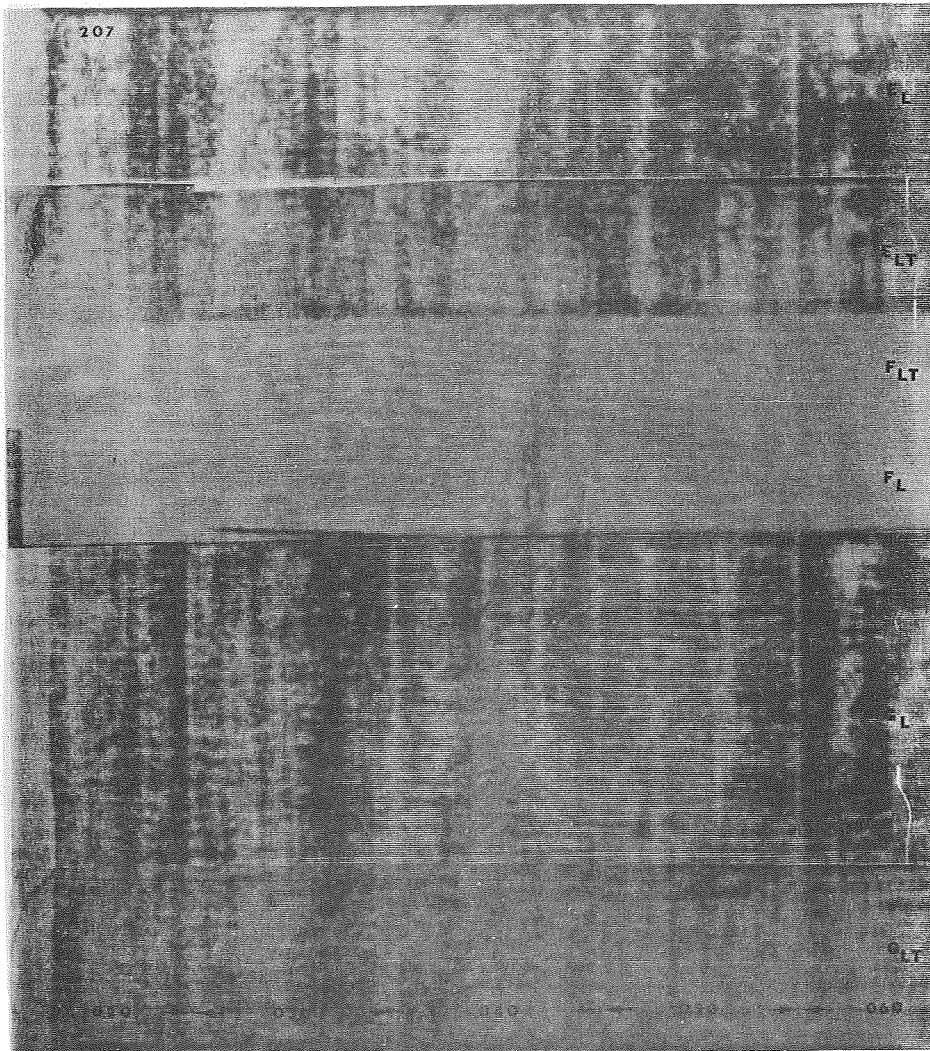


FIGURE 12. ULTRASONIC C-SCAN RECORDING AT 10 MHz OF THE FLAT GRAPHITE PANEL 207 SHOWING THE BACKING INCLUSION IN AREAS F_L AND F_{LT}

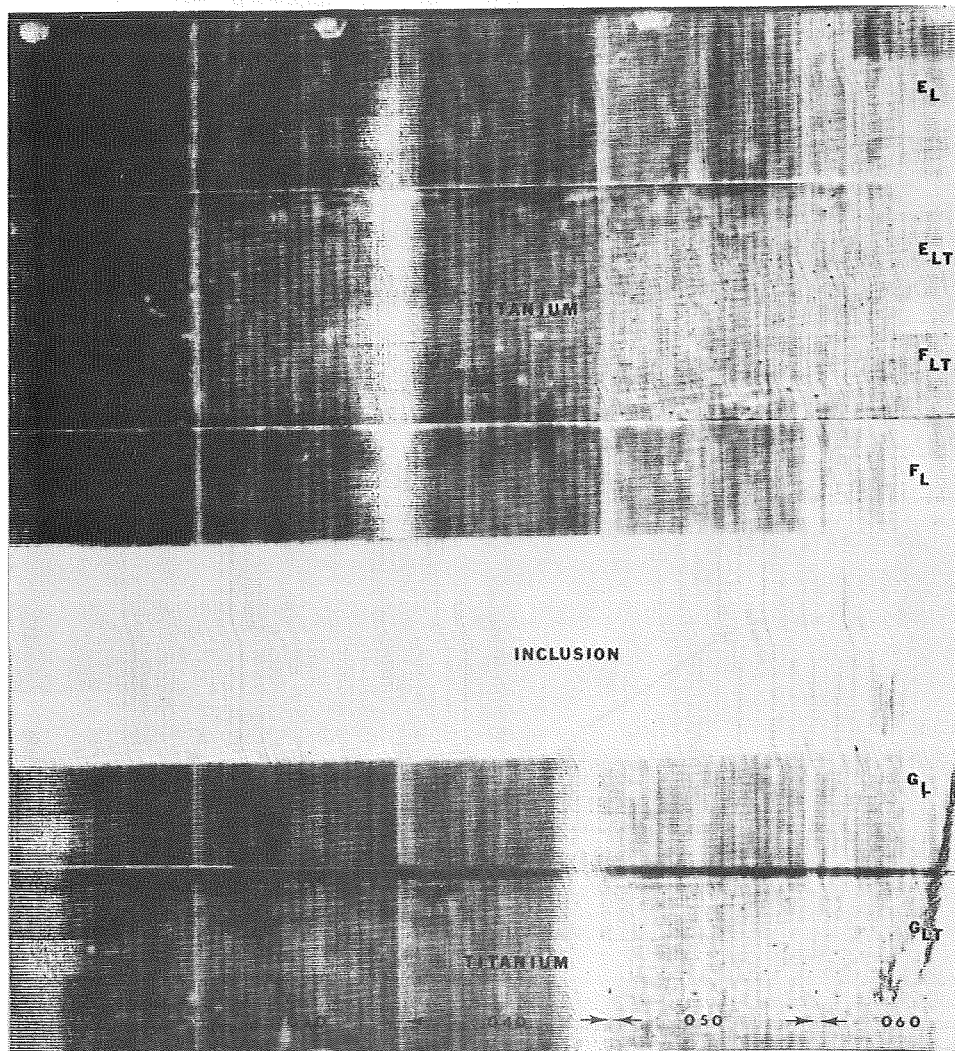


FIGURE 13. ULTRASONIC C-SCAN RECORDING AT 10 mHz OF THE FLAT BORON PANEL 210 SHOWING THE BACKING INCLUSION IN AREA G_L (MISPLACED FROM AREAS F_L AND F_{LT})

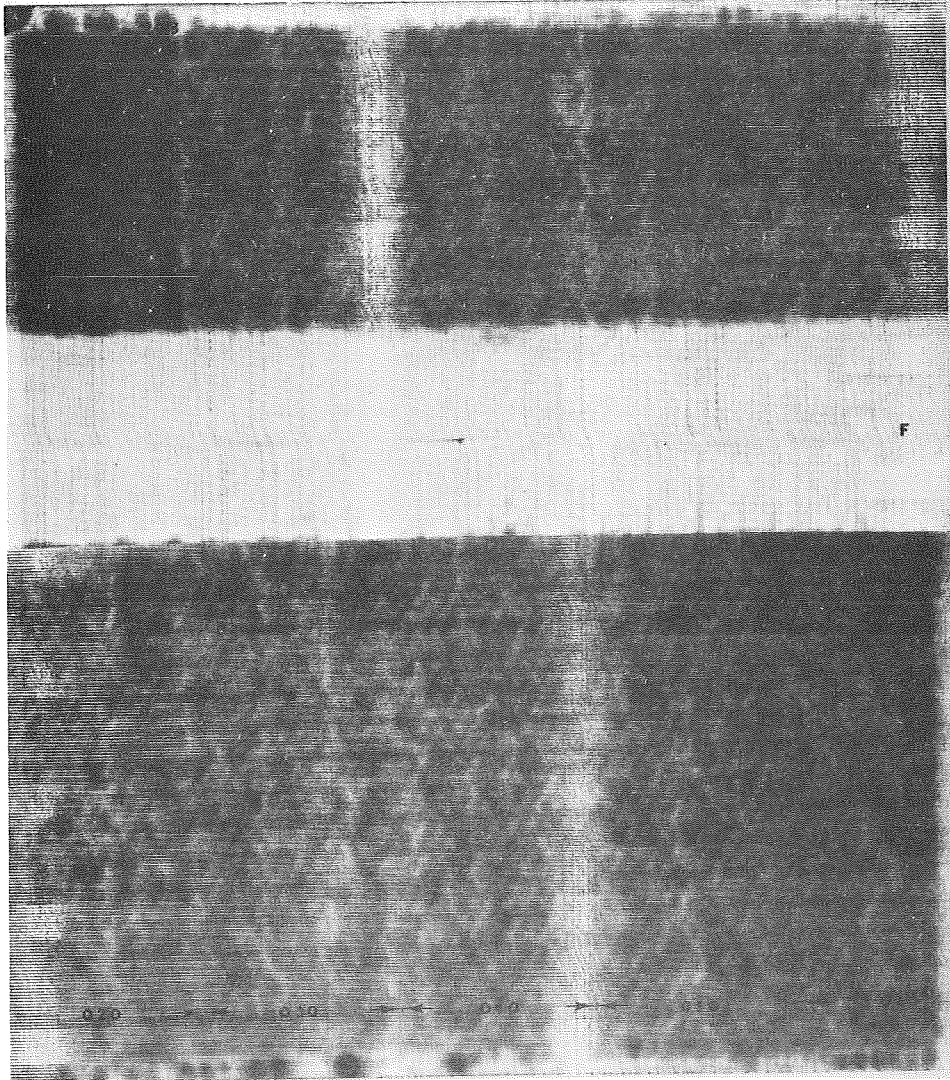


FIGURE 14. ULTRASONIC C-SCAN RECORDING AT 2.25 MHz OF THE 1/2-INCH GRAPHITE/HONEYCOMB PANEL 208 SHOWING THE BACKING INCLUSION IN AREA F

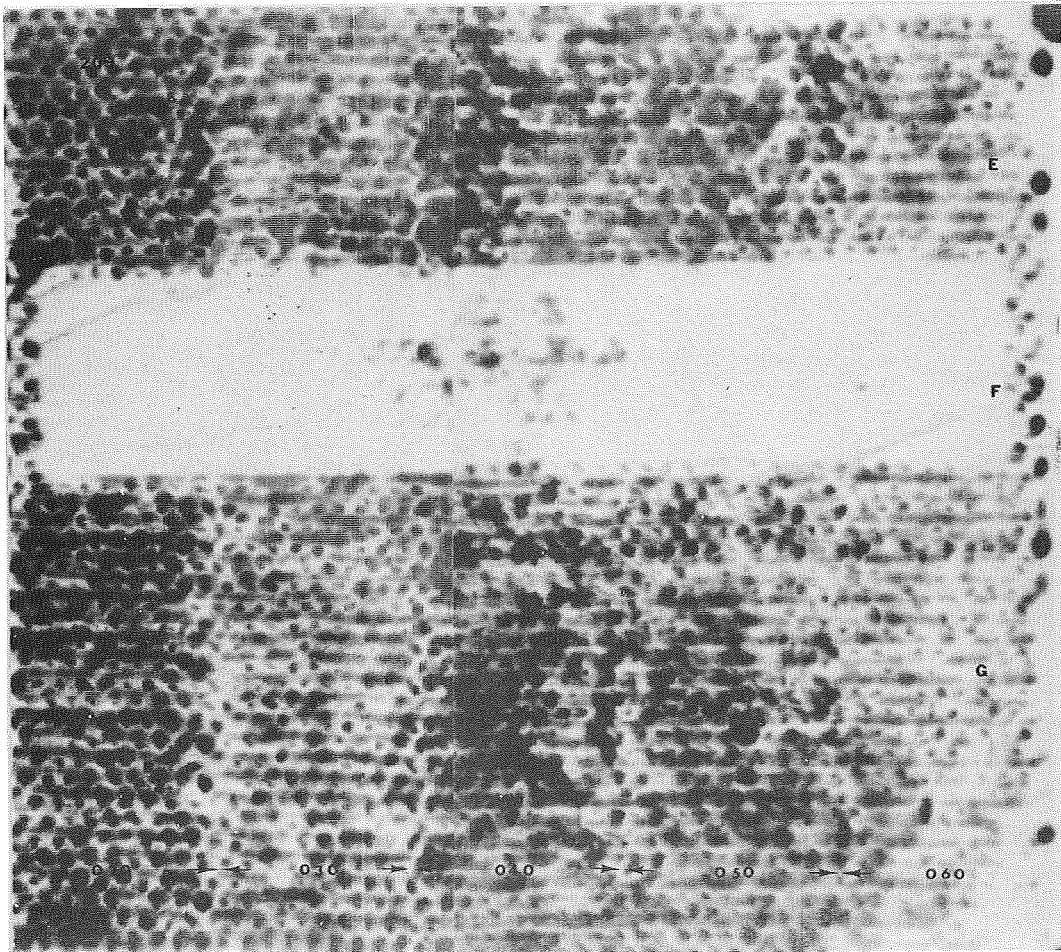


FIGURE 15. ULTRASONIC C-SCAN RECORDING AT 2.25 mHz OF THE 1-INCH GRAPHITE/HONEYCOMB PANEL 209 SHOWING THE BACKING INCLUSION IN AREA F

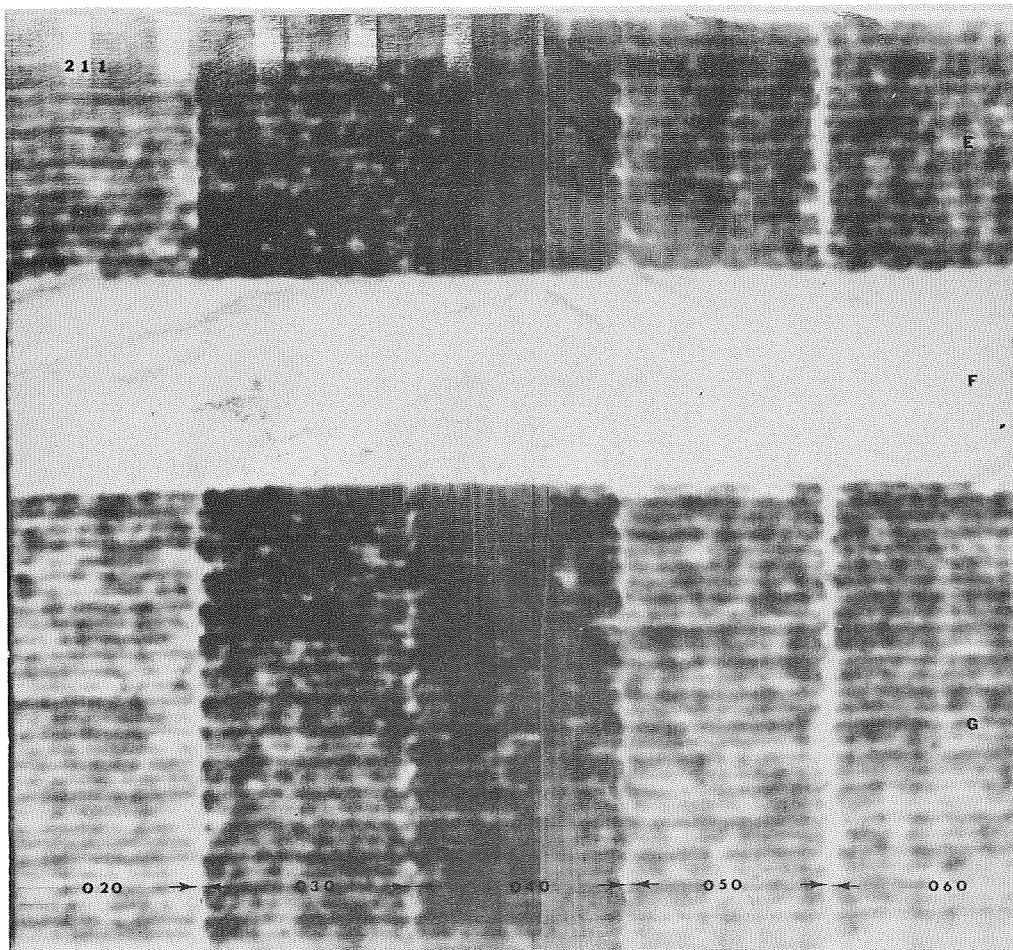


FIGURE 16. ULTRASONIC C-SCAN RECORDING AT 2.25 MHz OF THE 1/2-INCH BORON/HONEYCOMB PANEL 211 SHOWING THE BACKING INCLUSION IN AREA F

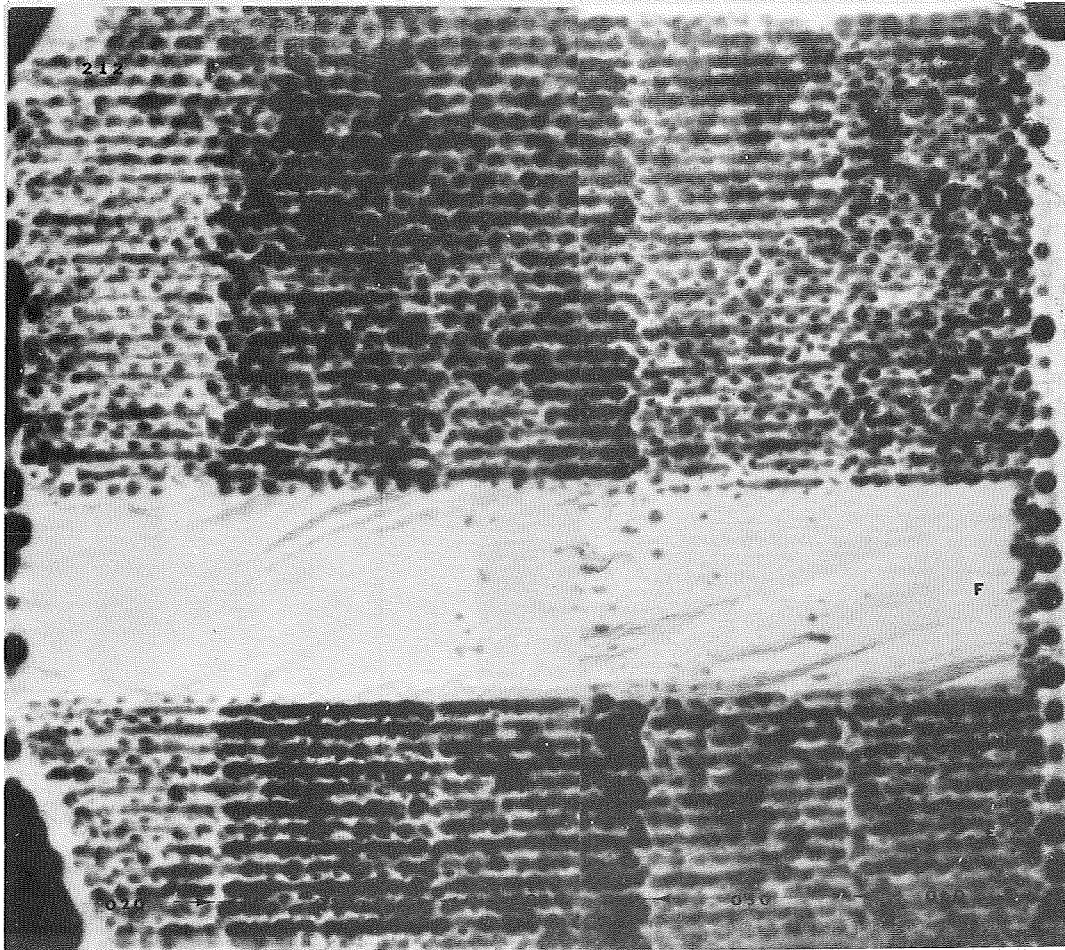


FIGURE 17. ULTRASONIC C-SCAN RECORDING AT 2.25 MHz OF THE 1-INCH BORON/HONEYCOMB PANEL 212 SHOWING THE BACKING INCLUSION IN AREA F

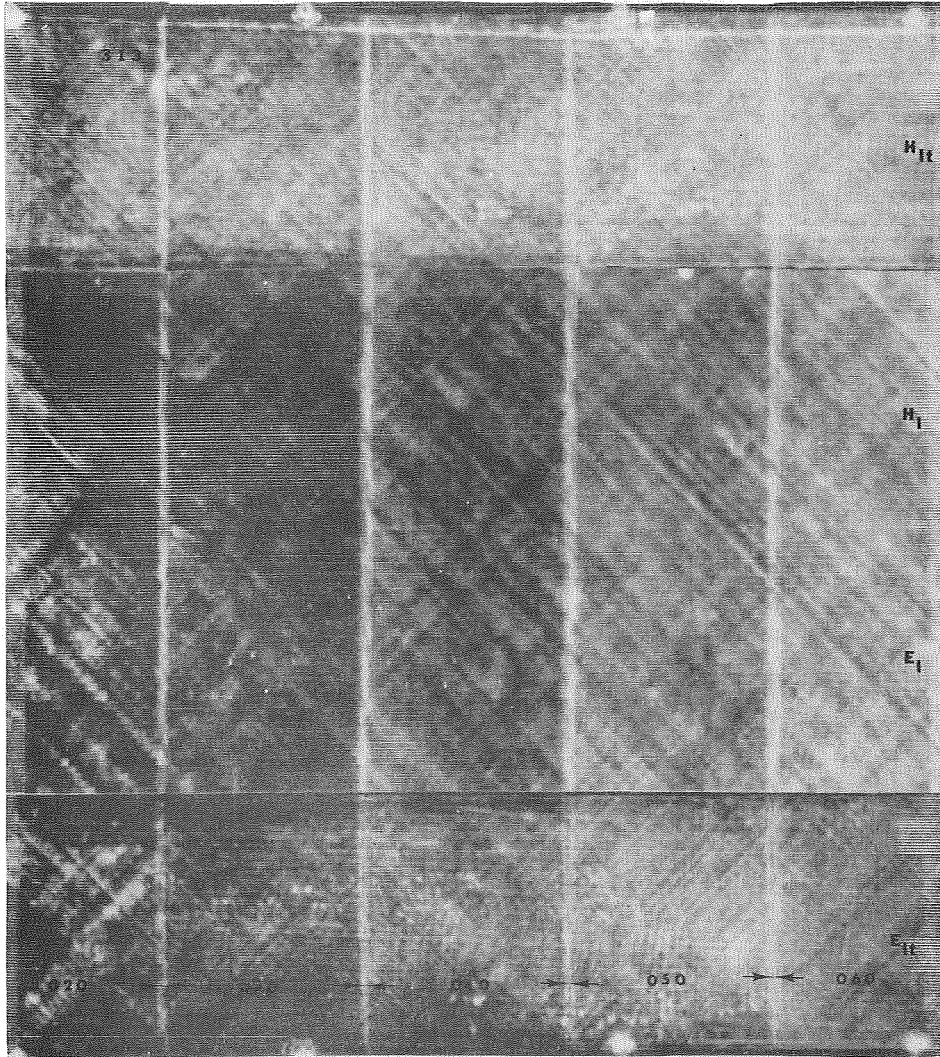


FIGURE 18. ULTRASONIC C-SCAN RECORDING AT 10 mHz OF THE FLAT GRAPHITE PANEL 313 SHOWING GROSS FIBER ORIENTATIONS

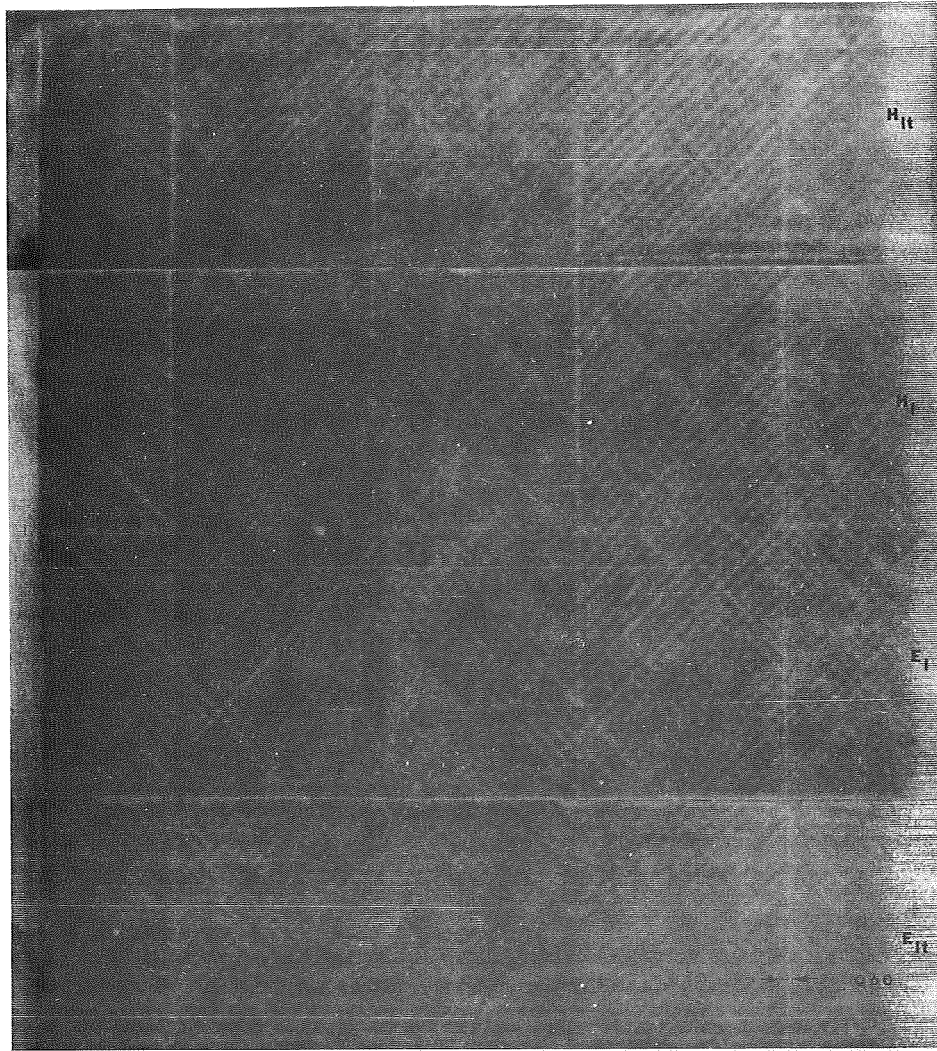


FIGURE 19. ULTRASONIC C-SCAN RECORDING AT 10 MHz OF THE FLAT BORON PANEL 316 SHOWING GROSS FIBER ORIENTATIONS

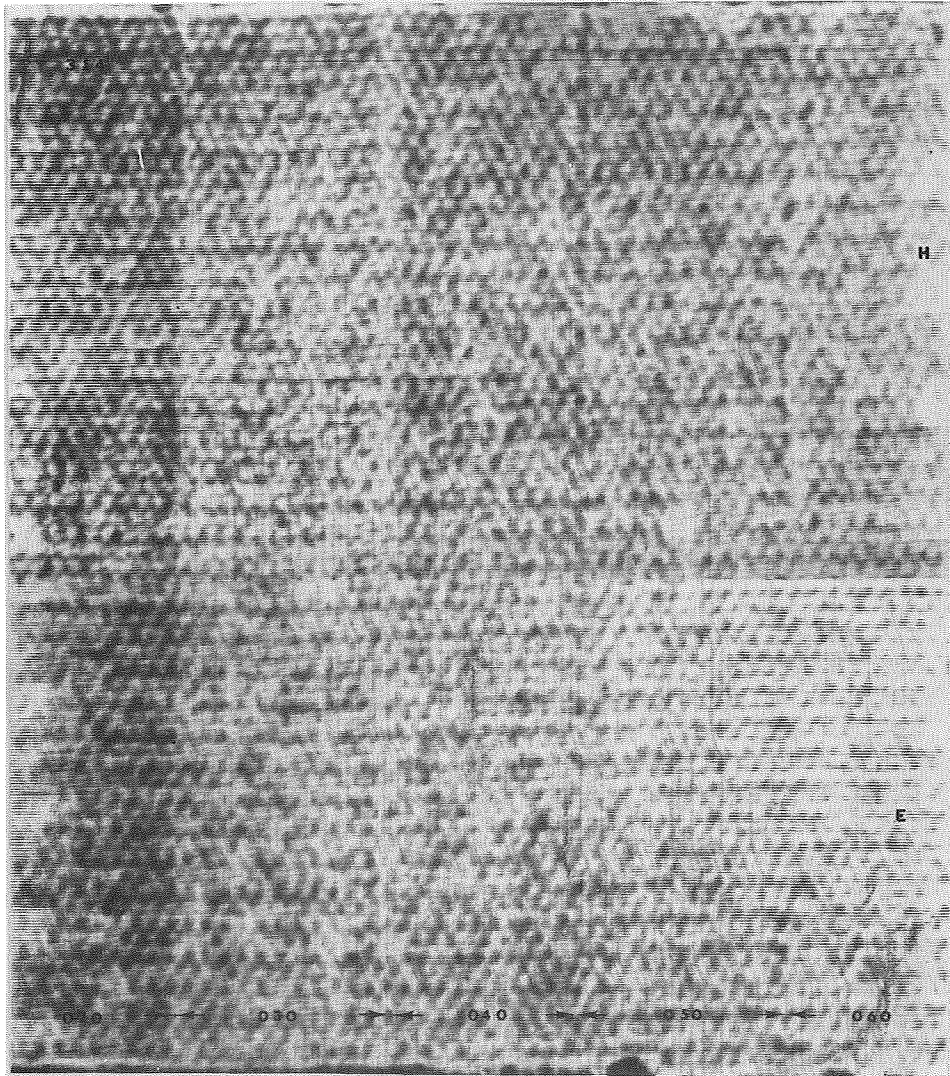


FIGURE 20. ULTRASONIC C-SCAN RECORDING AT 2.25 MHz OF THE 1/2-INCH GRAPHITE/HONEYCOMB PANEL 314

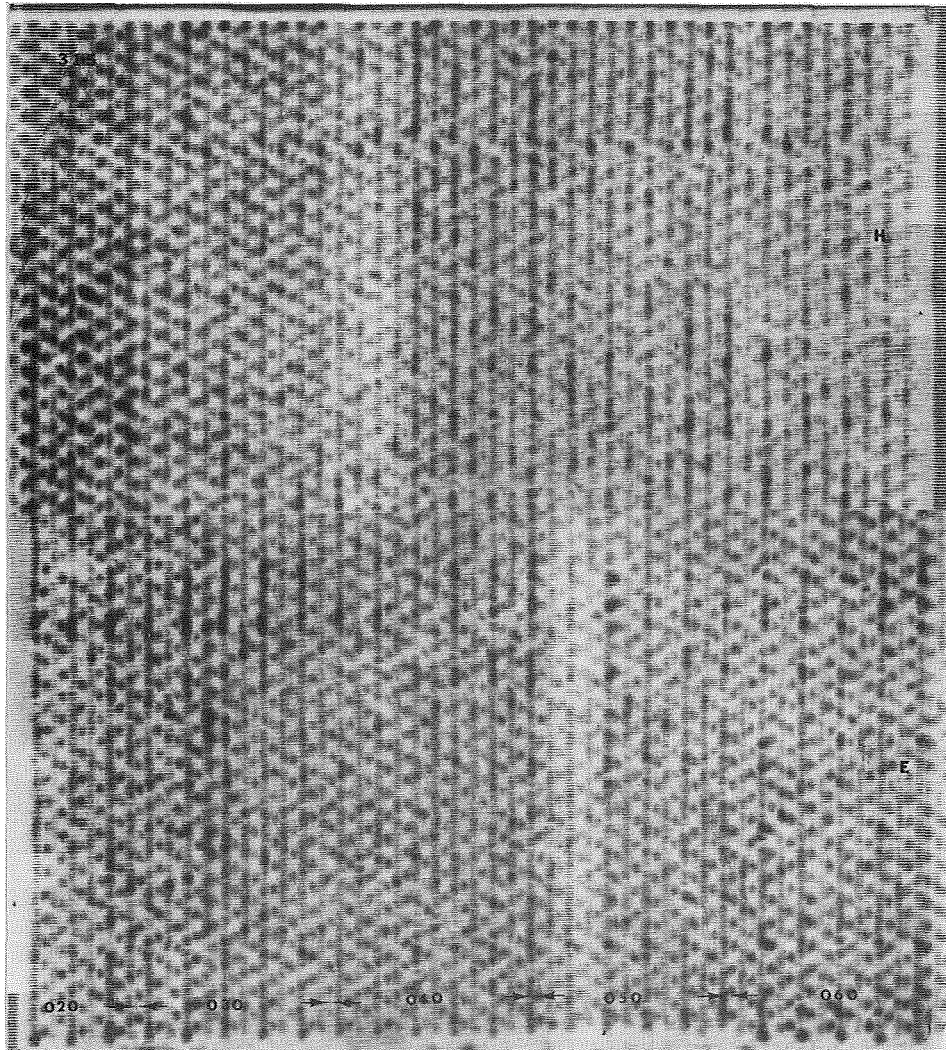


FIGURE 21. ULTRASONIC C-SCAN RECORDING AT 2.25 MHz OF THE 1-INCH GRAPHITE/HONEYCOMB PANEL 315

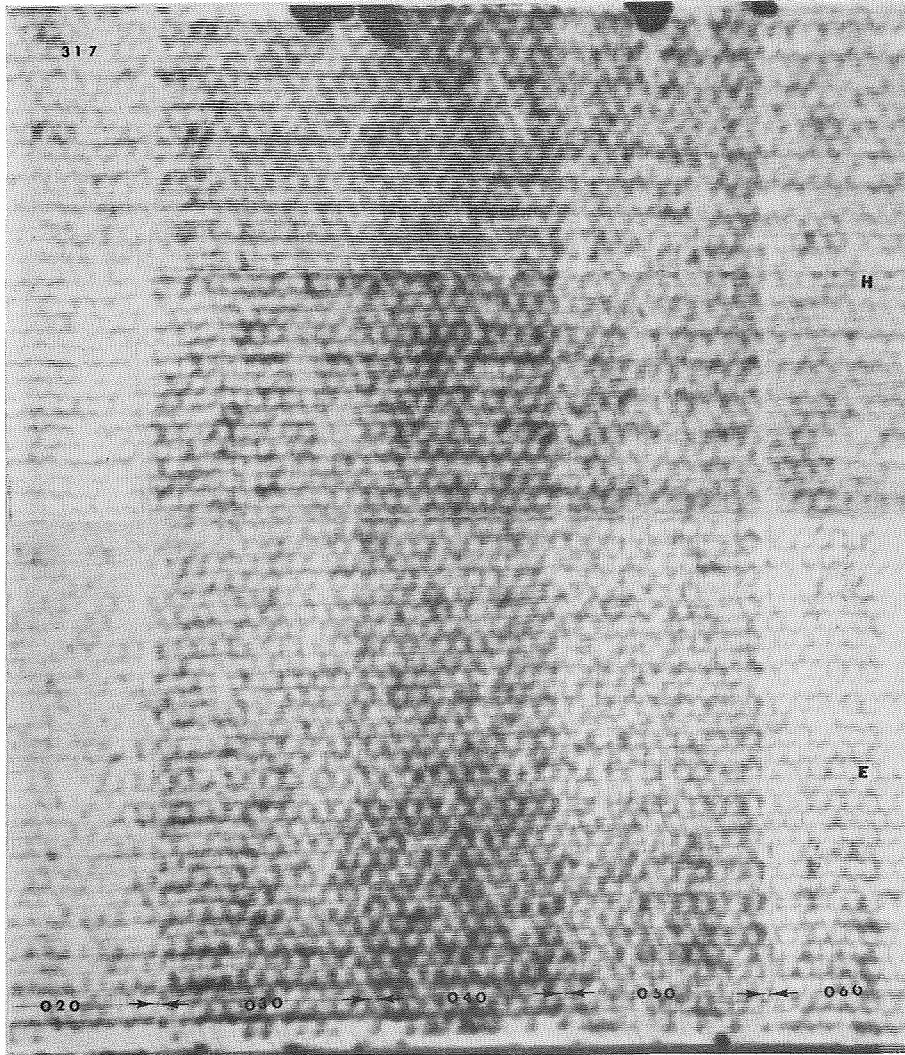


FIGURE 22. ULTRASONIC C-SCAN RECORDING AT 2.25 MHz OF THE 1/2-INCH BORON/HONEYCOMB PANEL 317

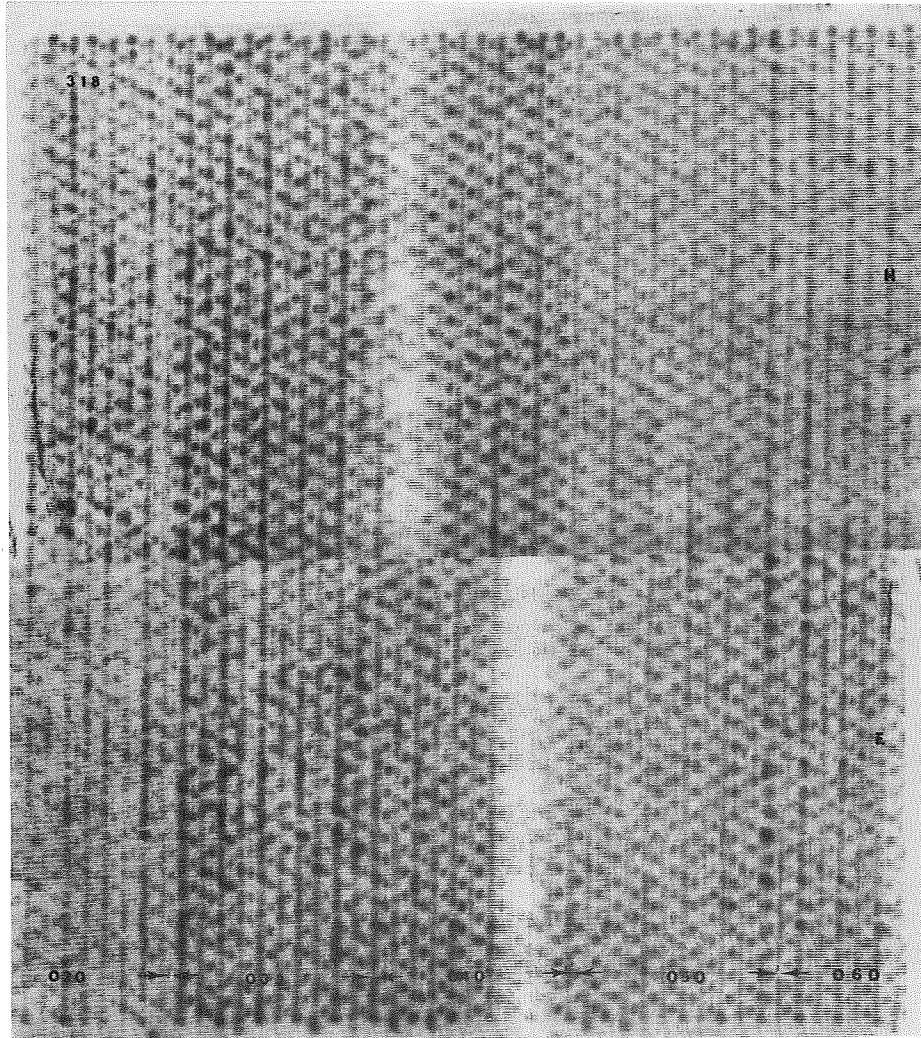


FIGURE 23. ULTRASONIC C-SCAN RECORDING AT 2.25 MHz OF THE 1-INCH BORON/HONEYCOMB PANEL 318

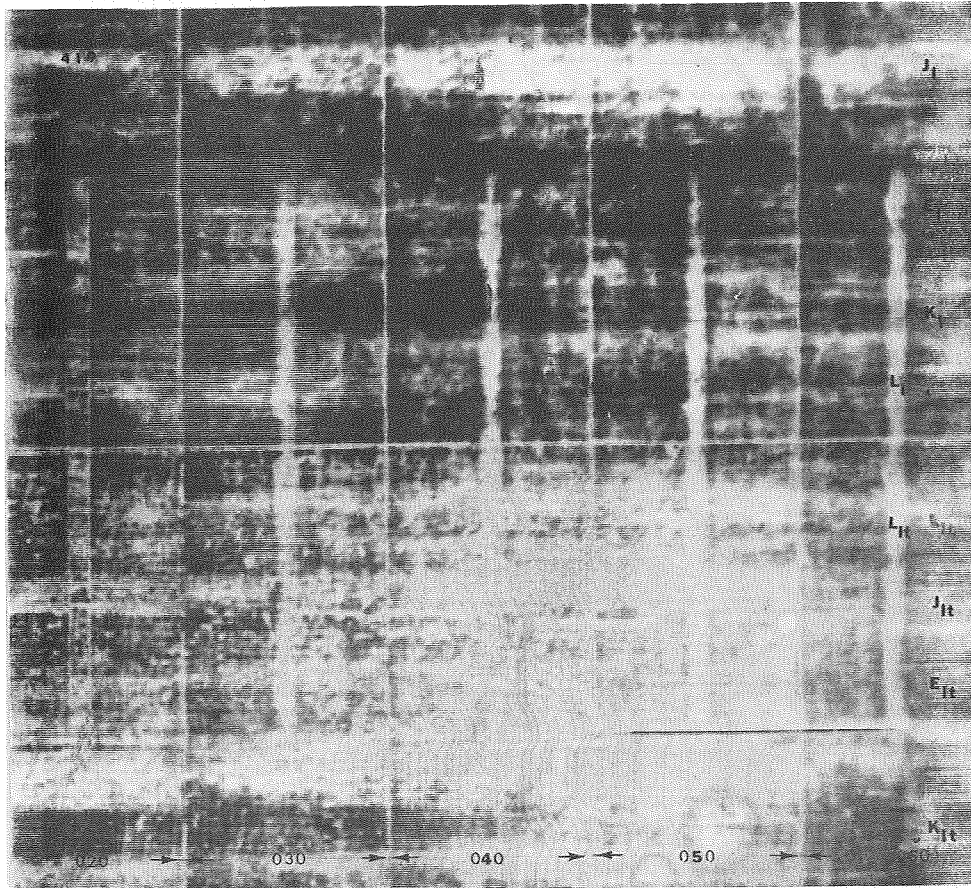


FIGURE 24. ULTRASONIC C-SCAN RECORDING AT 10 mHz OF THE FLAT GRAPHITE PANEL 419 SHOWING THE 1/4-INCH SLOTS (L_I, L_{II}), OVERLAPS (J_I, J_{II}), AND SPACING VOIDS (K_I, K_{II}) IN THE FIBER PLYS

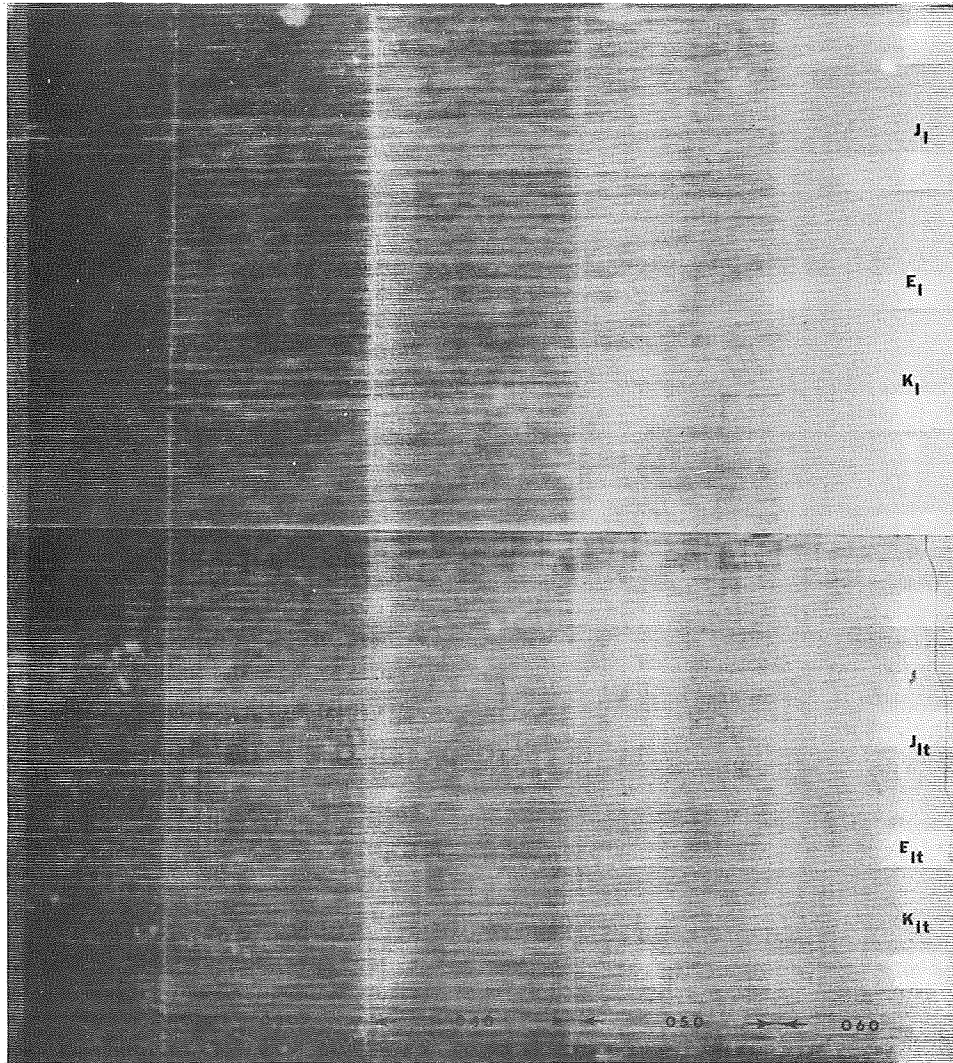


FIGURE 25. ULTRASONIC C-SCAN RECORDING AT 10 MHz OF THE FLAT BORON PANEL 422 SHOWING THE FILAMENT PLY OVERLAPS (J_I, J_{It}) AND SPACING VOIDS (K_I, K_{It})

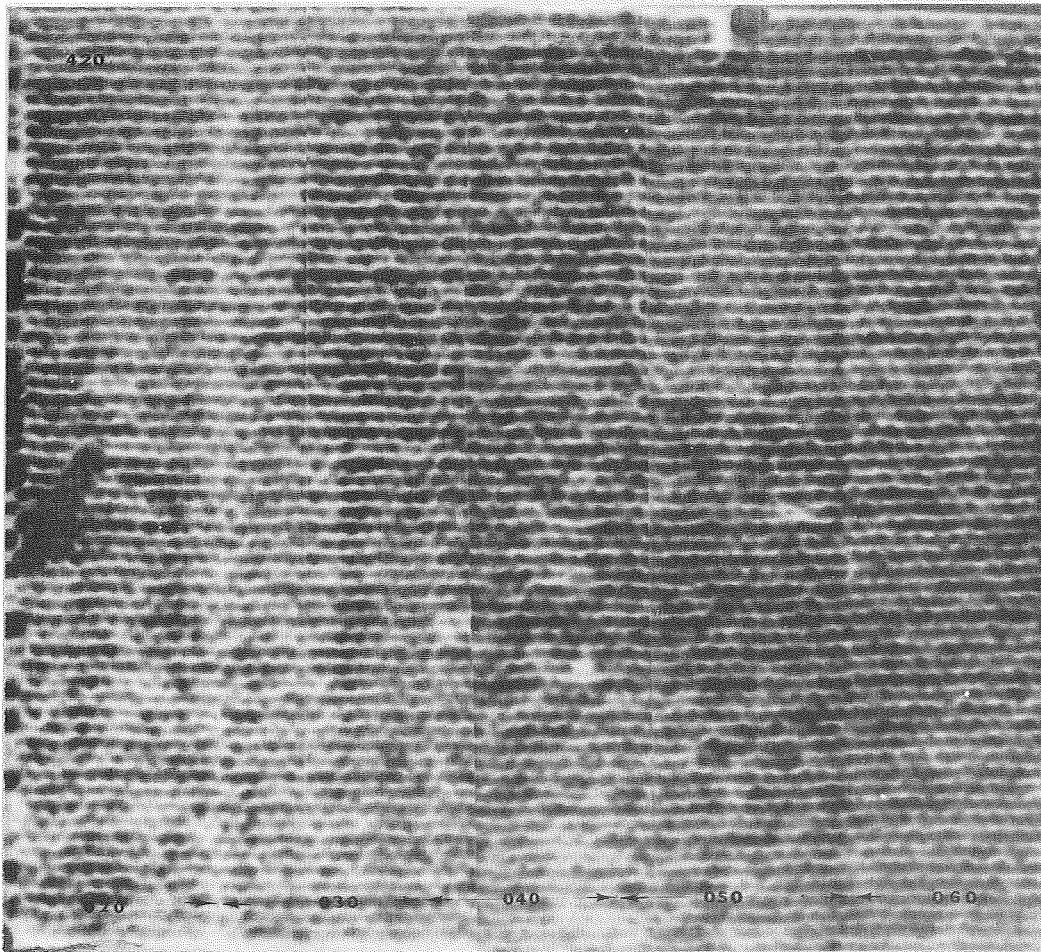


FIGURE 26. ULTRASONIC C-SCAN RECORDING AT 2.25 MHz OF THE 1/2-INCH GRAPHITE/HONEYCOMB PANEL 420

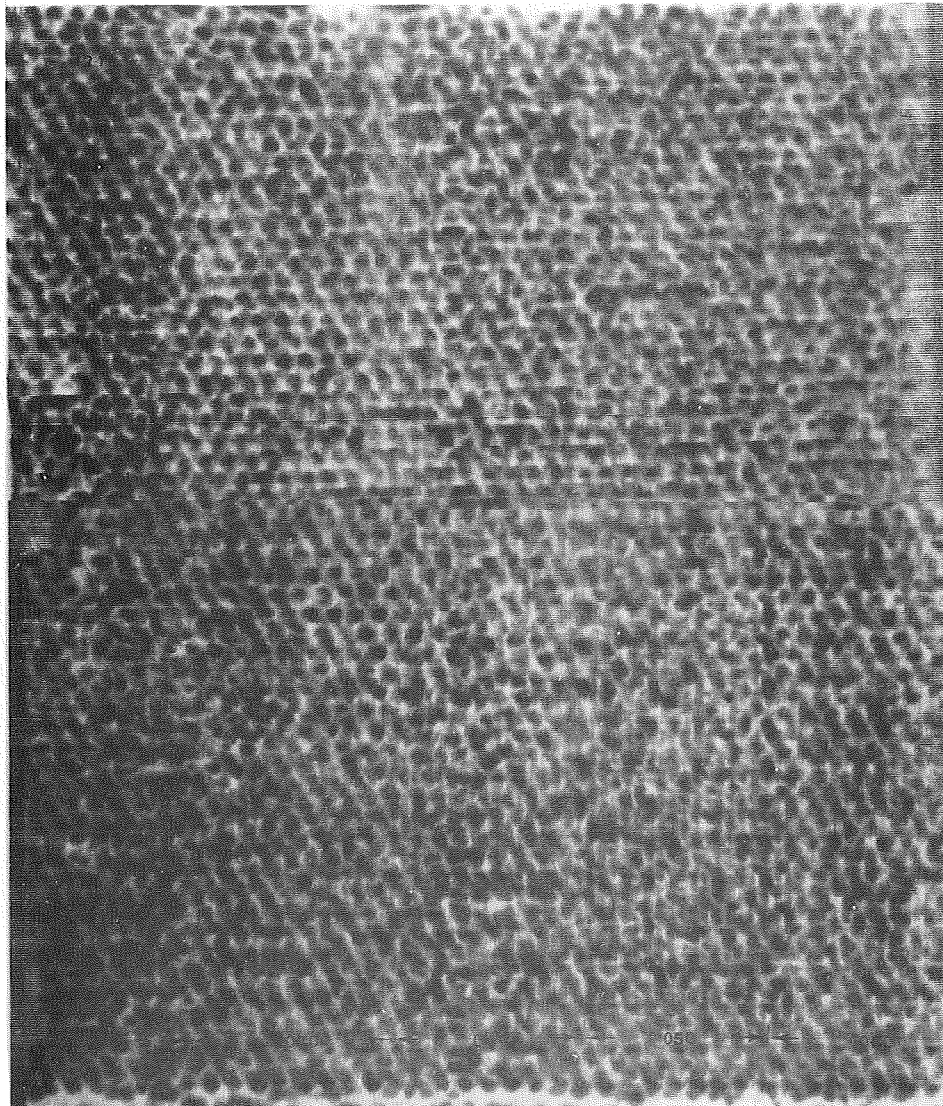


FIGURE 27. ULTRASONIC C-SCAN RECORDING AT 2.25 MHz OF THE 1-INCH GRAPHITE/HONEYCOMB PANEL 421

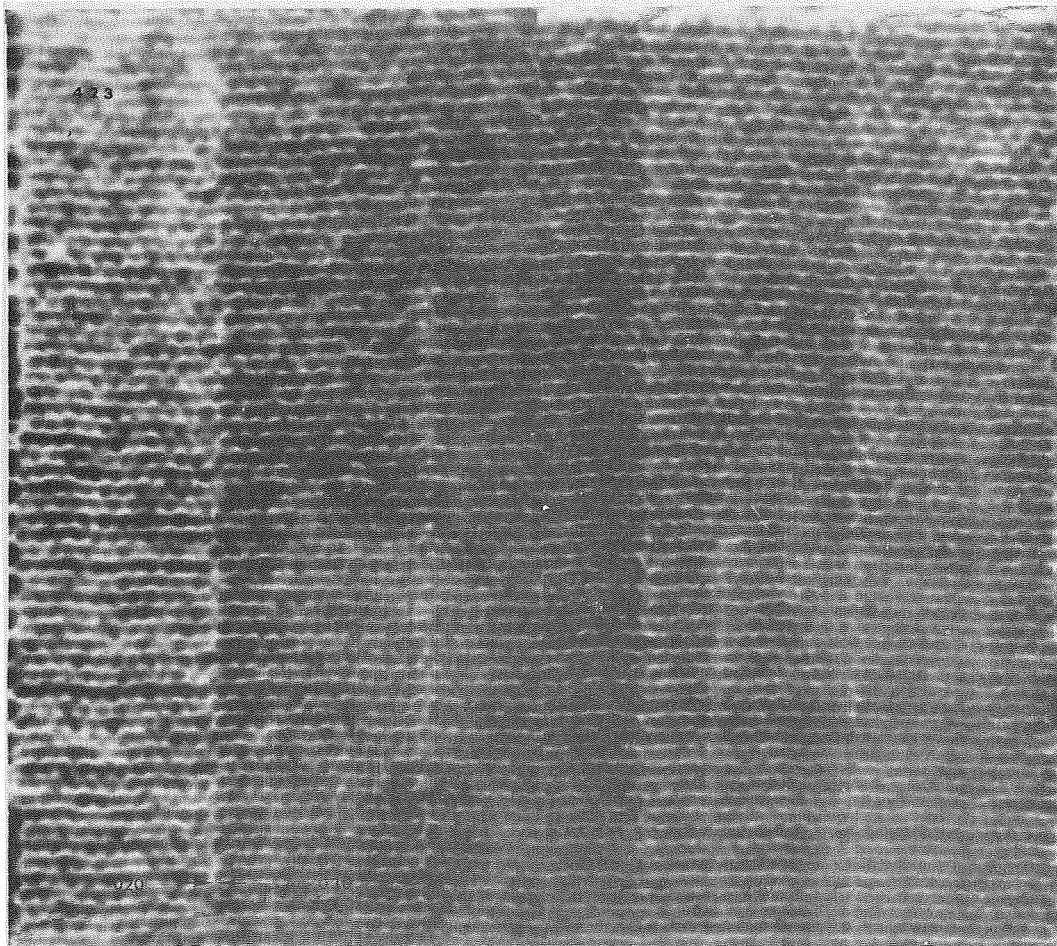


FIGURE 28. ULTRASONIC C-SCAN RECORDING AT 2.25 MHz OF THE 1/2-INCH BORON/HONEYCOMB PANEL 423

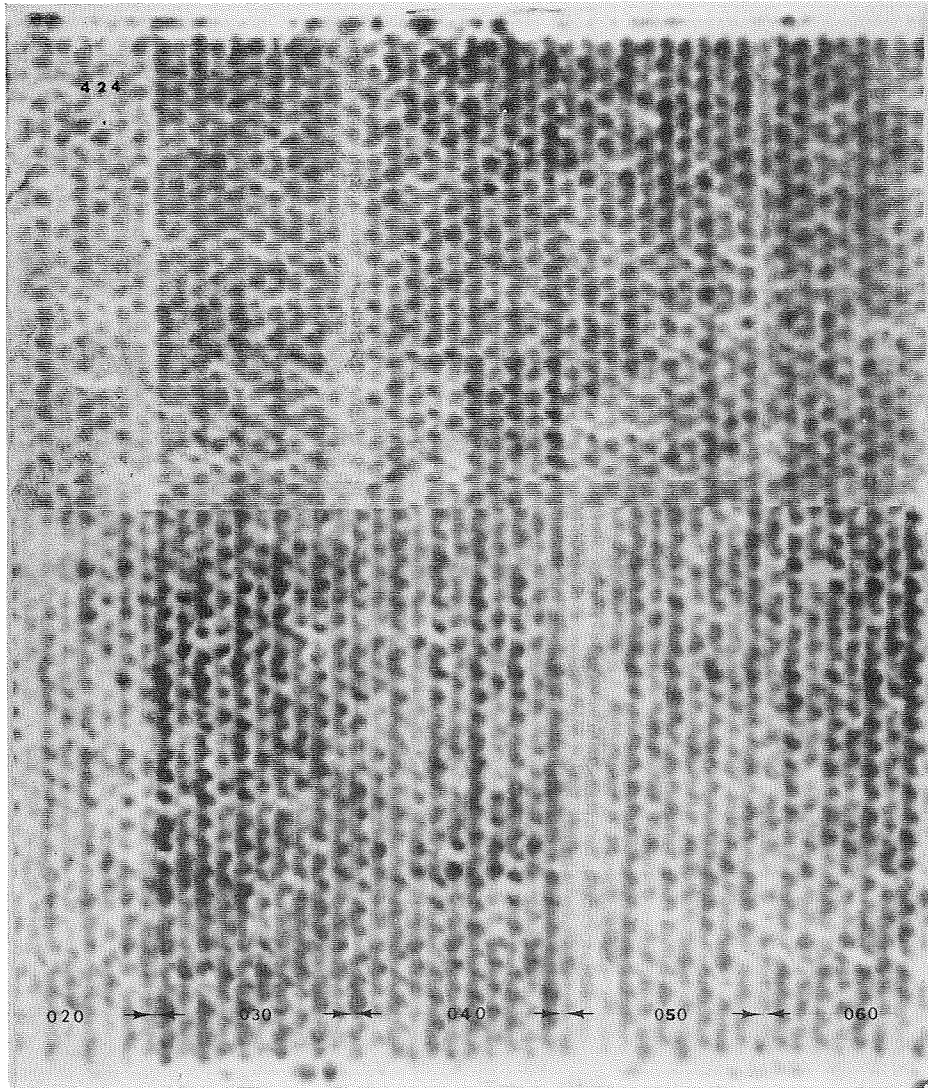


FIGURE 29. ULTRASONIC C-SCAN RECORDING AT 2.25 MHz OF THE 1-INCH BORON/HONEYCOMB PANEL 424

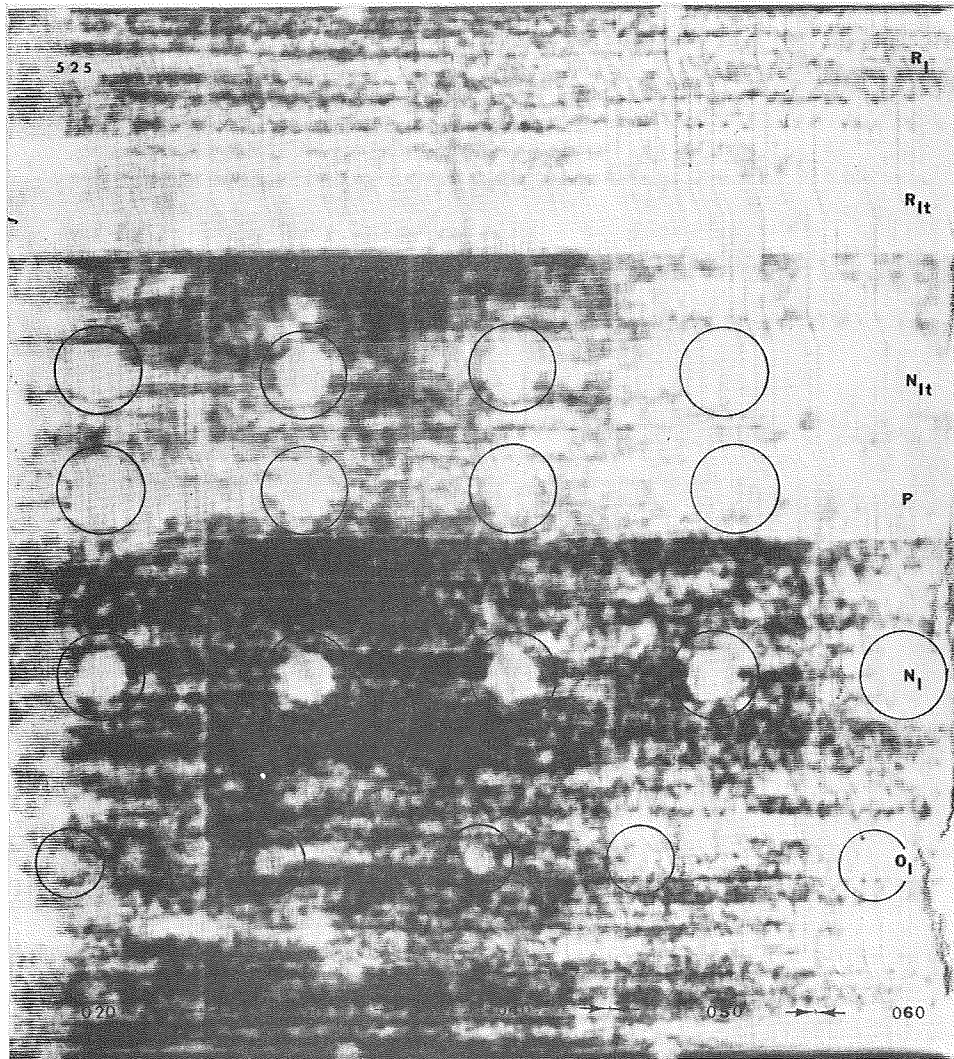


FIGURE 30. ULTRASONIC C-SCAN RECORDING AT 10 mHz OF THE FLAT GRAPHITE PANEL 525, THE SIMULATED INTERLAMINAR (O_I, N_I, N_{It}) AND ADHESIVE DISBONDS (P), AND THE GENERAL DISBOND DUE TO MATERIAL PRE-AGED 60 DAYS (R_I, R_{It})

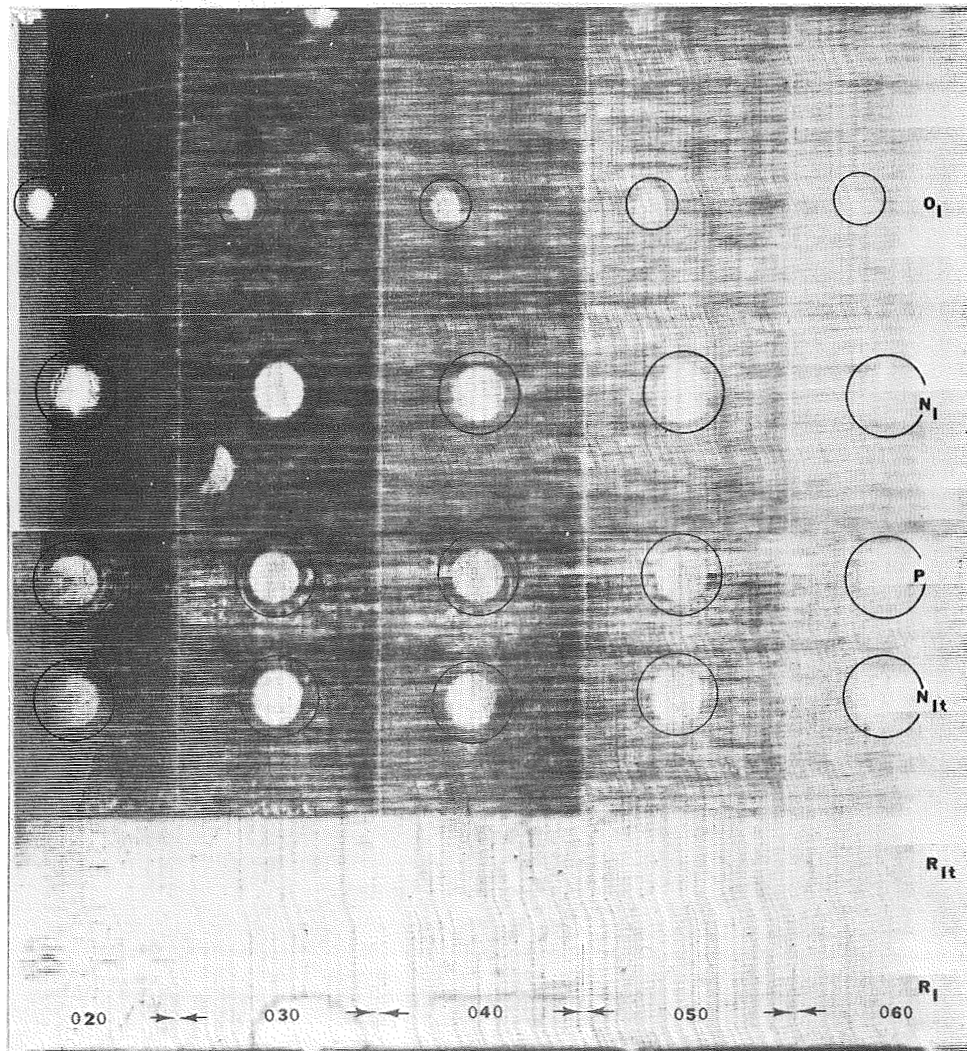


FIGURE 31. ULTRASONIC C-SCAN RECORDING AT 10 MHz OF THE FLAT BORON PANEL 526 SHOWING THE SIMULATED INTERLAMINAR (O_I, N_I, N_{It}) AND ADHESIVE (P) DISBONDS AND THE GENERAL DISBOND AREA PRODUCED BY USE OF MATERIAL PRE-AGED 60 DAYS (R_I, R_{It})

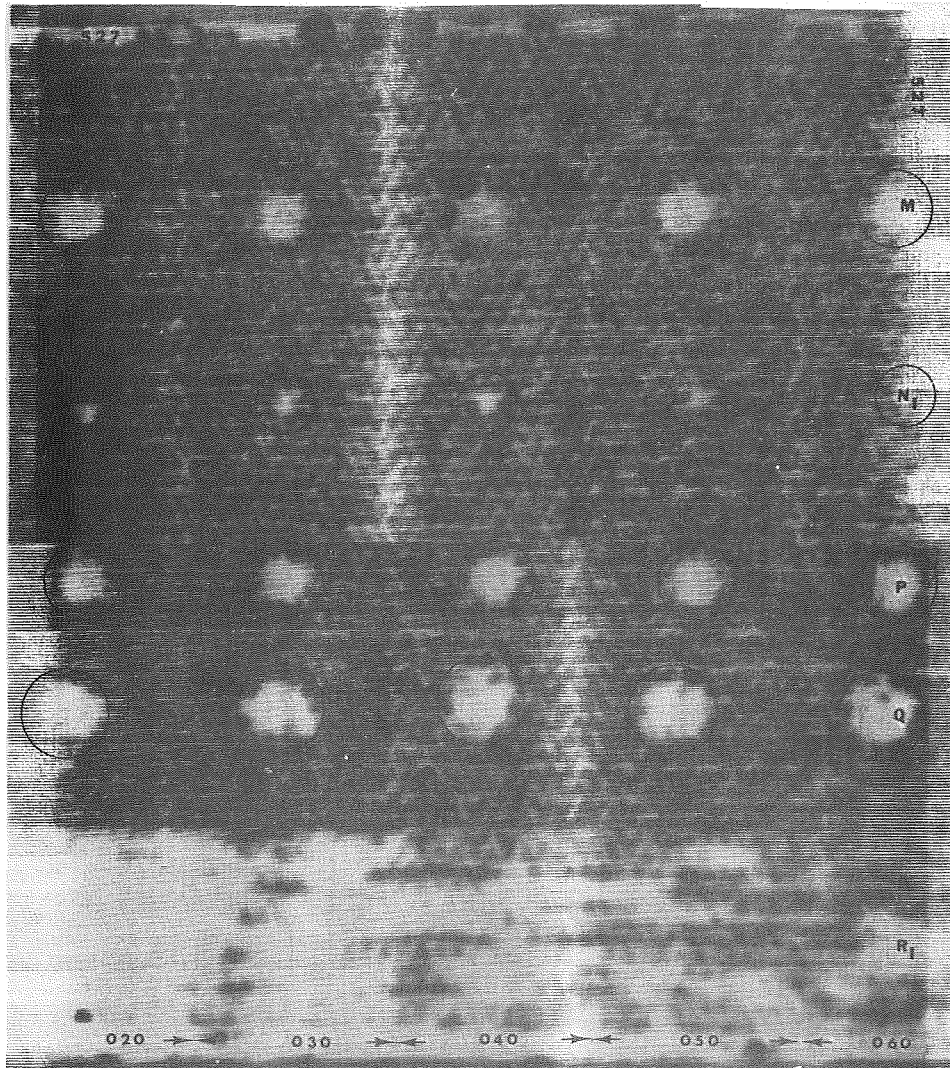


FIGURE 32. ULTRASONIC C-SCAN RECORDING AT 2.25 MHz OF THE 1/2-INCH GRAPHITE/HONEYCOMB PANEL 527 (#2) SHOWING ALL THE INTENDED DEFECTS AS WELL AS MANY UNINTENTIONAL DISBONDS

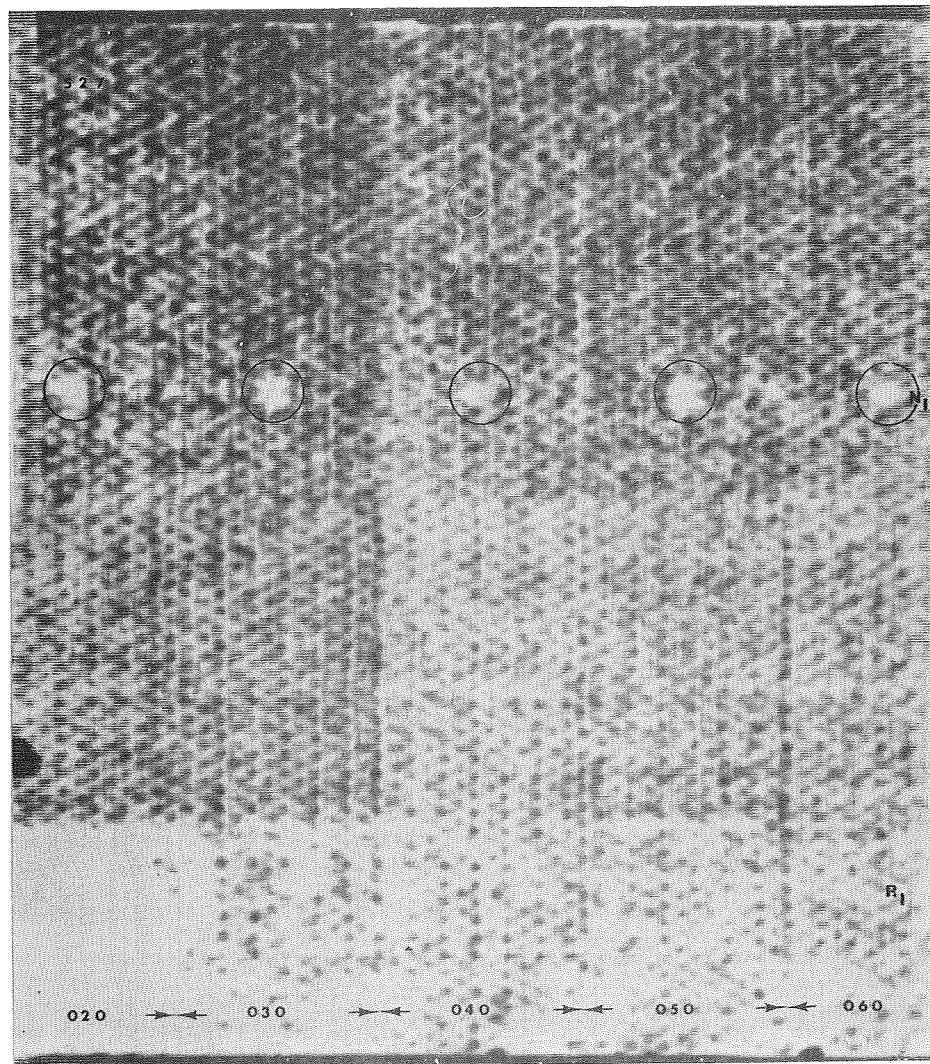


FIGURE 33. ULTRASONIC C-SCAN RECORDING AT 2.25 MHz OF THE 1/2-INCH GRAPHITE/HONEYCOMB PANEL 527 (#1) SHOWING ON THE 1/4-INCH INTERLAMINAR DISBONDS (N_1) AND THE PREAGED AREA (R_1)

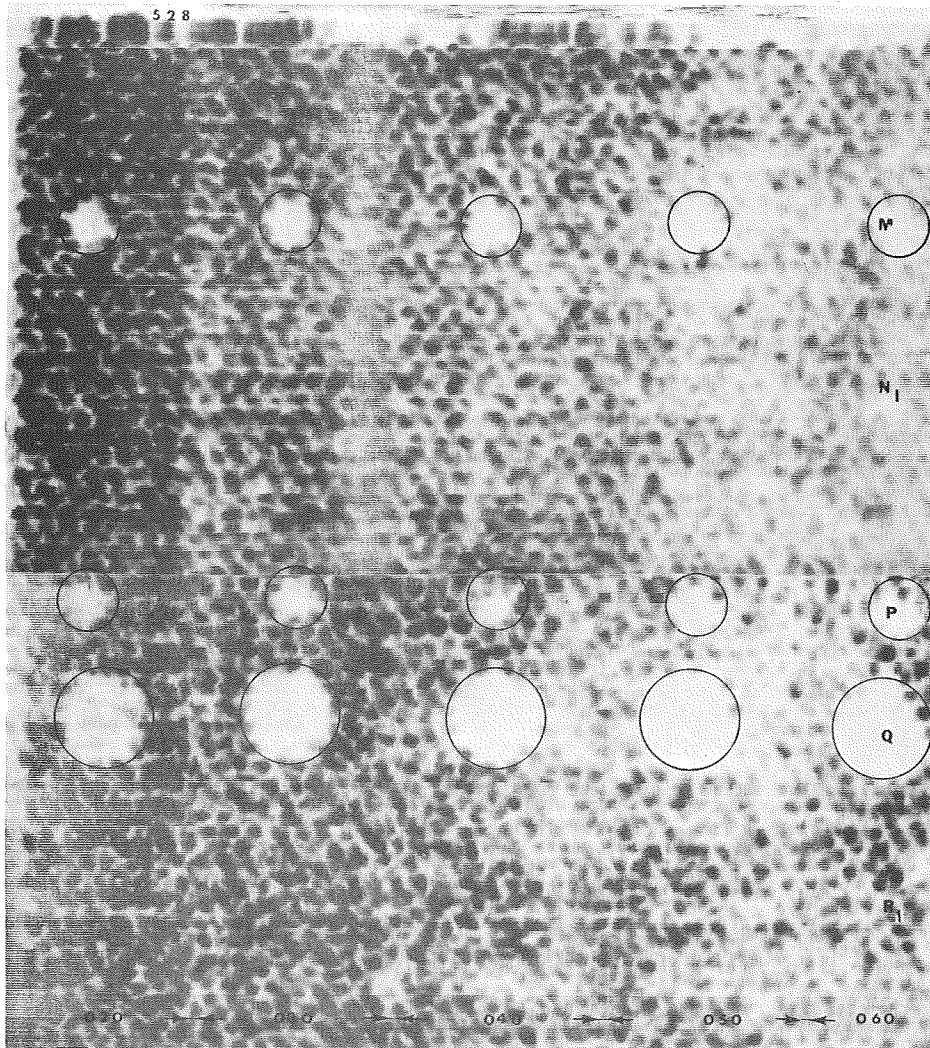


FIGURE 34. ULTRASONIC C-SCAN RECORDING AT 2.25 MHz OF THE 1-INCH GRAPHITE/HONEYCOMB PANEL 528 SHOWING THE INTER-LAMINAR (N₁), FAR-SIDE (M) AND NEAR-SIDE (P) ADHESIVE DISBONDS, AND THE CRUSHED CORE (Q)

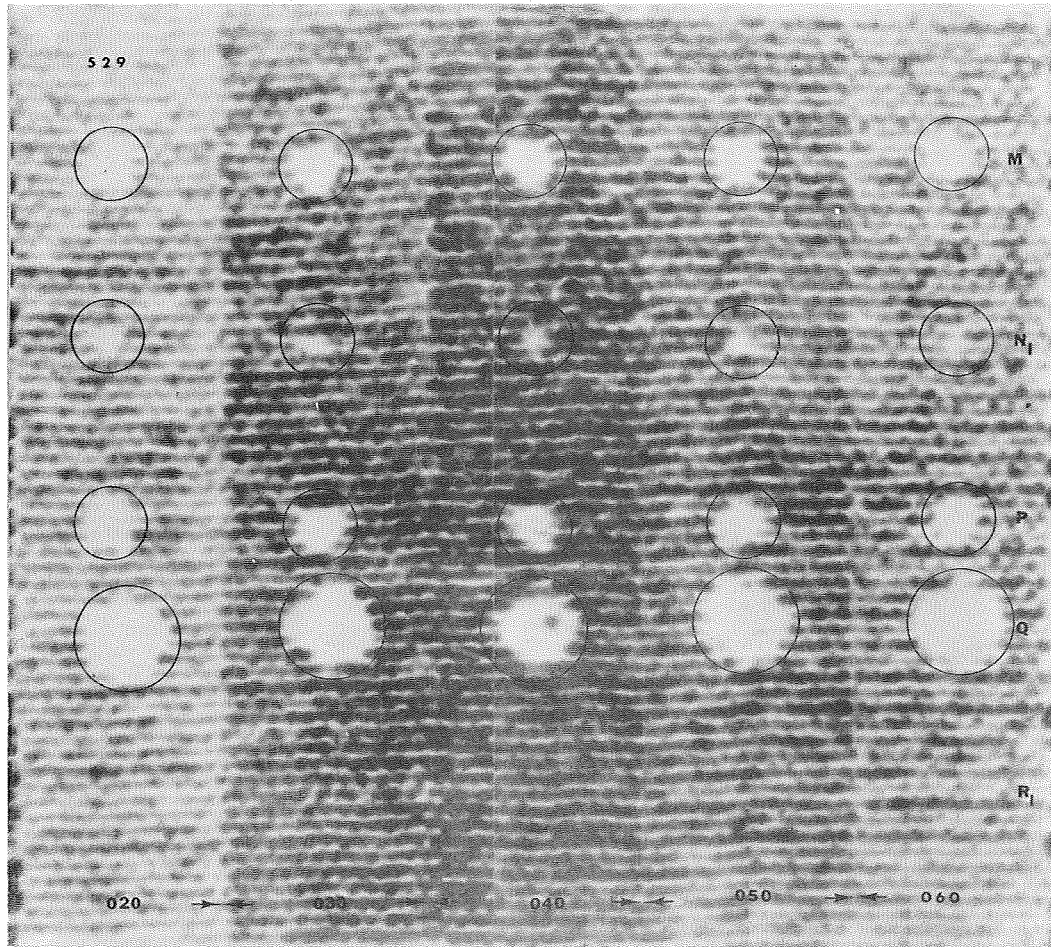


FIGURE 35. ULTRASONIC C-SCAN RECORDING AT 2.25 MHz OF THE 1/2-INCH BORON/HONEYCOMB PANEL 529 SHOWING THE INTERLAMINAR (N_f), FAR-SIDE (M) AND NEAR-SIDE (P) DISBONDS AND THE CRUSHED CORE (Q)

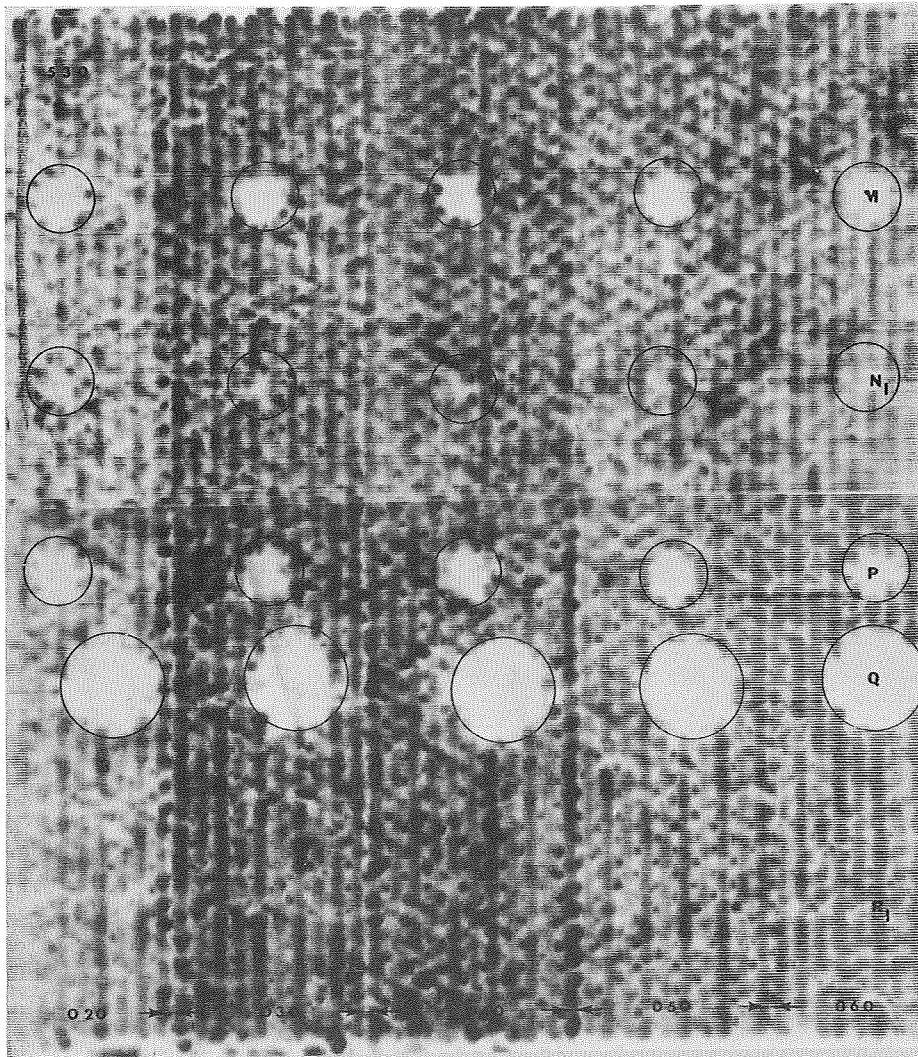


FIGURE 36. ULTRASONIC C-SCAN RECORDING AT 2.25 MHz OF THE 1-INCH BORON/HONEYCOMB PANEL 530 SHOWING THE INTERLAMINAR (N_1), FAR-SIDE (M) AND NEAR-SIDE (P) DISBONDS AND THE CRUSHED CORE (Q)

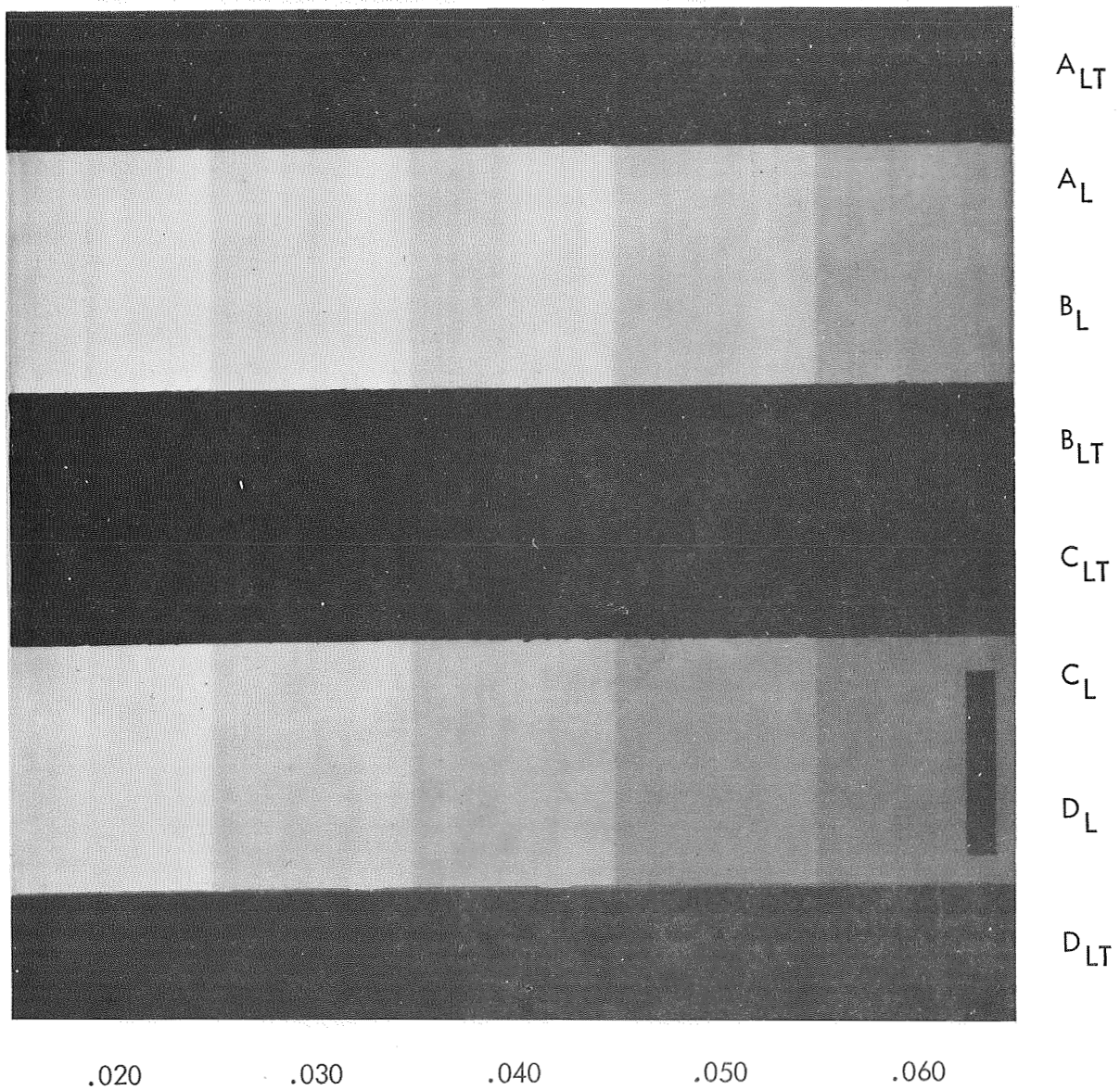


FIGURE 37. RADIOGRAPHIC PRINT OF THE FLAT GRAPHITE PANEL 101 (POROSITY AND RESIN VARIATIONS NOT DISCERNIBLE)

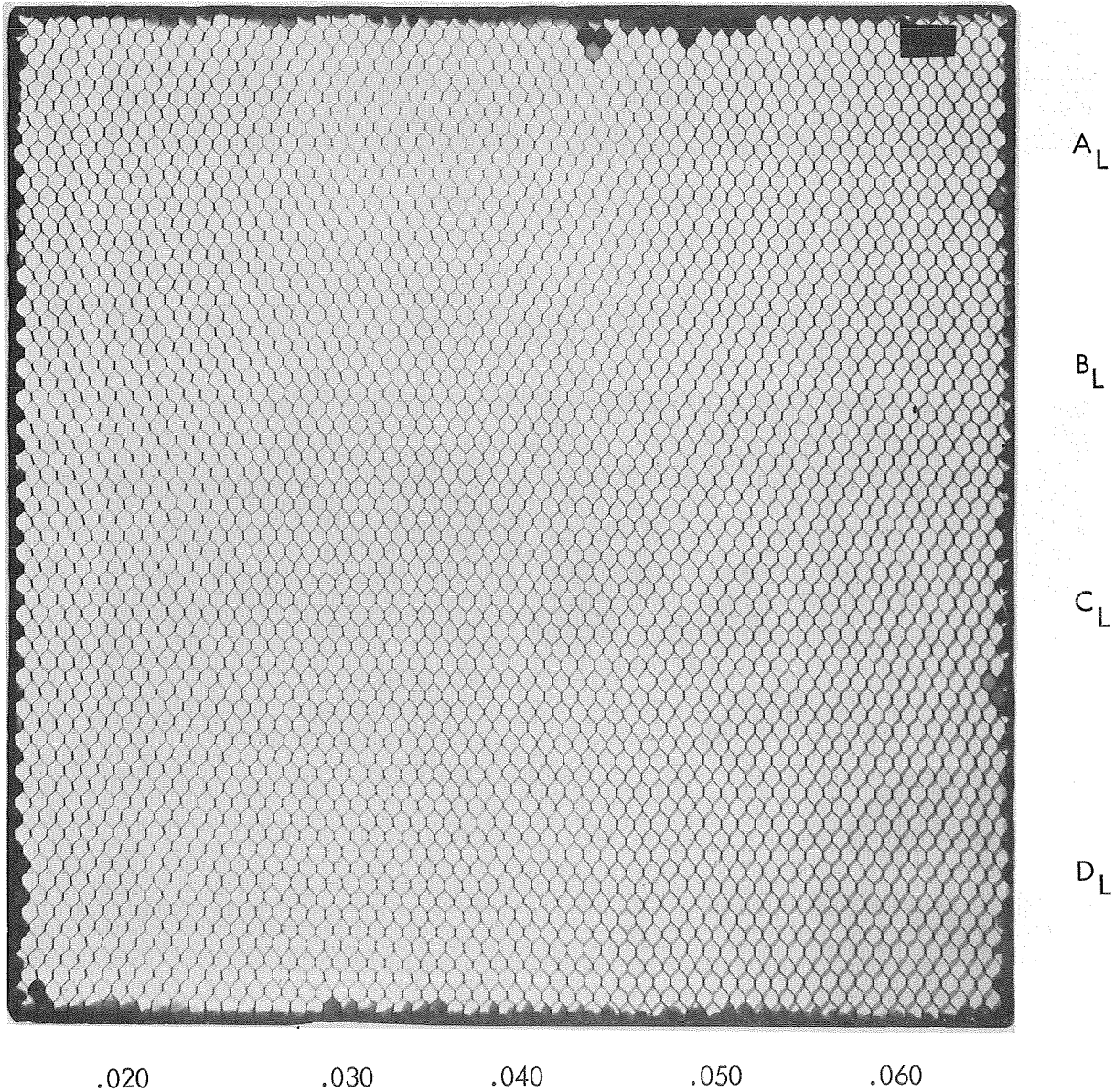


FIGURE 38. RADIOGRAPHIC PRINT OF THE 1/2-INCH GRAPHITE/HONEYCOMB PANEL 102 (POROSITY AND RESIN VARIATIONS NOT DISCERNIBLE)

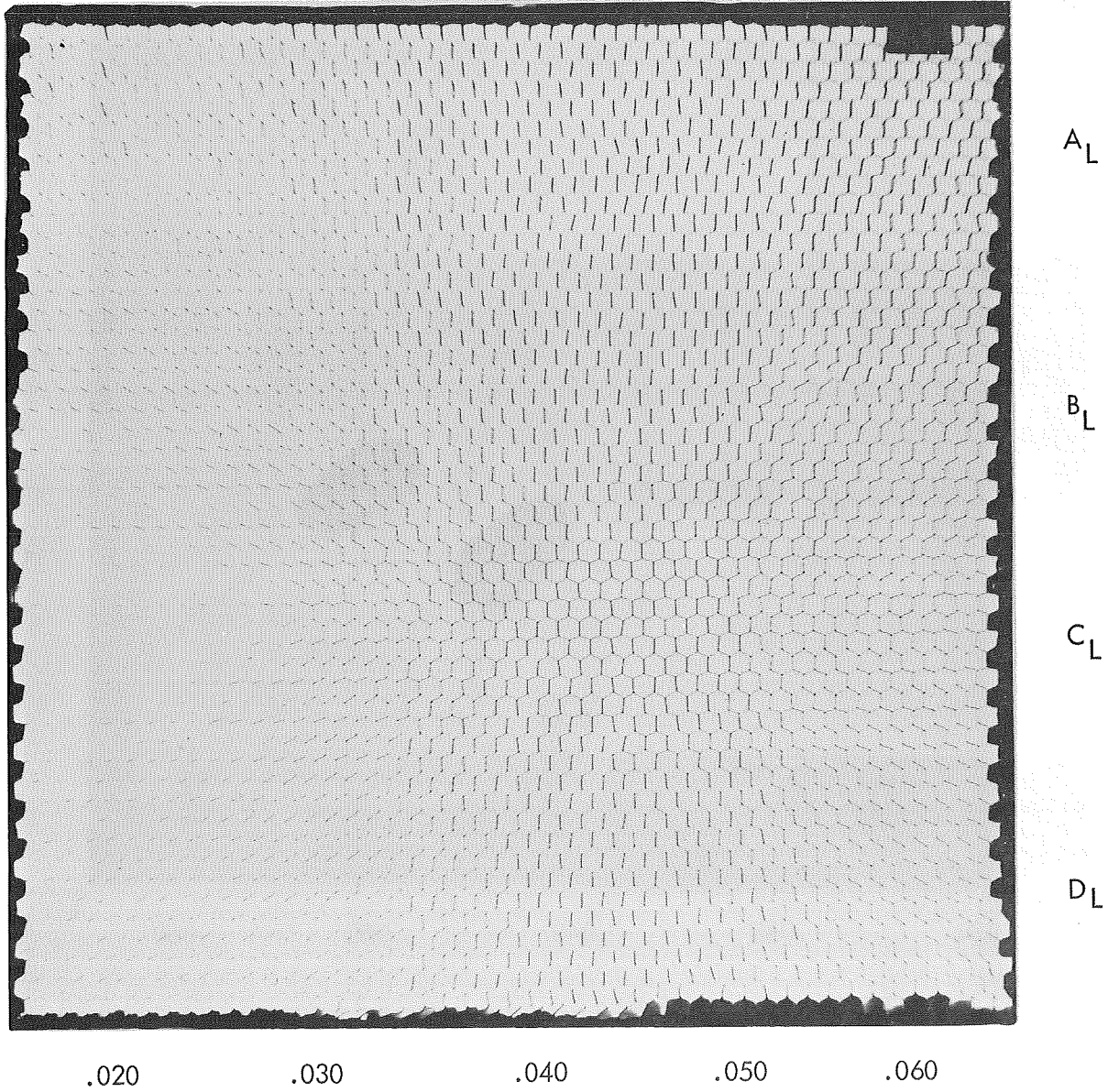


FIGURE 39. RADIOGRAPHIC PRINT OF THE 1-INCH GRAPHITE/HONEYCOMB PANEL 103 (POROSITY AND RESIN VARIATIONS NOT DISCERNIBLE)

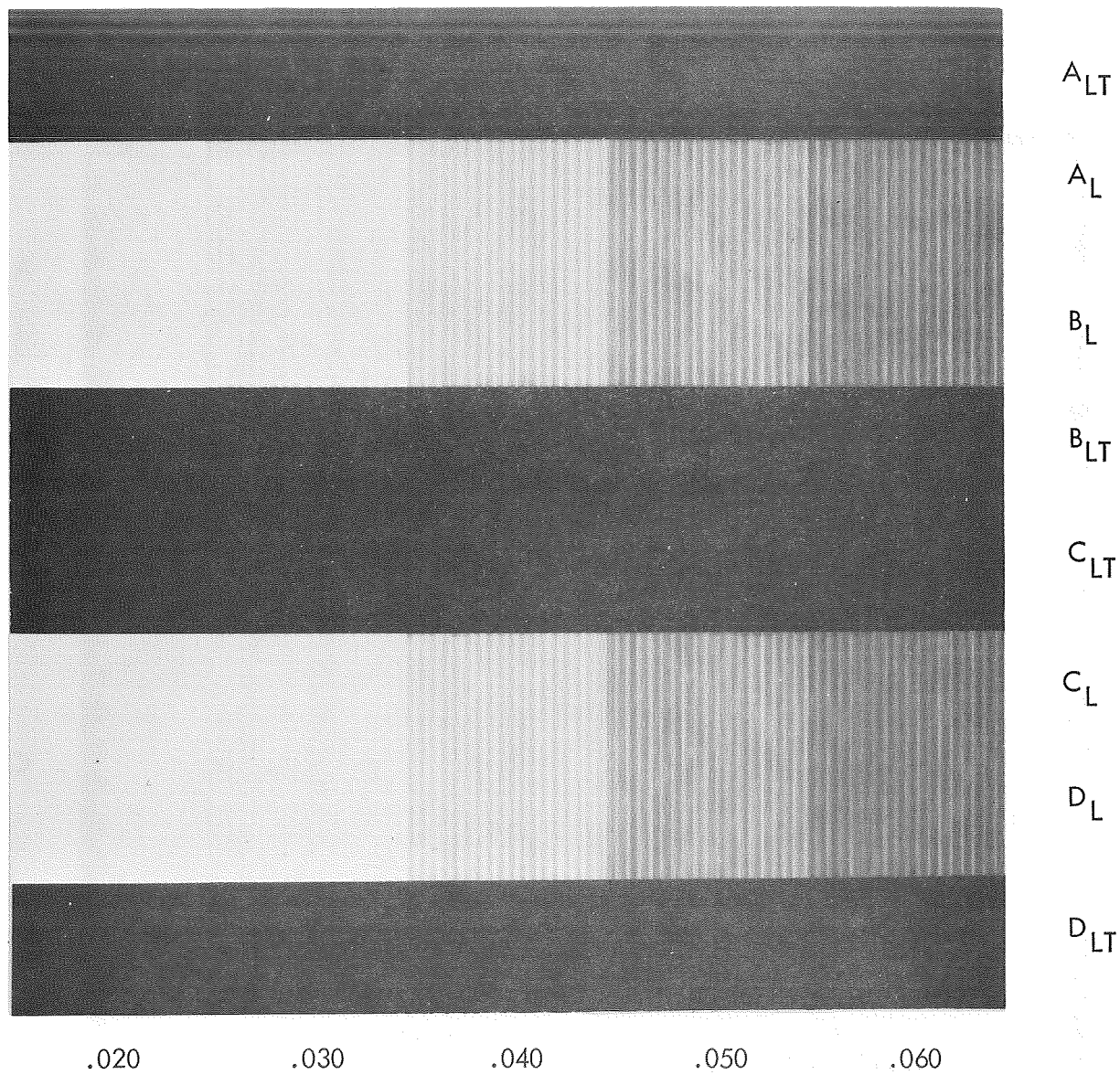


FIGURE 40. RADIOGRAPHIC PRINT OF THE FLAT BORON PANEL 104 (POROSITY AND RESIN VARIATIONS NOT DISCERNIBLE)

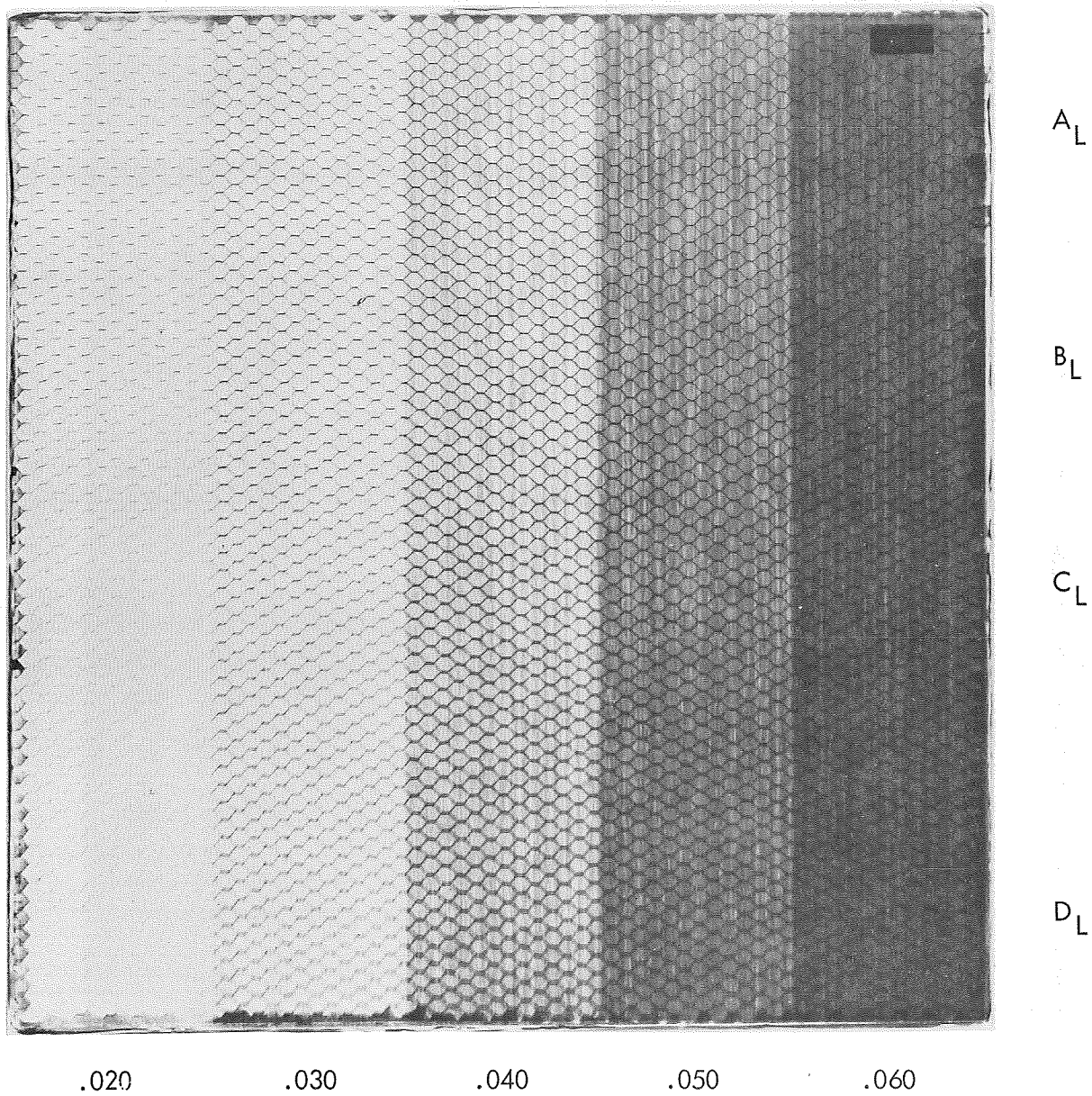


FIGURE 41. RADIOGRAPHIC PRINT OF THE 1/2-INCH BORON/HONEYCOMB PANEL 105 (POROSITY AND RESIN VARIATIONS NOT DISCERNIBLE)

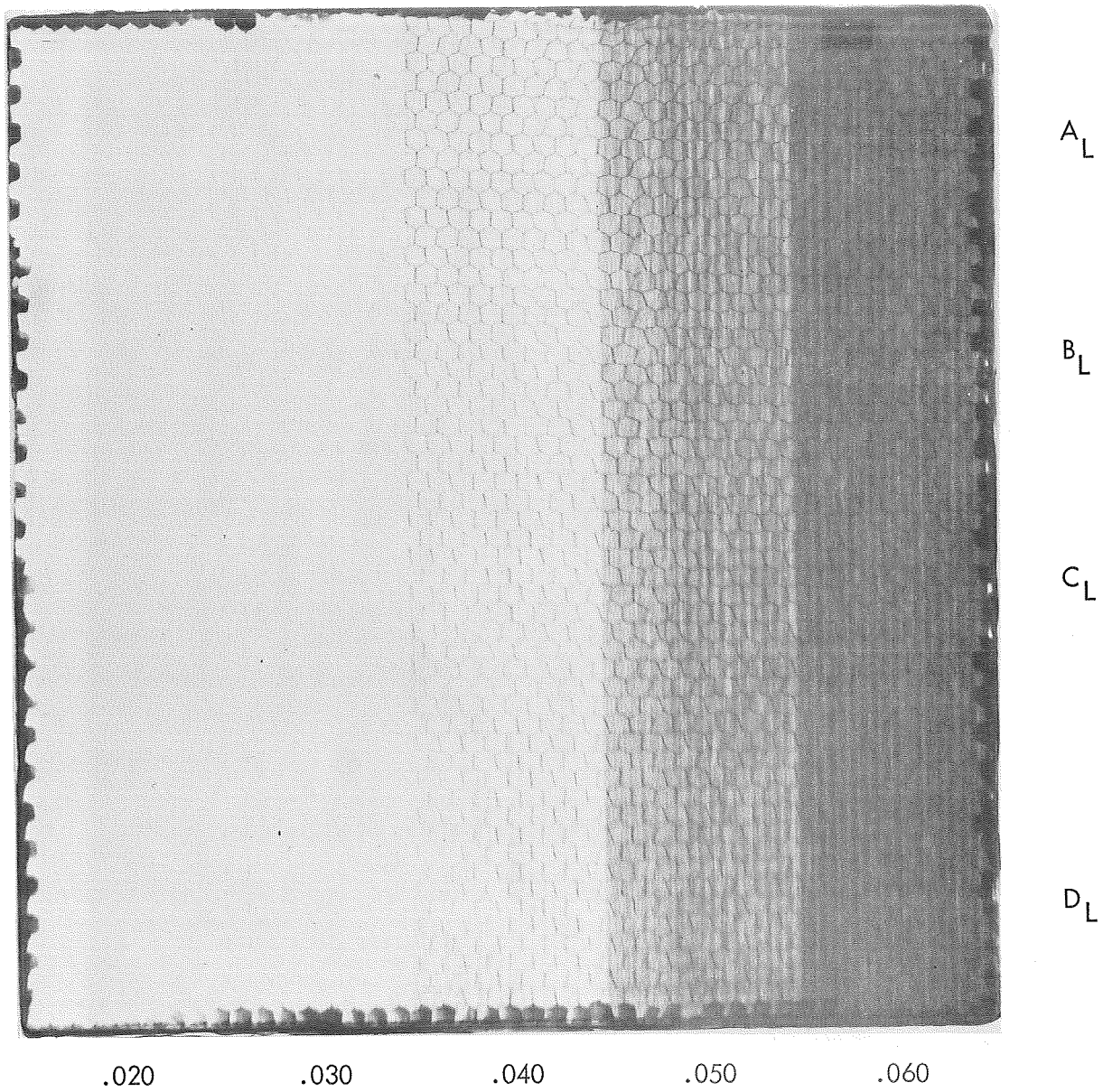


FIGURE 42. RADIOGRAPHIC PRINT OF THE 1-INCH BORON/HONEYCOMB PANEL 106 (POROSITY AND RESIN VARIATIONS NOT DISCERNIBLE)

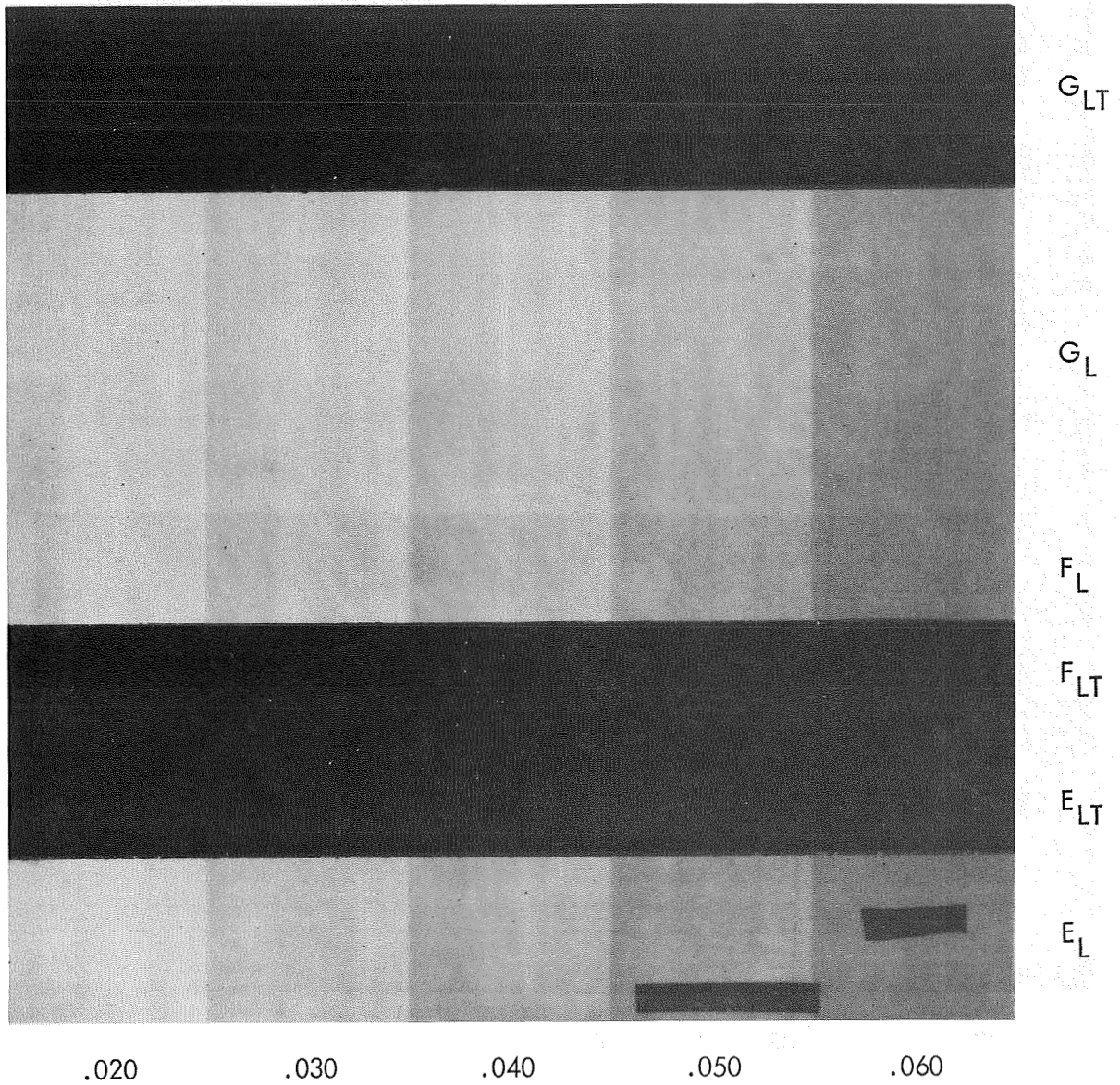


FIGURE 43. RADIOGRAPHIC PRINT OF THE FLAT GRAPHITE PANEL 207 (SHOWING THE BACKING INCLUSION (F_L))

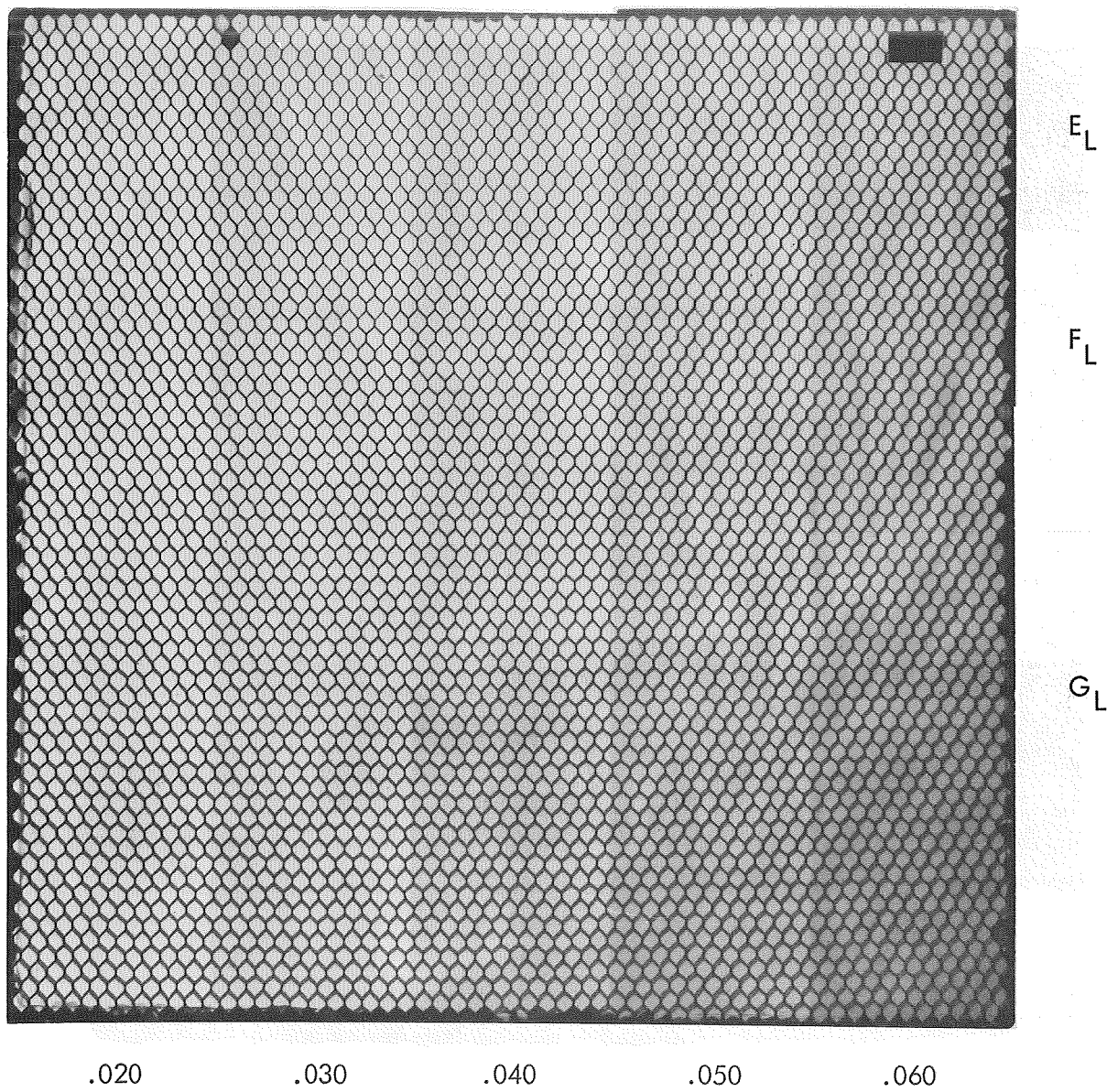


FIGURE 44. RADIOGRAPHIC PRINT OF THE 1/2-INCH GRAPHITE/HONEYCOMB PANEL 208. BACKING INCLUSION (F_L) AND UNDERCURE (G_L) ARE NOT DISCERNIBLE.

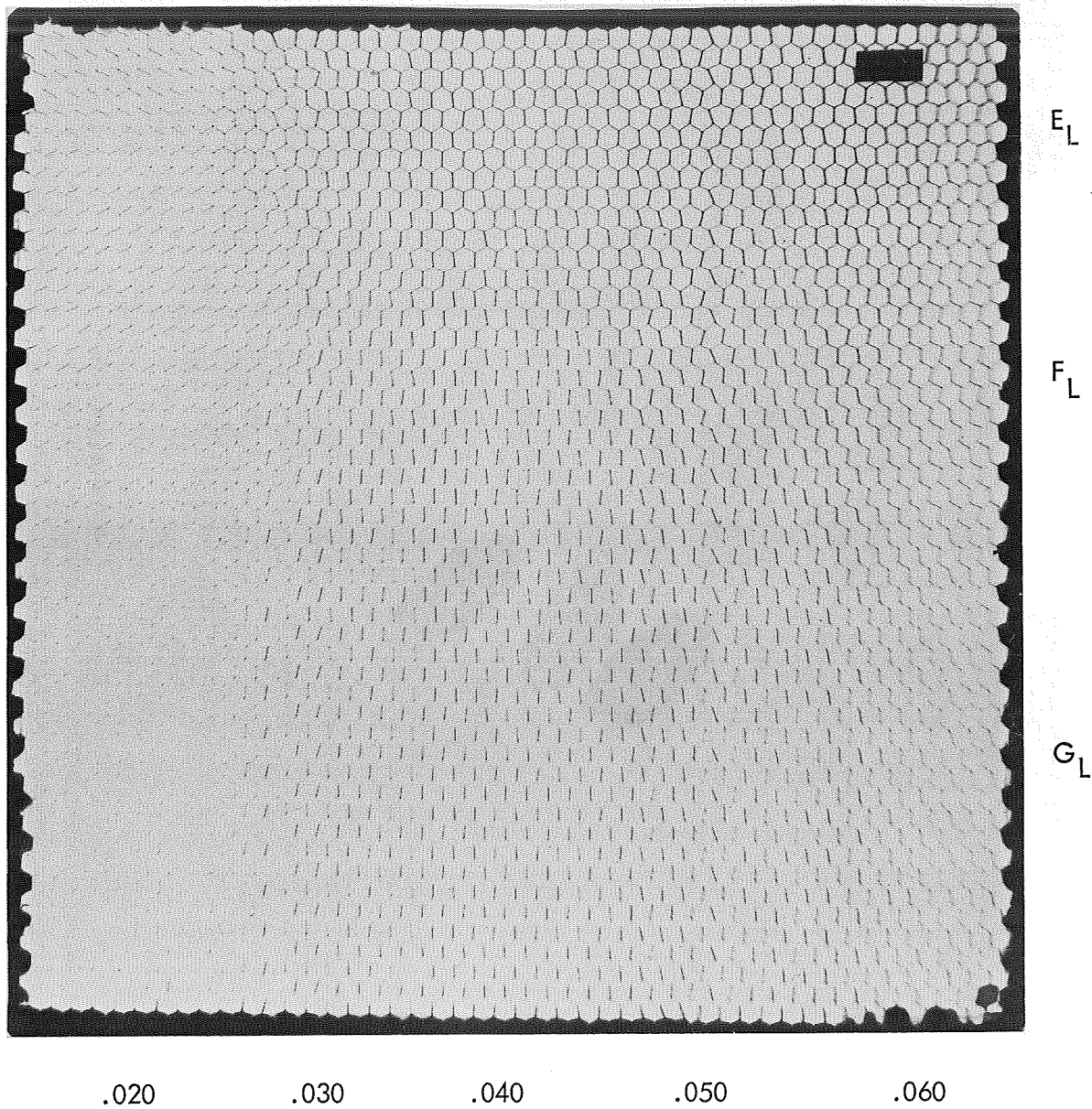


FIGURE 45. RADIOGRAPHIC PRINT OF THE 1-INCH GRAPHITE/HONEYCOMB PANEL 209. BACKING INCLUSION (F_L) AND UNDERCURE (G_L) ARE NOT DISCERNIBLE.

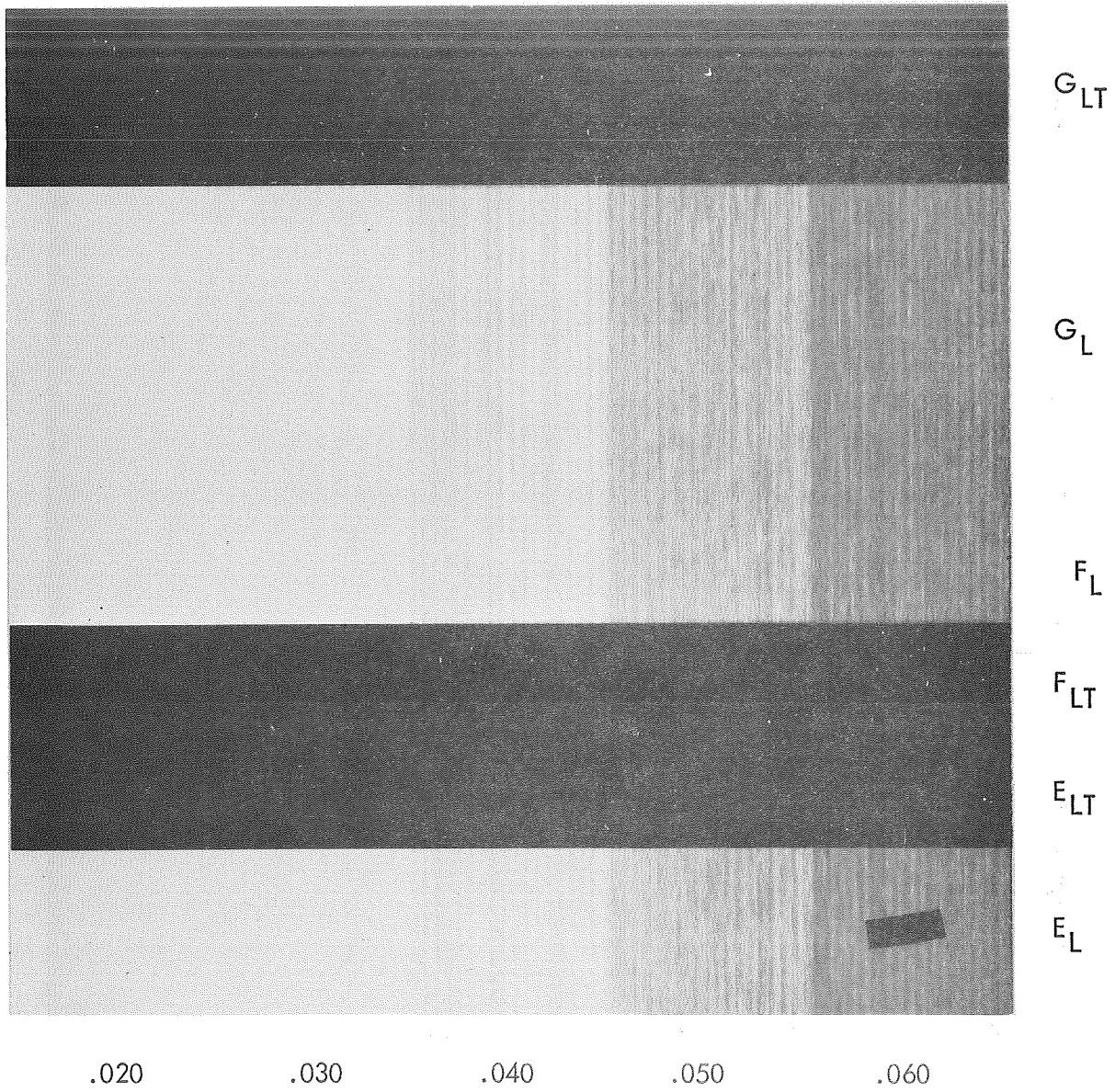


FIGURE 46. RADIOGRAPHIC PRINT OF THE FLAT BORON PANEL 210. BACKING INCLUSION (F_L) AND UNDERCURE (G_L) ARE NOT DISCERNIBLE.

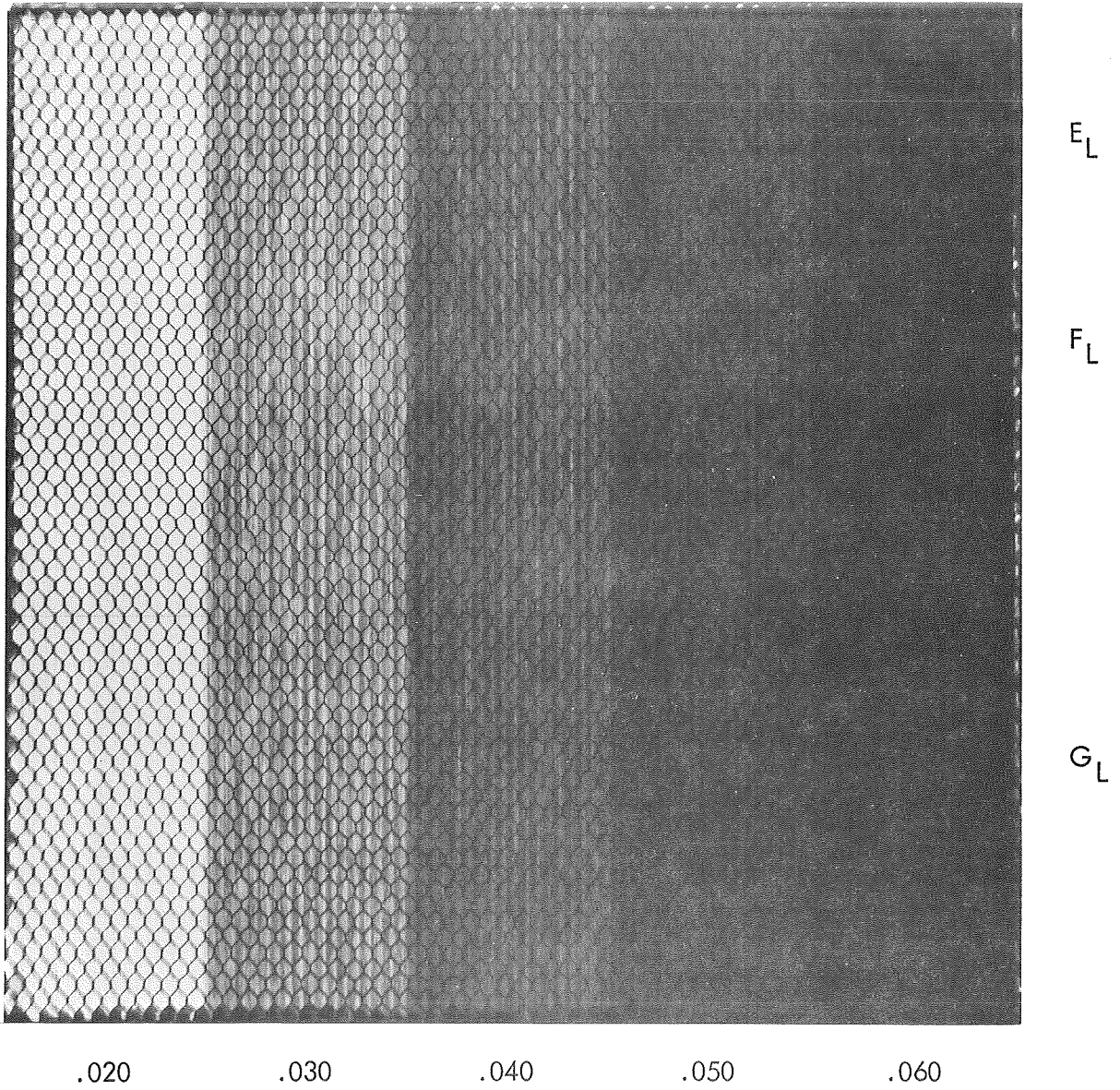


FIGURE 47. RADIOGRAPHIC PRINT OF THE 1/2-INCH BORON/HONEYCOMB PANEL 211. BACKING INCLUSION (F_L) AND UNDERCURE (G_L) ARE NOT DISCERNIBLE.

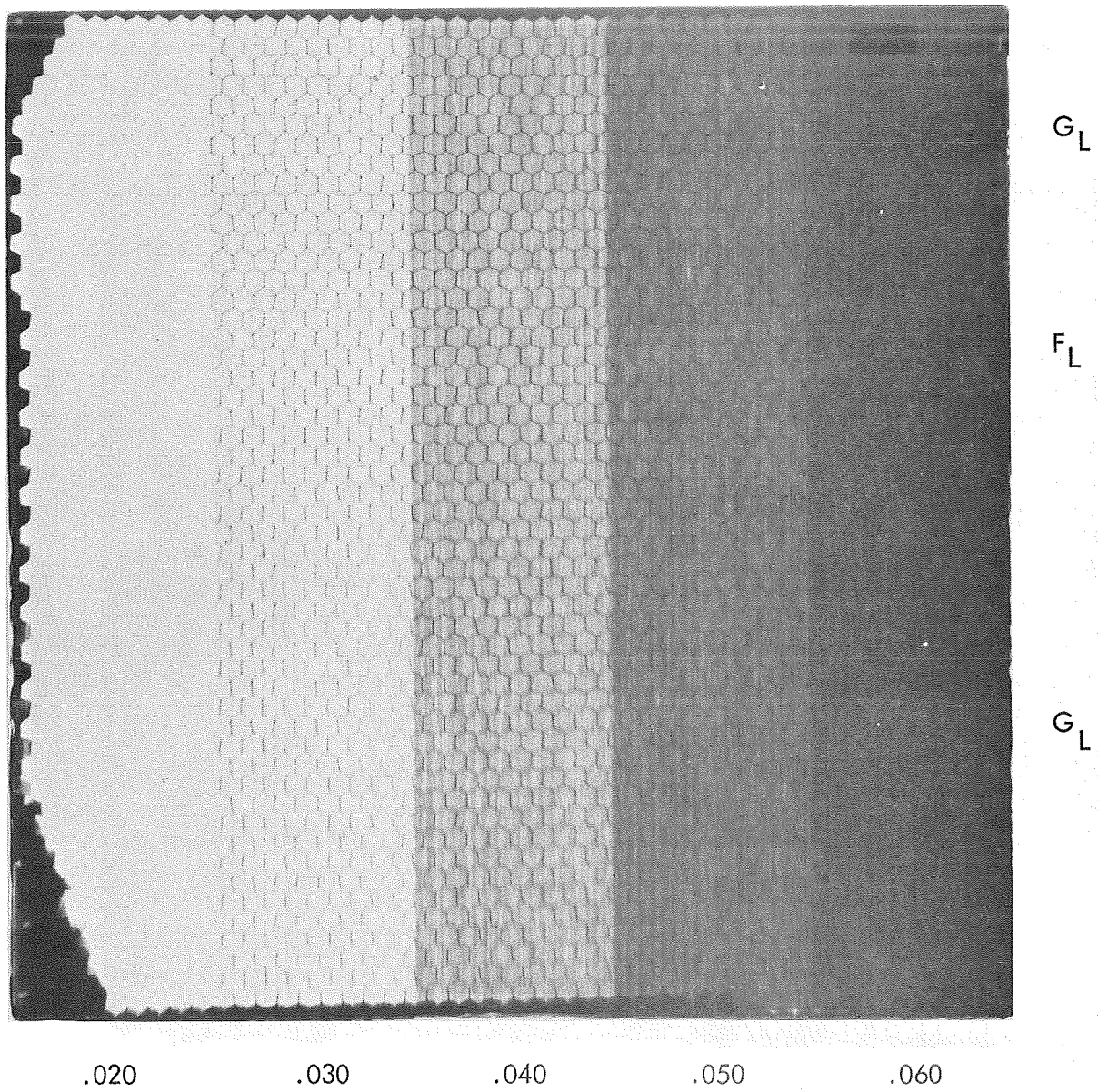


FIGURE 48. RADIOGRAPHIC PRINT OF THE 1-INCH BORON/HONEYCOMB PANEL 212. BACKING INCLUSION (F_L) AND UNDERCURE (G_L) ARE NOT DISCERNIBLE.

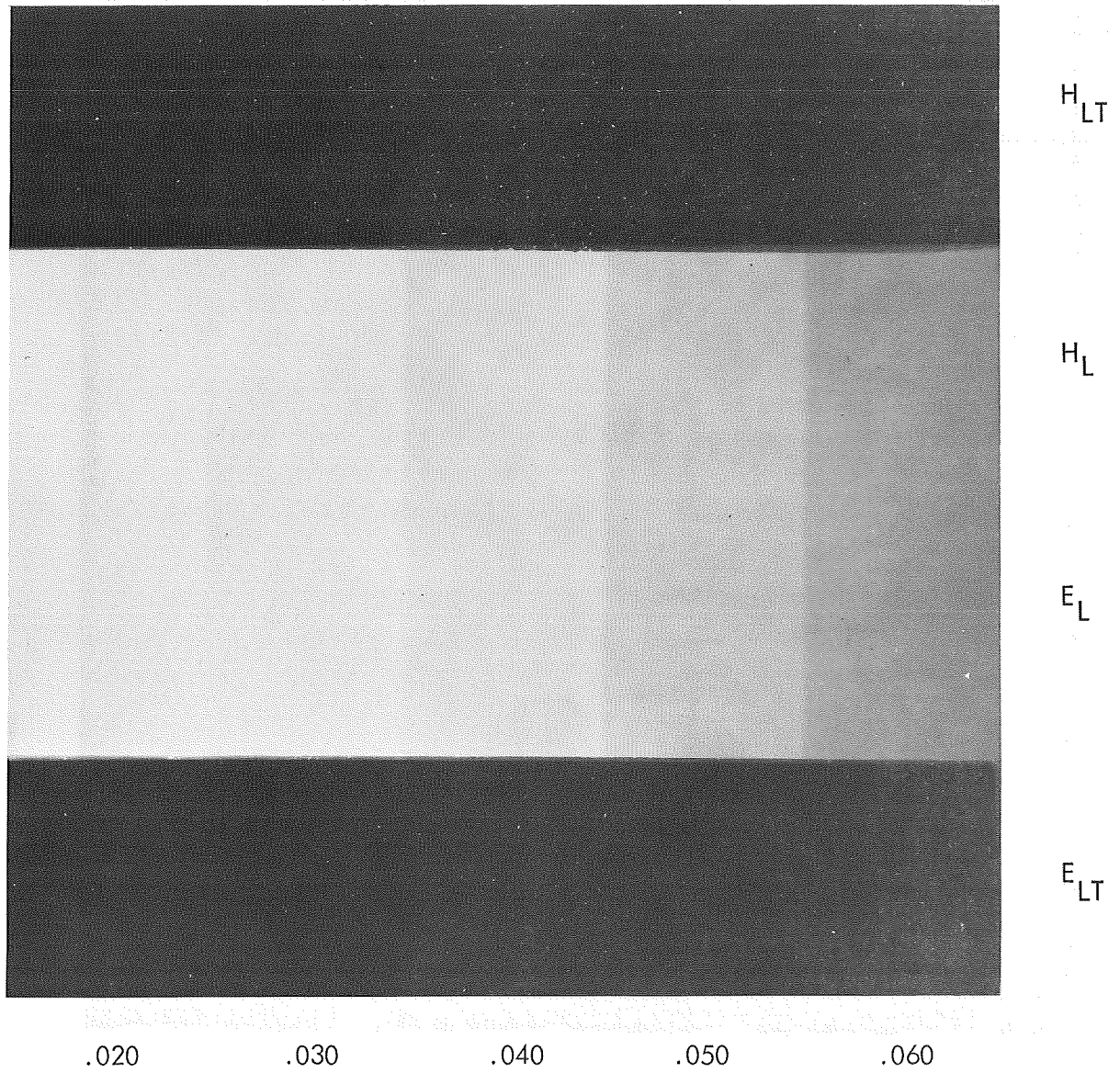


FIGURE 49. RADIOGRAPHIC PRINT OF THE FLAT GRAPHITE PANEL 313 SHOWING THE MISALIGNED PLY (H_L) AS A SLIGHTLY DARKER REGION

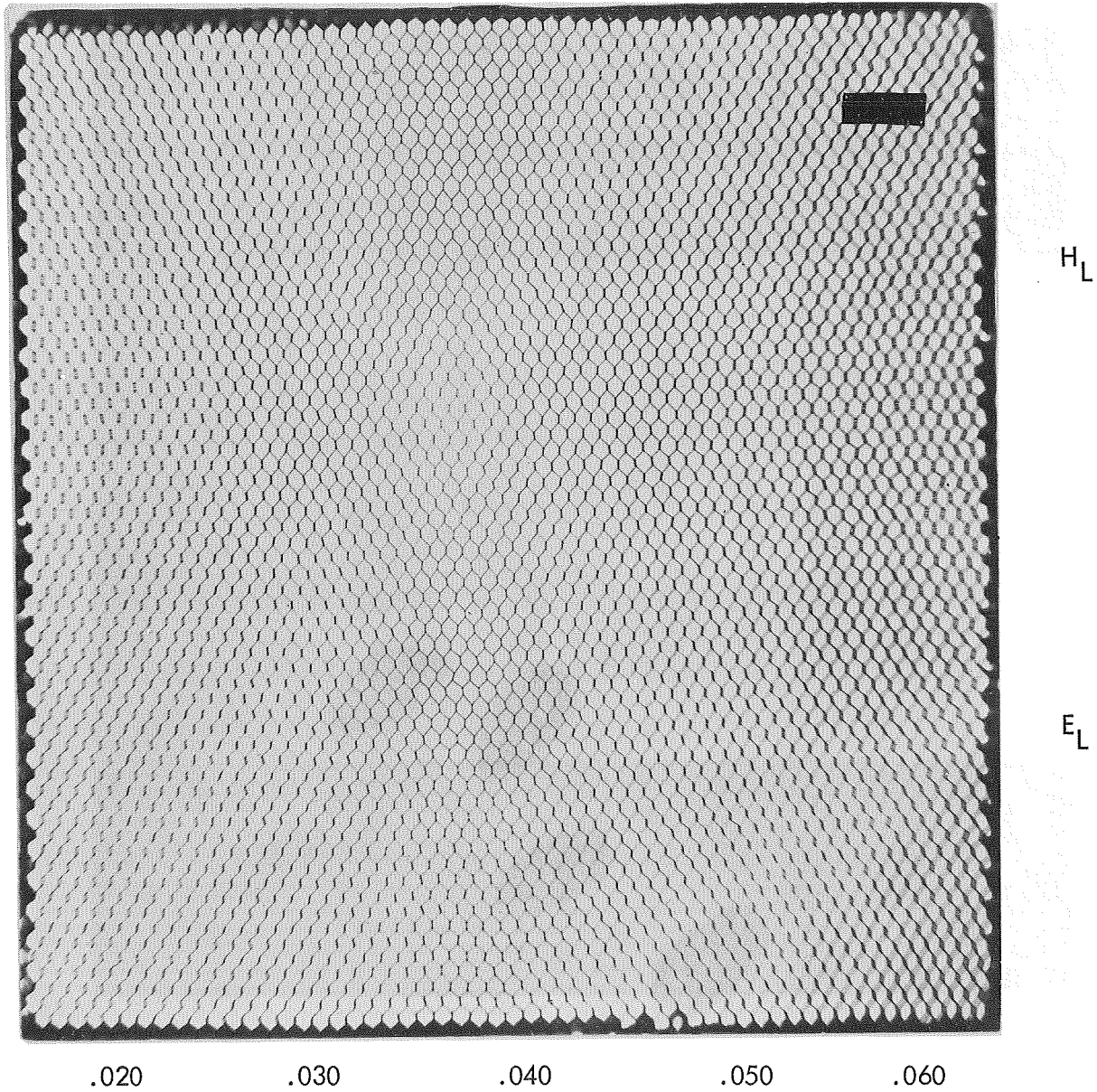


FIGURE 50. RADIOGRAPHIC PRINT OF THE 1/2-INCH GRAPHITE/HONEYCOMB PANEL 314. MISALIGNED PLY (H_L) IN FACE SHEET IS NOT DISCERNIBLE.

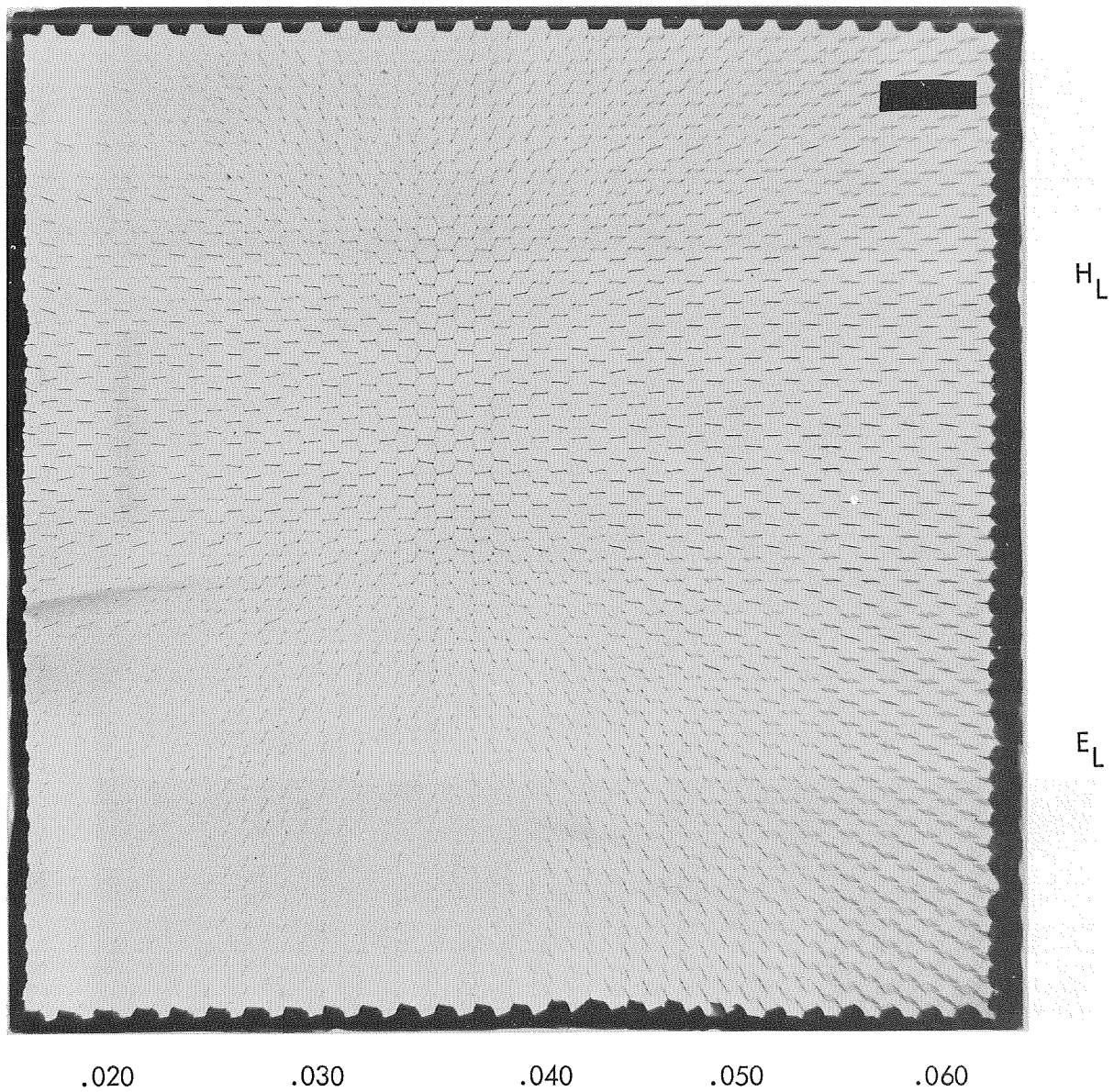


FIGURE 51. RADIOGRAPHIC PRINT OF THE 1-INCH GRAPHITE/HONEYCOMB PANEL 315. MISALIGNED PLY (H_L) IN FACE SHEET IS NOT DISCERNIBLE.

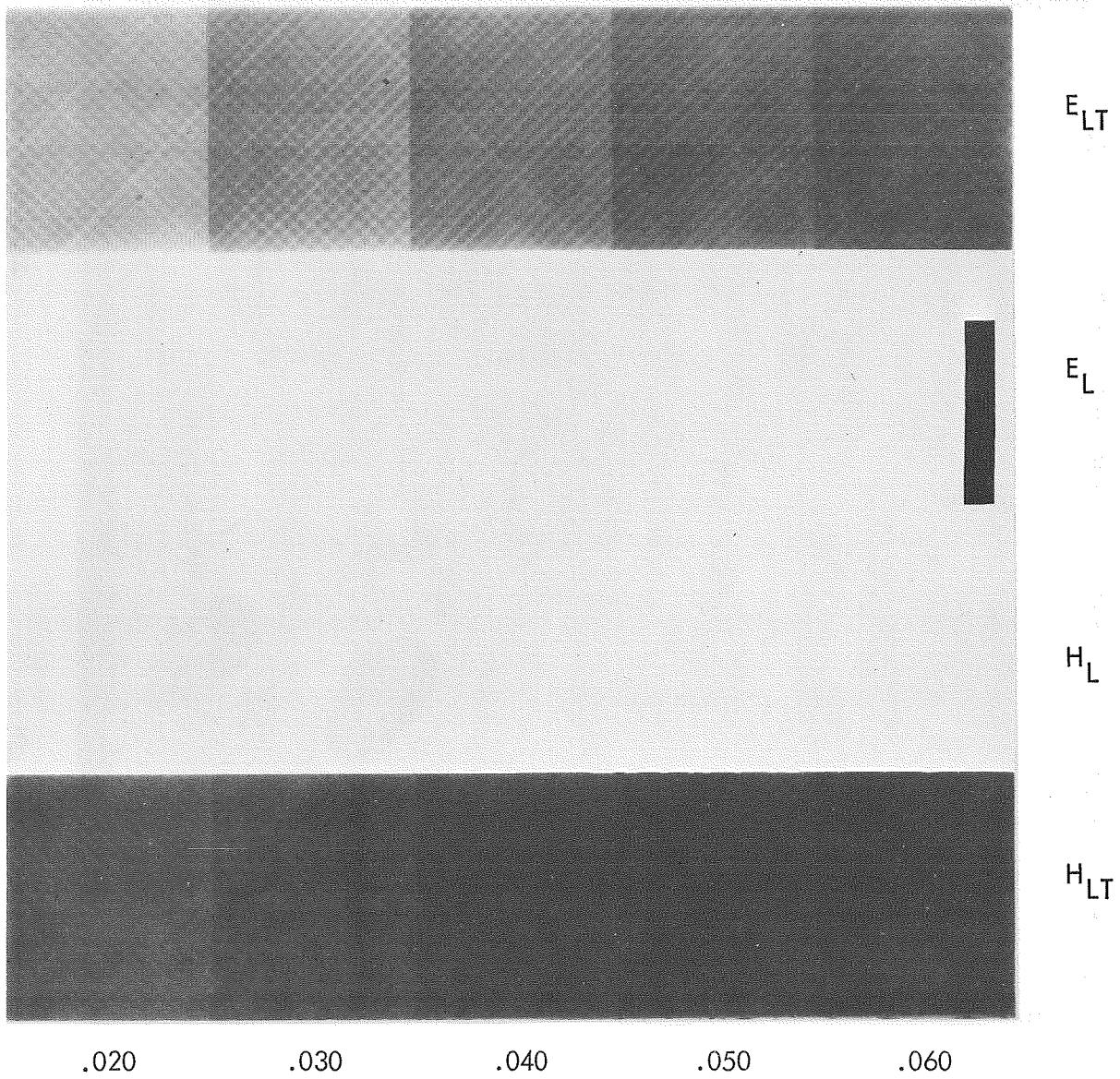


FIGURE 52. RADIOGRAPHIC PRINT OF THE FLAT BORON PANEL 316, SHOWING FIBER MISALIGNMENT IN THE LEFT-HAND PORTION OF H_{LT}

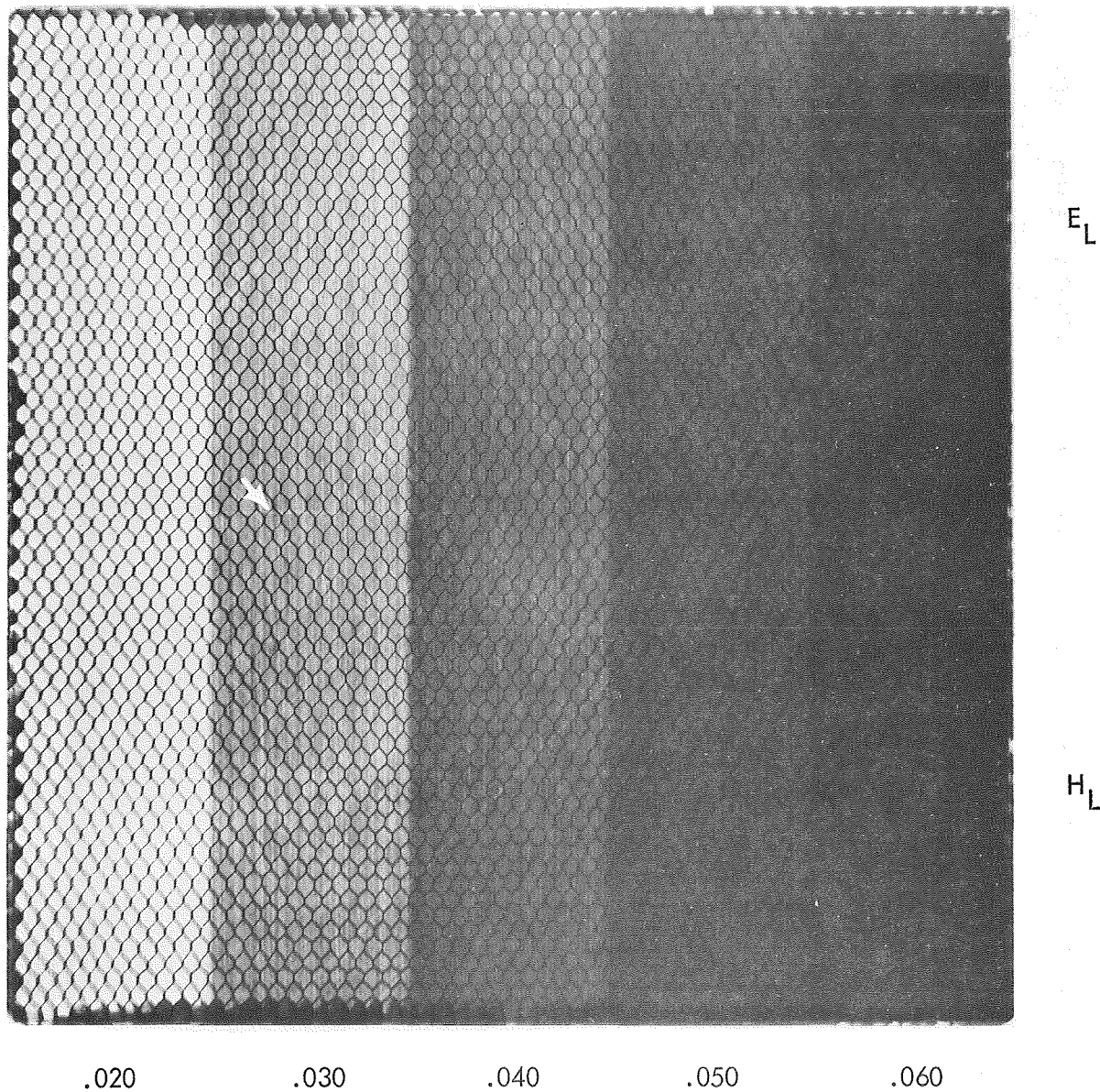


FIGURE 53. RADIOGRAPHIC PRINT OF THE 1/2-INCH BORON/HONEYCOMB PANEL 317 SHOWING PLY SEPARATION DUE TO BUTT JOINT MISALIGNMENT (ARROW)

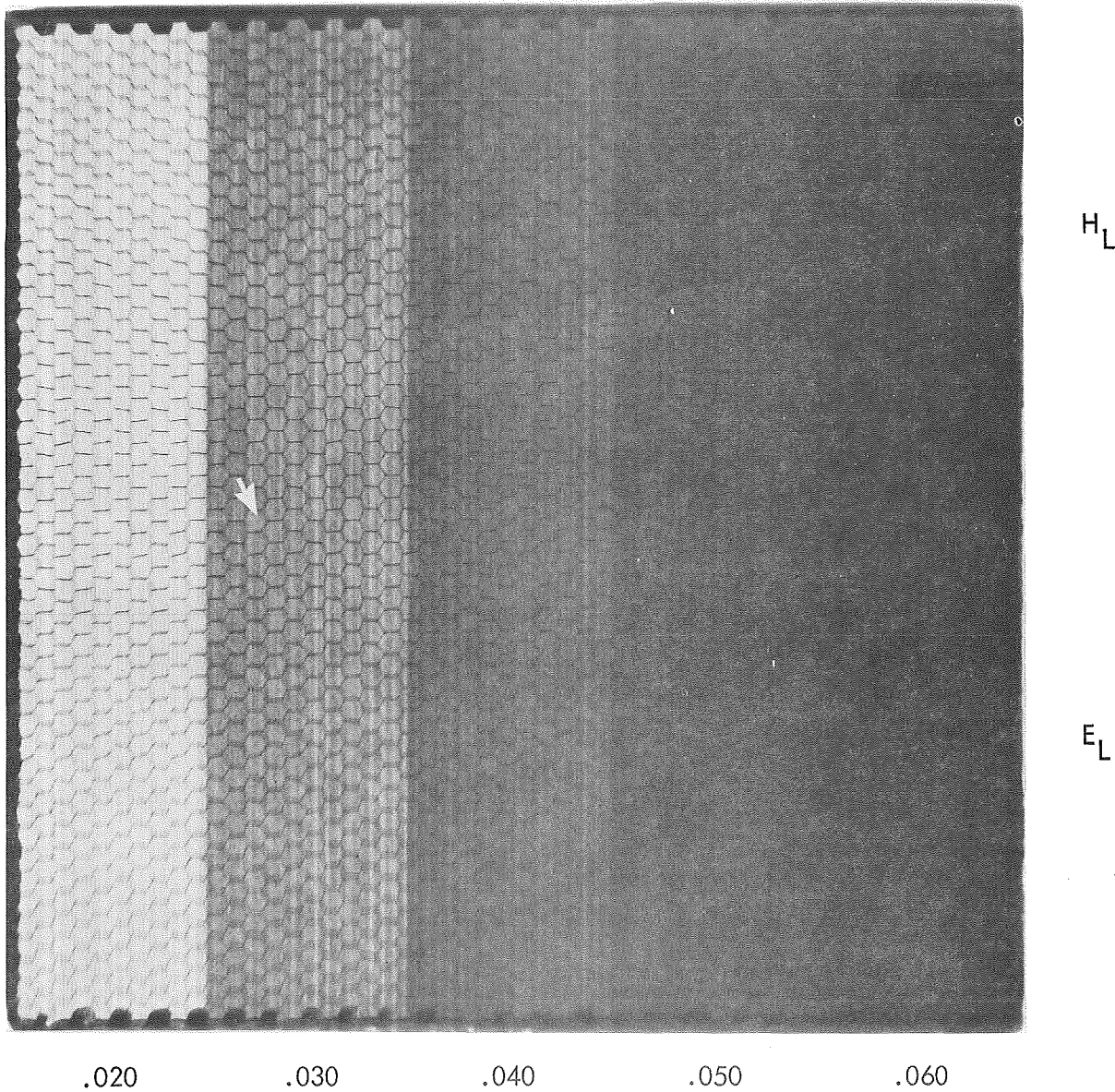


FIGURE 54. RADIOGRAPHIC PRINT OF THE 1-INCH BORON/HONEYCOMB PANEL 318 SHOWING PLY SEPARATION DUE TO BUTT JOINT MISALIGNMENT (ARROW)

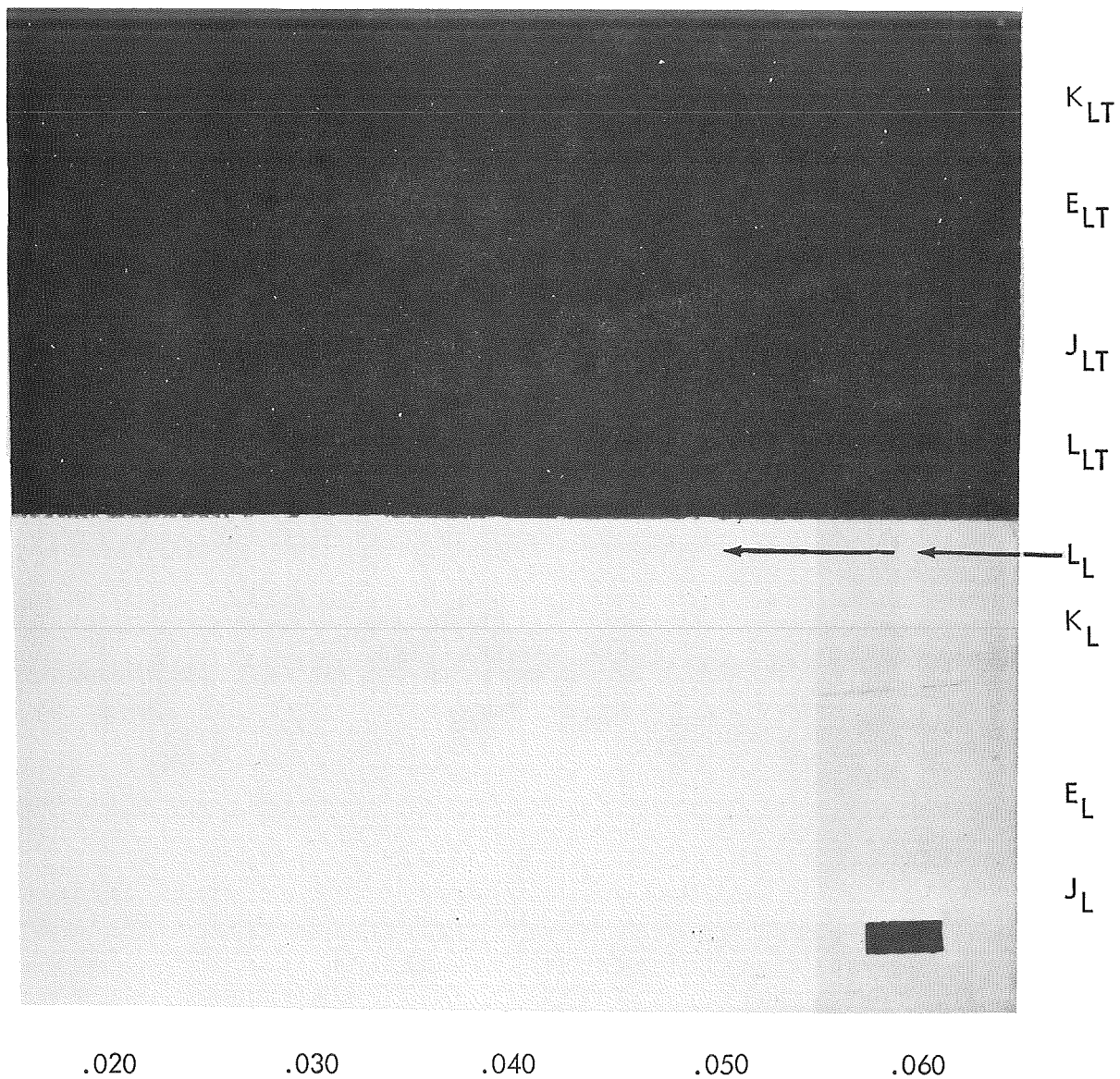


FIGURE 55. RADIOGRAPHIC PRINT OF THE FLAT GRAPHITE PANEL 419 SHOWING THE 1/4" SLOTS, OVERLAPS AND SPACING VOIDS IN THE FIBER PLYS (MOST INDICATIONS LOST IN REPRODUCTION)

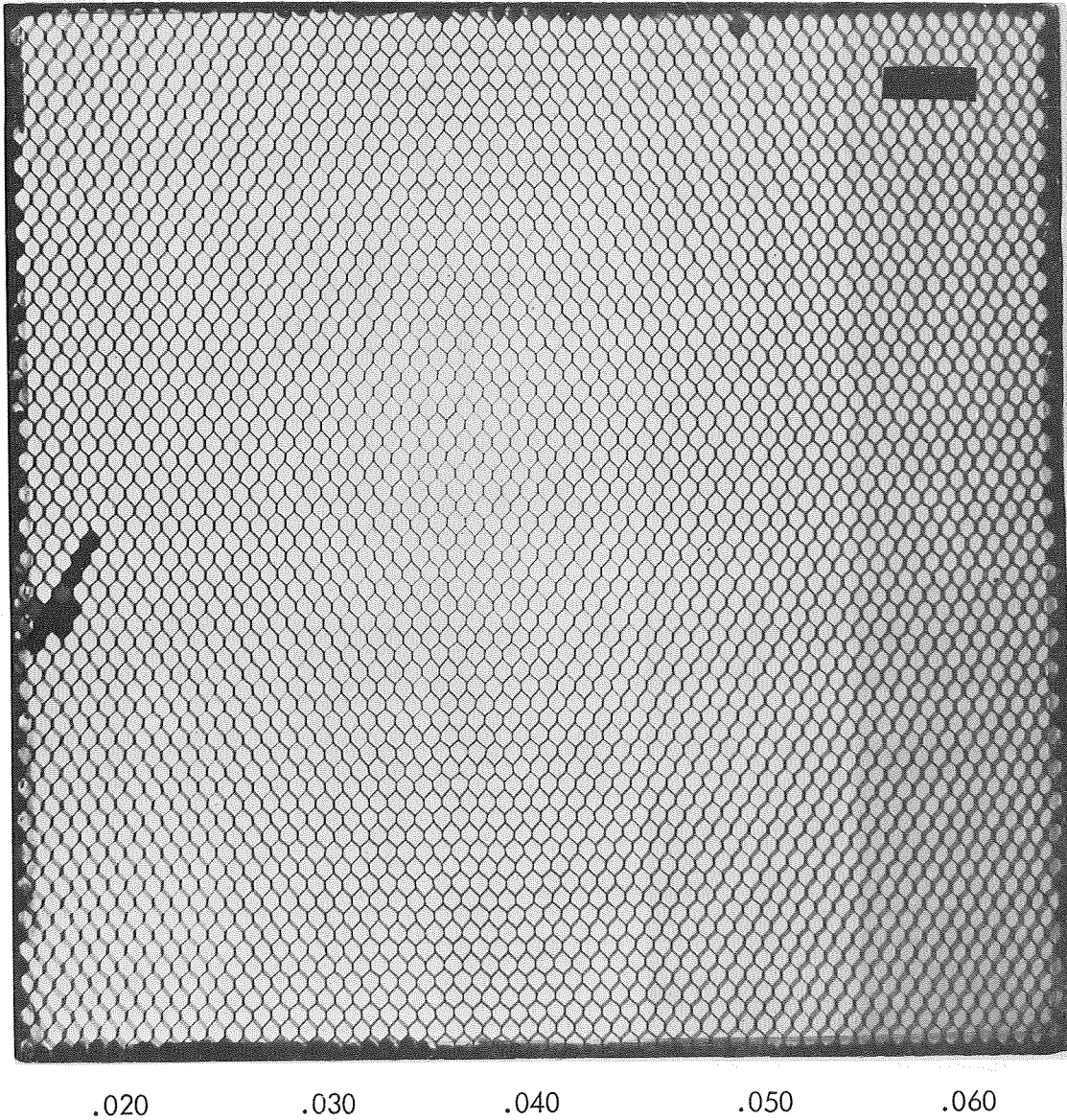


FIGURE 56. RADIOGRAPHIC PRINT OF THE 1/2-INCH GRAPHITE/HONEYCOMB PANEL 420 SHOWING THE OVERLAPS AND SPACING VOIDS IN THE FIBER PLIES (LOST IN REPRODUCTION)

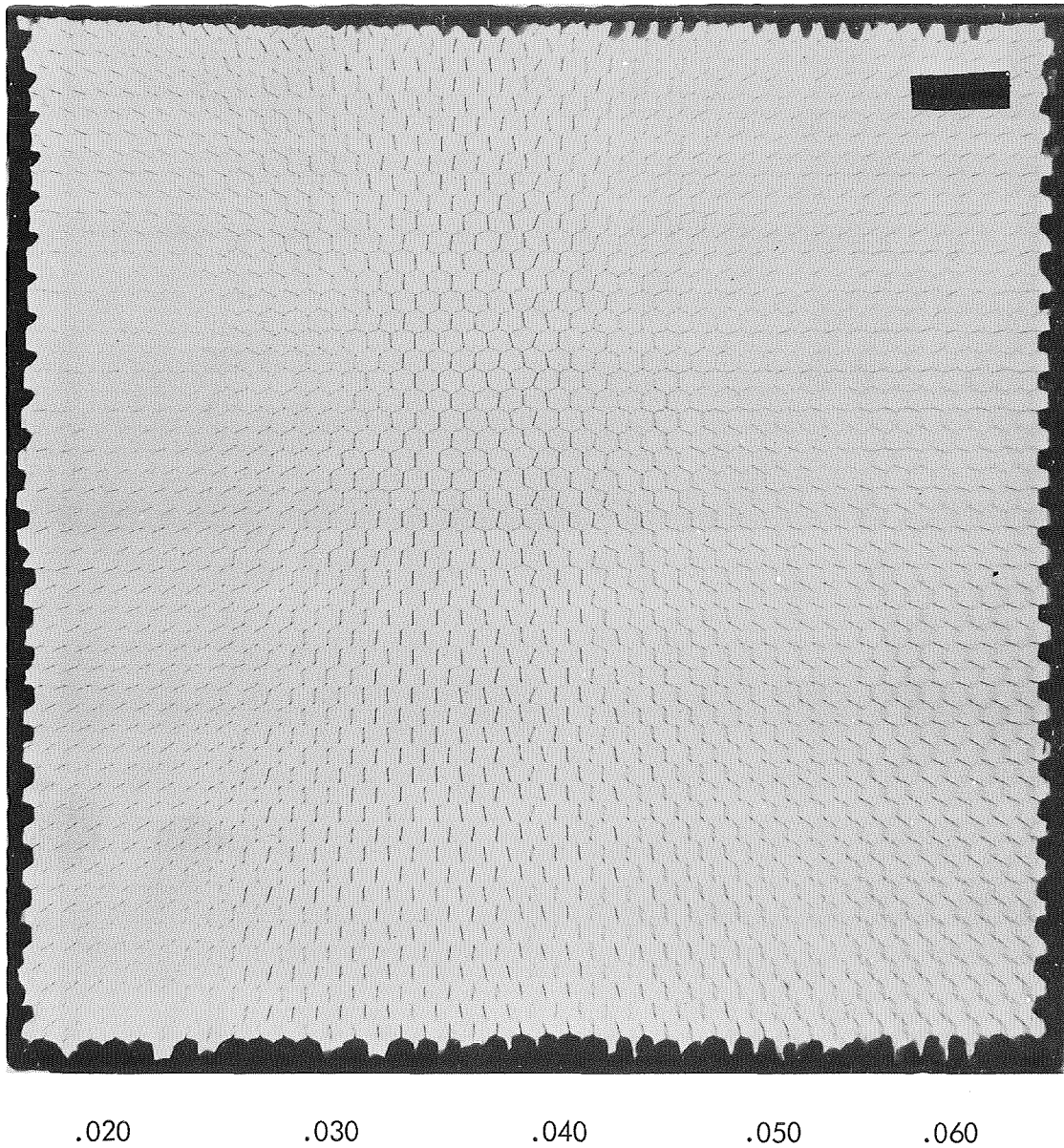


FIGURE 57. RADIOGRAPHIC PRINT OF THE 1-INCH GRAPHITE/HONEYCOMB PANEL 421 SHOWING THE 1/4-INCH SLOT (IN THE 0.020-INCH THICK SECTION), THE OVERLAPS, AND THE SPACING VOIDS IN THE FIBER PLYS (LOST IN REPRODUCTION)

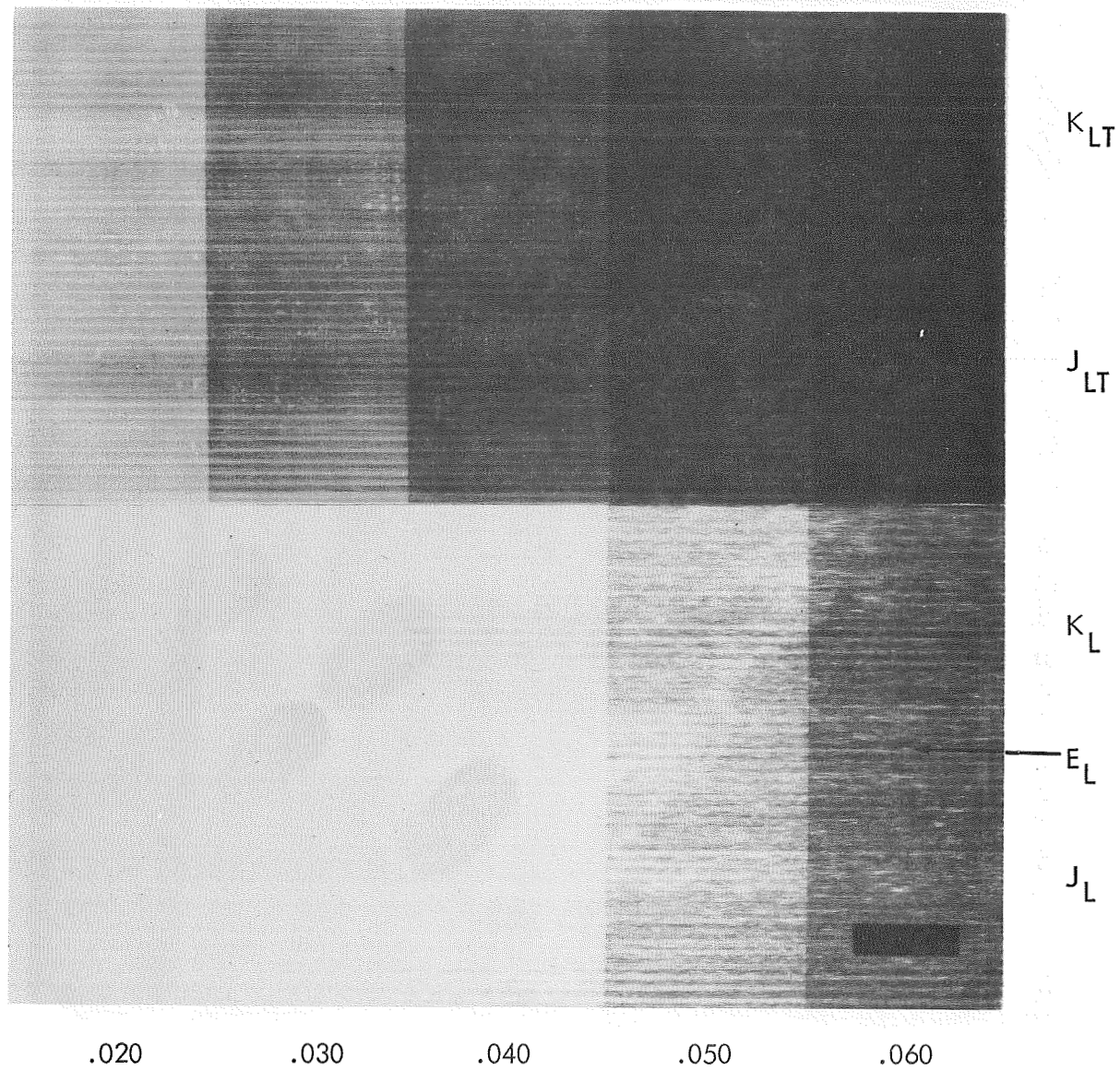


FIGURE 58. RADIOGRAPHIC PRINT OF THE FLAT BORON PANEL 422 SHOWING THE SLITS, OVERLAPS, AND SPACING VOIDS IN THE FILAMENT PLIES (SOME INDICATIONS LOST IN REPRODUCTION)

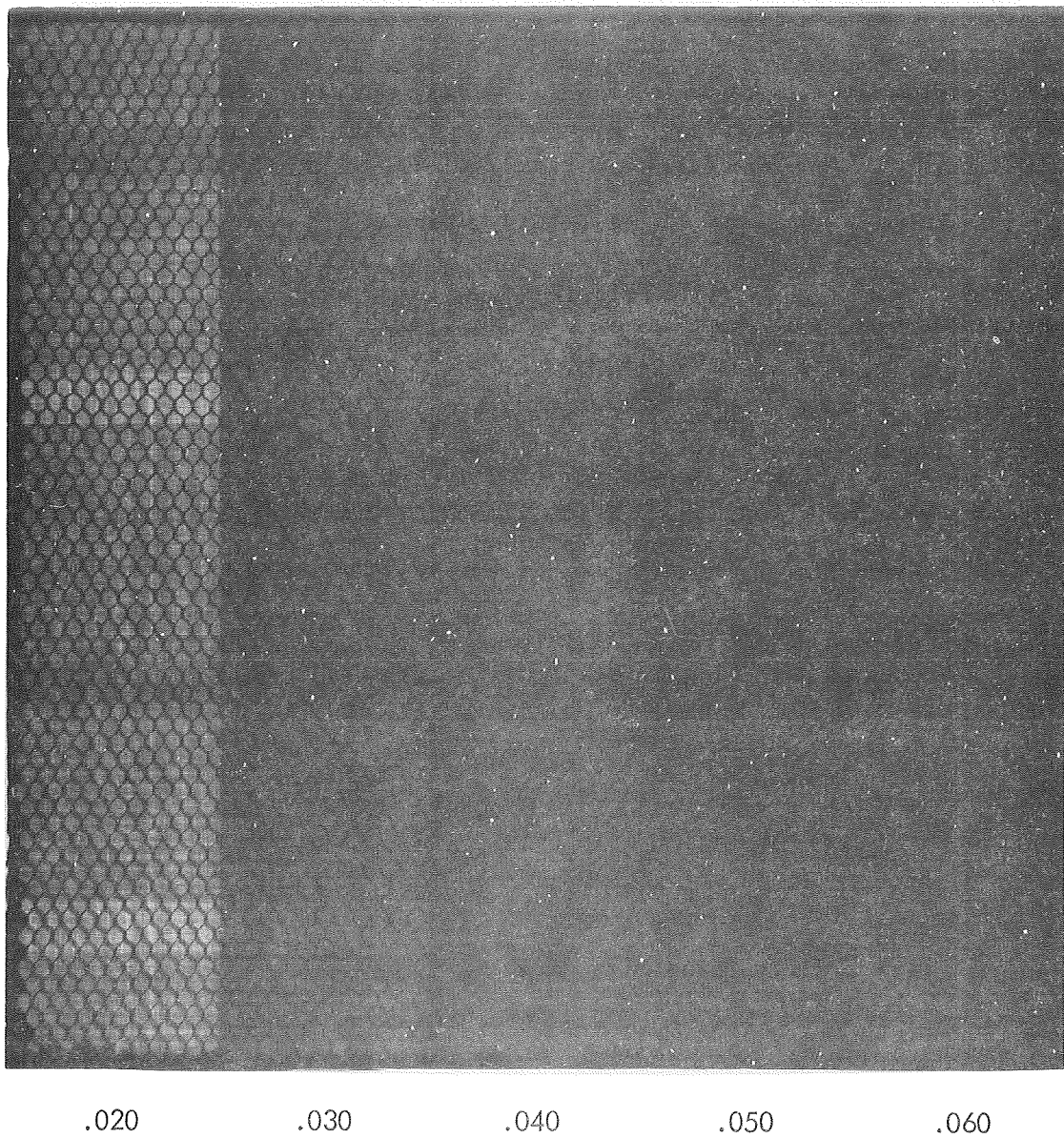


FIGURE 59. RADIOGRAPHIC PRINT OF THE 1/2-INCH BORON/HONEYCOMB PANEL 423 SHOWING THE OVERLAPS (DARK HORIZONTAL BANDS) AND SPACING VOIDS (LIGHT HORIZONTAL BANDS) IN THE FILAMENT PLYS

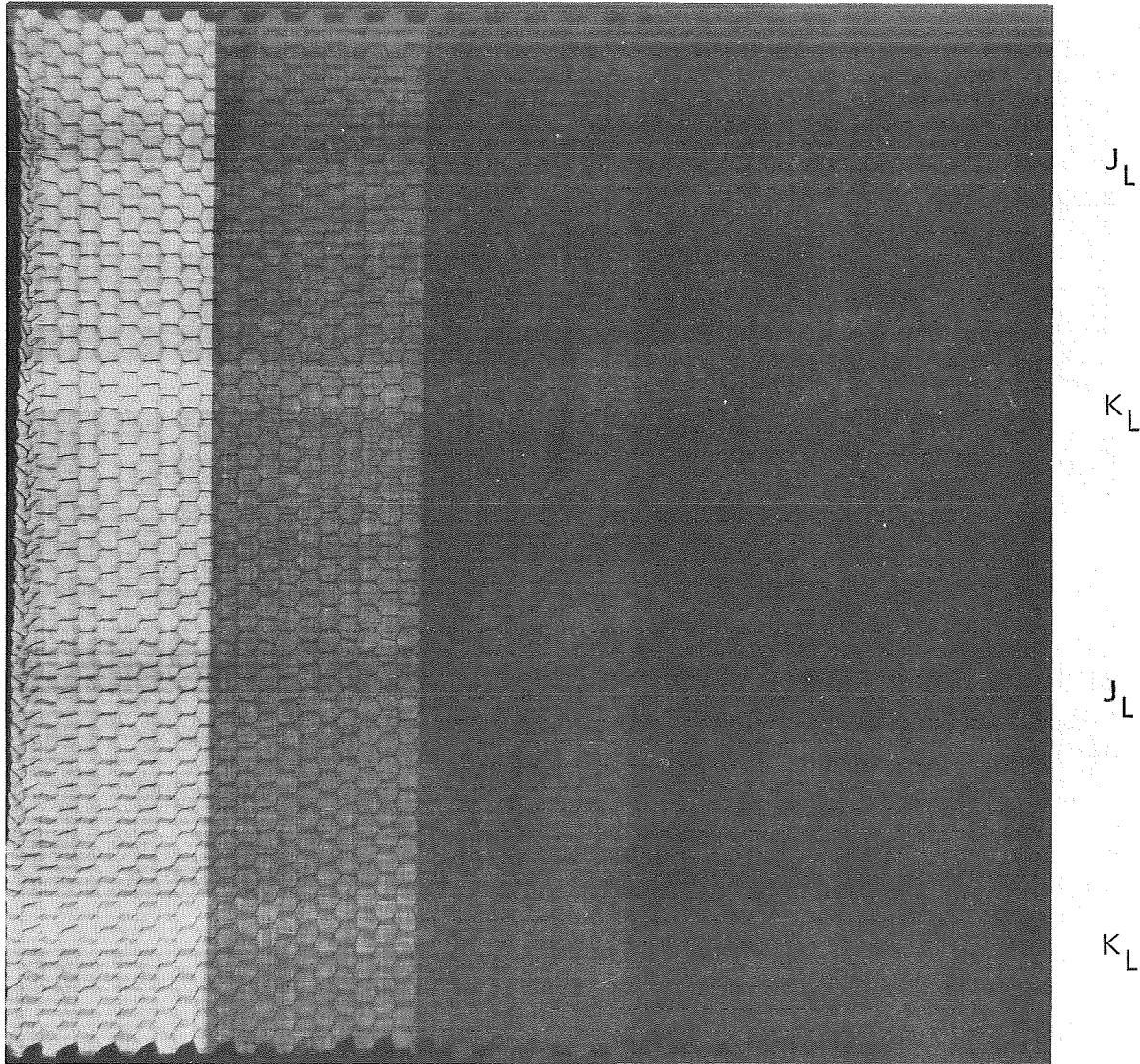


FIGURE 60. RADIOGRAPHIC PRINT OF THE 1-INCH BORON/HONEYCOMB PANEL 424 SHOWING THE OVERLAPS (DARK HORIZONTAL BANDS) AND SPACING VOIDS (LIGHT HORIZONTAL BANDS) IN THE FILAMENT PLIES

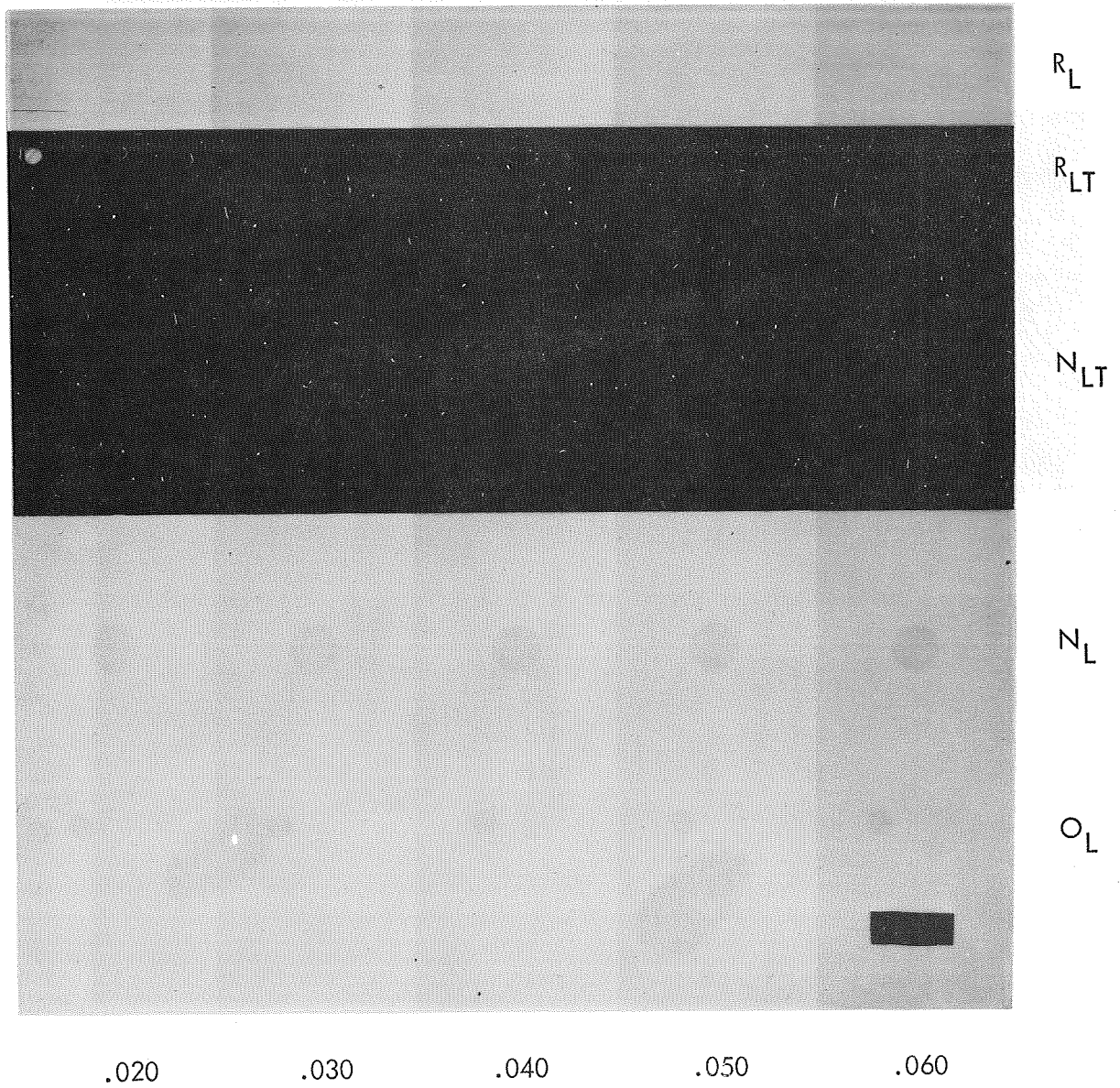


FIGURE 61. RADIOGRAPHIC PRINT OF THE FLAT GRAPHITE PANEL 525
 SHOWING THE 1/4-INCH AND 1/2-INCH INSERTS
 CAUSING DISBONDS

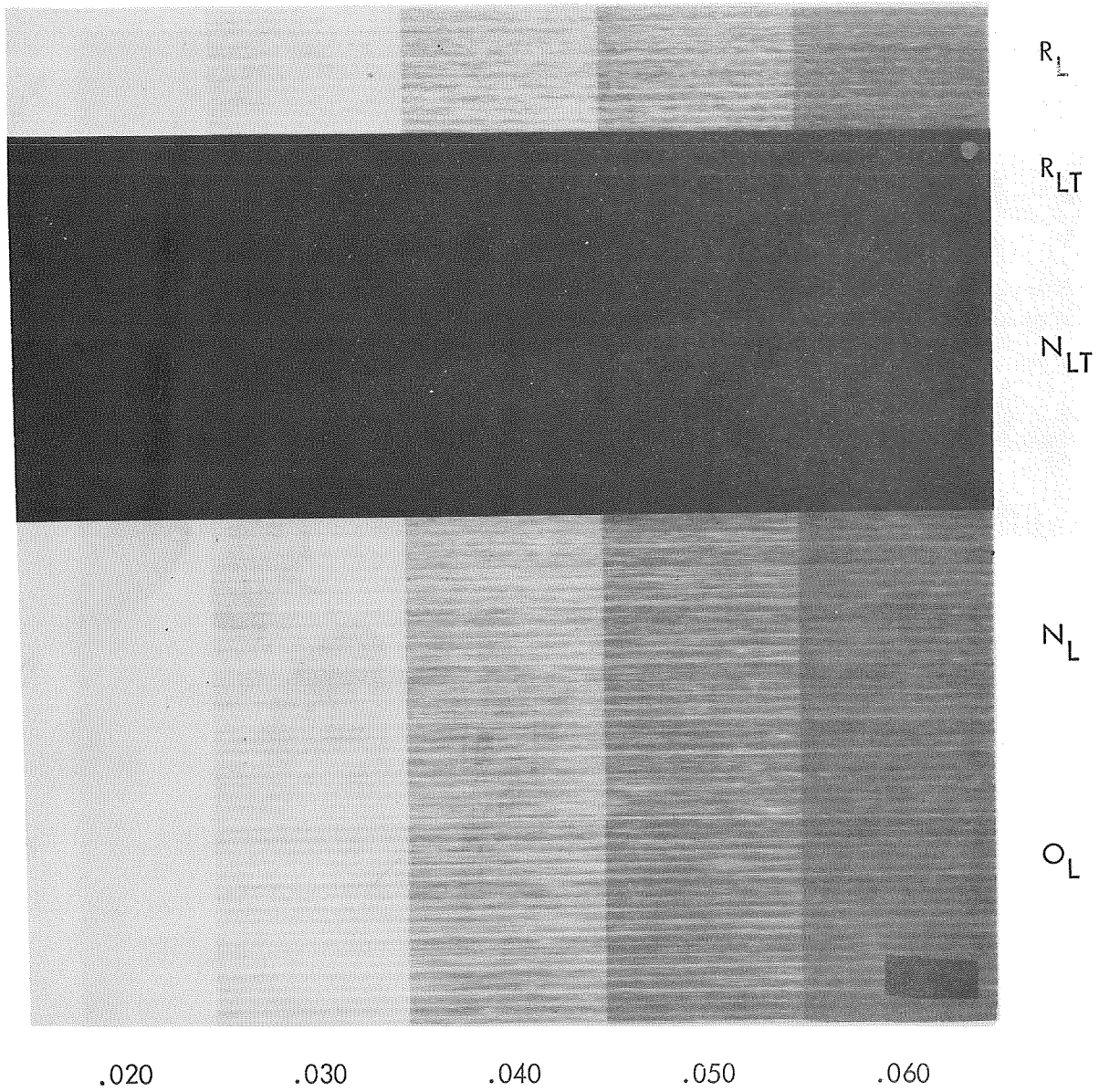
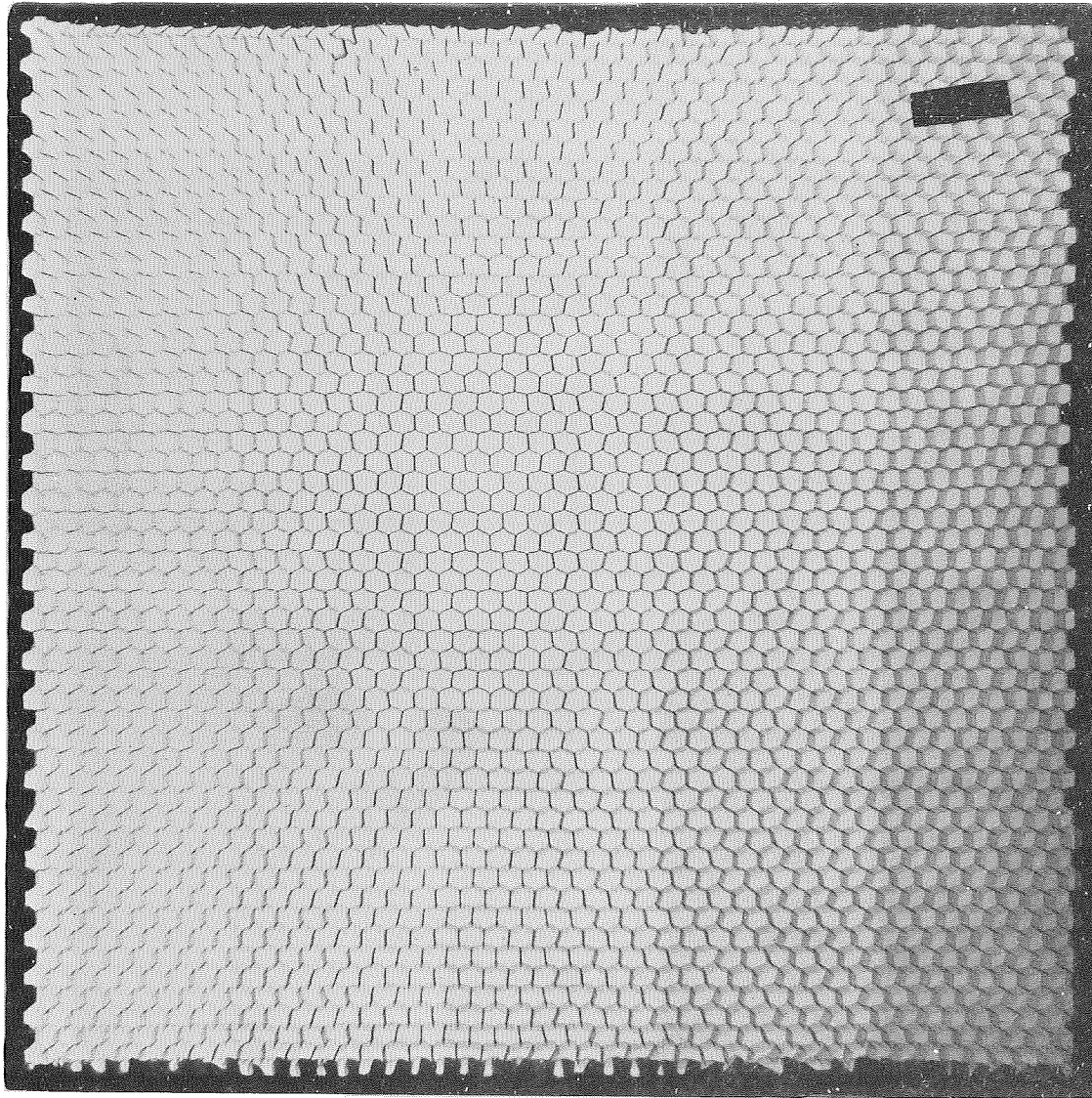


FIGURE 62. RADIOGRAPHIC PRINT OF THE FLAT BORON PANEL 526
(INSERTS NOT DISCERNIBLE)



R_L

.020 .030 .040 .050 .060

FIGURE 63. RADIOGRAPHIC PRINT OF THE 1-INCH GRAPHITE/HONEYCOMB PANEL 528, CONTAINING THE CRUSHED CORE AND THE INTER-LAMINAR, NEAR-SIDE, AND FAR-SIDE DISBONDS (NOT DISCERNIBLE IN THIS REPRODUCTION)

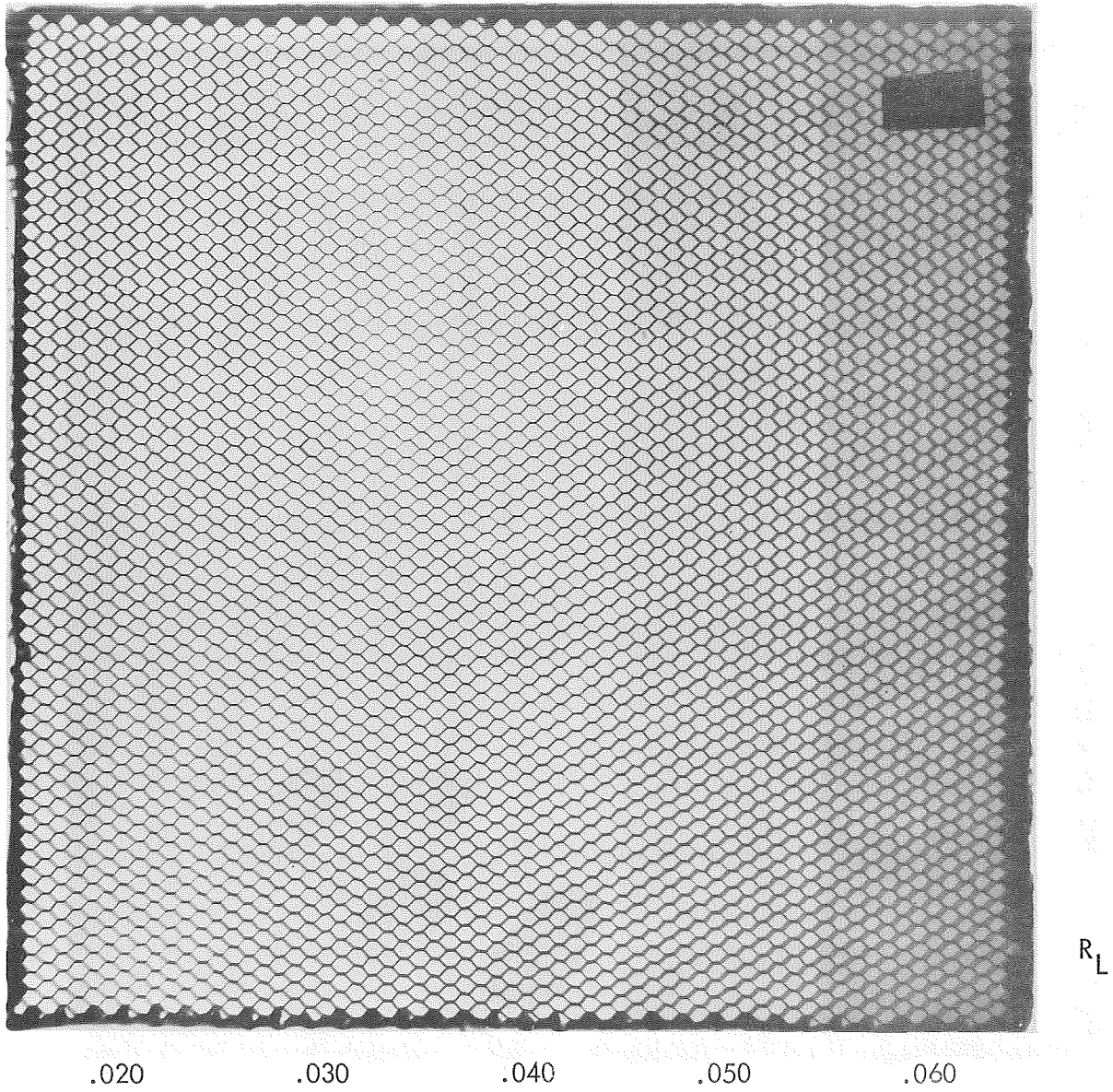
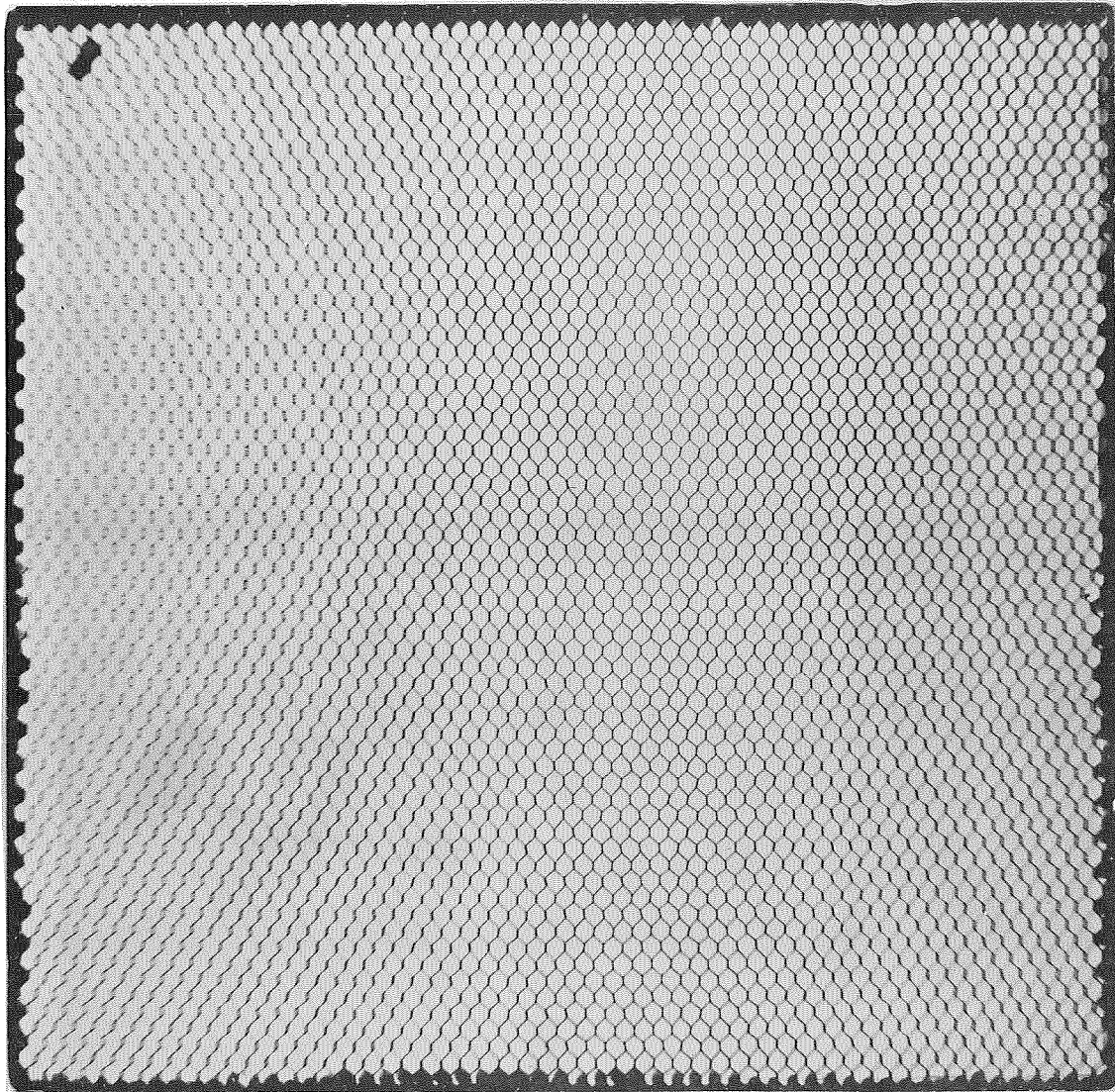


FIGURE 64. RADIOGRAPHIC PRINT OF THE 1/2-INCH GRAPHITE/HONEYCOMB PANEL 527 (#1), CONTAINING THE 1/4-INCH INSERTS FOR INTERLAMINAR DISBONDS



R_L

.020 .030 .040 .050 .060

FIGURE 65. RADIOGRAPHIC PRINT OF THE 1/2-INCH GRAPHITE/HONEYCOMB PANEL 527 (#2), CONTAINING INTERLAMINAR, FAR-SIDE, NEAR-SIDE, AND GENERAL DISBONDS AND CRUSHED CORE (NOT DISCERNIBLE IN THIS REPRODUCTION)

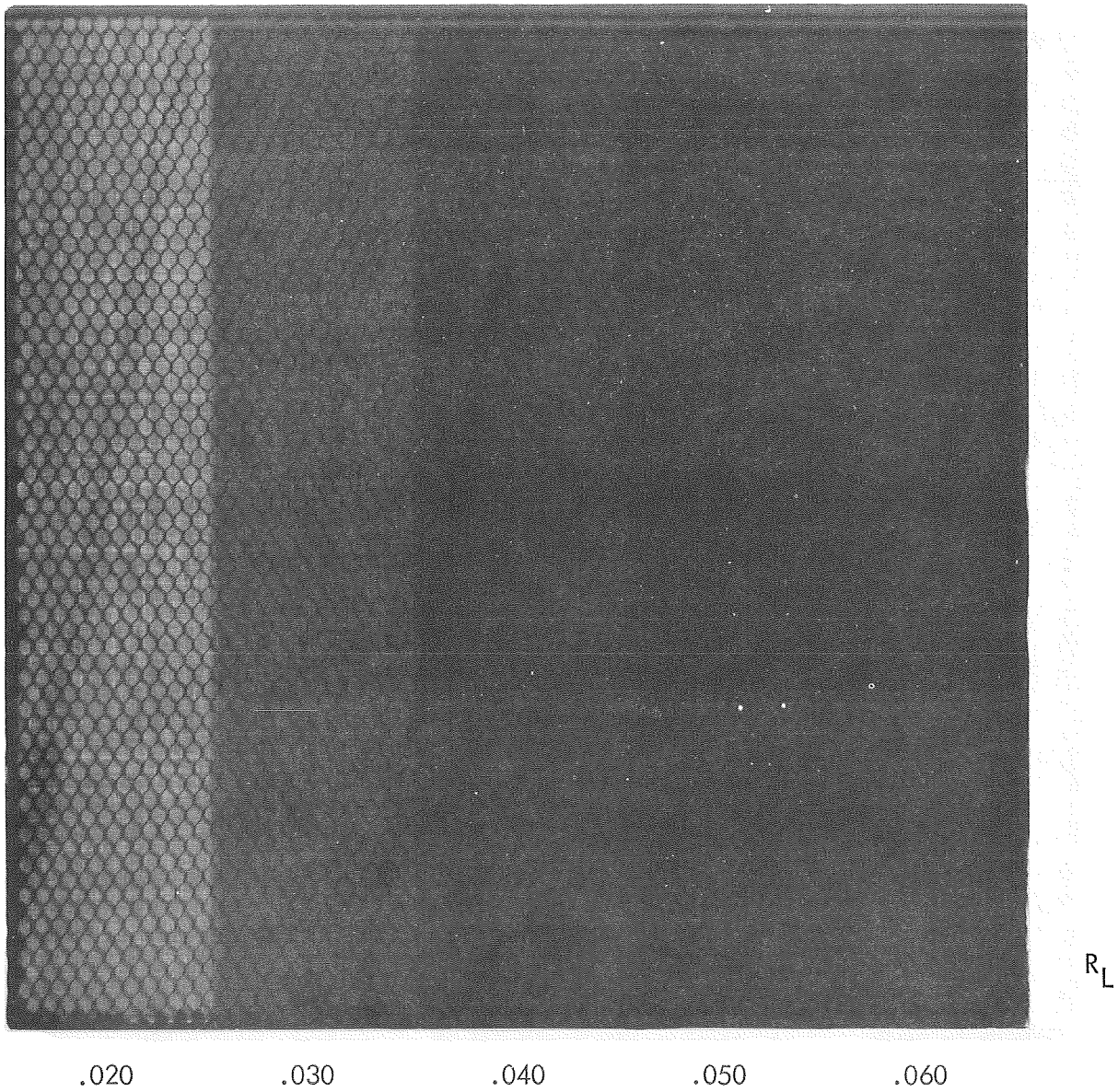
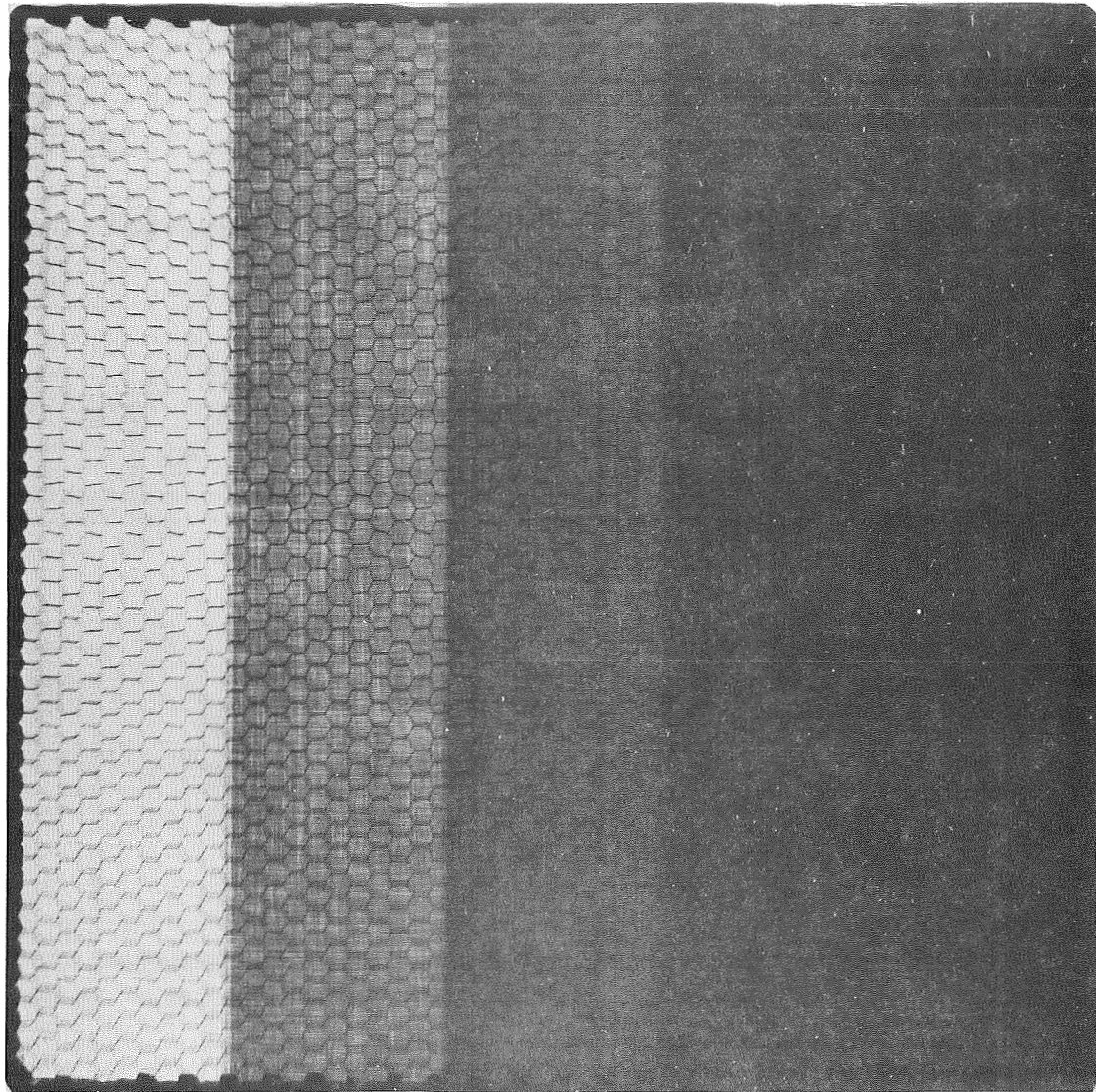


FIGURE 66. RADIOGRAPHIC PRINT OF THE 1/2-INCH BORON/HONEYCOMB PANEL 529 CONTAINING CRUSHED CORE AND INTERLAMINAR, FAR-SIDE, AND NEAR-SIDE DISBONDS (NOT DISCERNIBLE IN THIS REPRODUCTION)



.020

.030

.040

.050

.060

R_L

FIGURE 67. RADIOGRAPHIC PRINT OF THE 1-INCH BORON/HONEYCOMB PANEL 530 CONTAINING CRUSHED CORE AND INTERLAMINAR, FAR-SIDE, AND NEAR-SIDE DISBONDS (NOT DISCERNIBLE IN THIS REPRODUCTION)

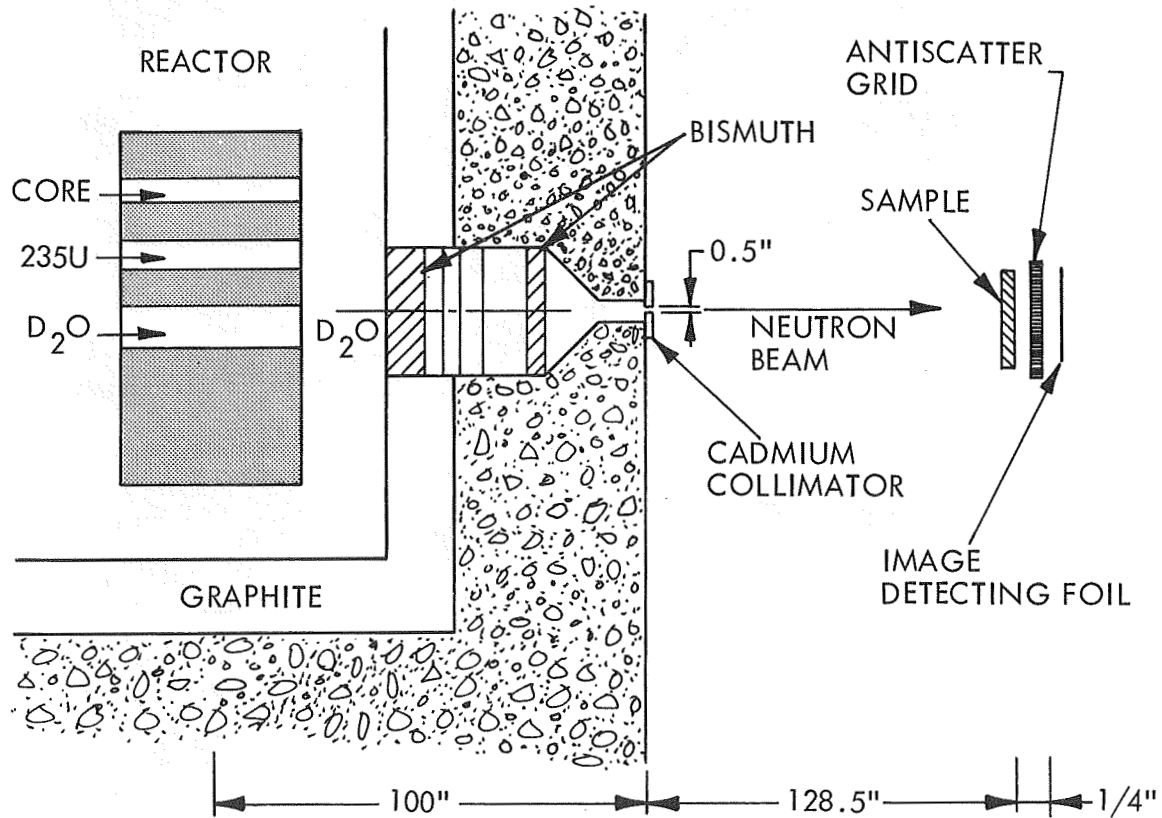


FIGURE 68. CROSS-SECTION OF NEUTRON RADIOGRAPHIC FACILITY LOCATED AT THE GEORGIA INSTITUTE OF TECHNOLOGY.

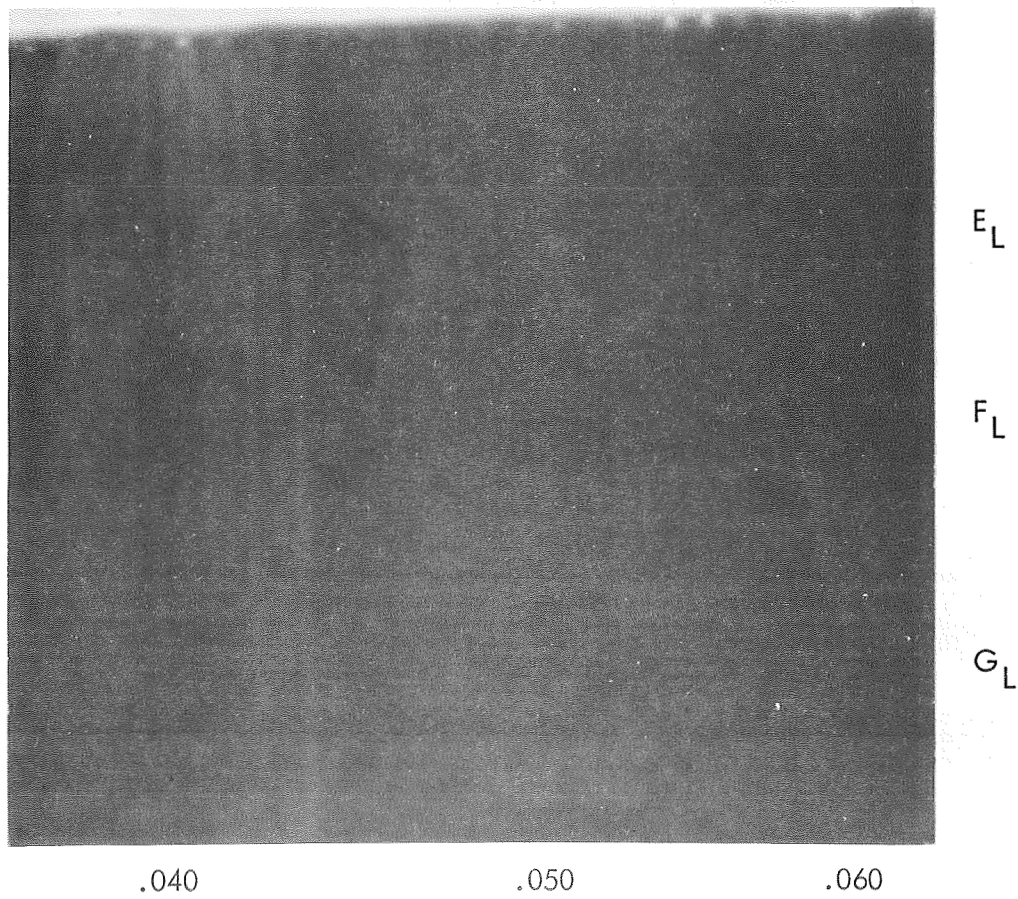
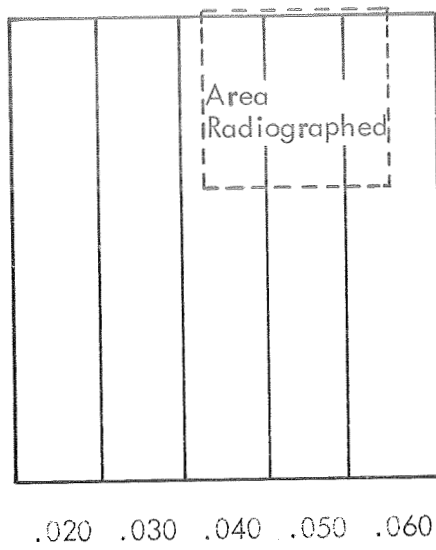


FIGURE 69. POSITIVE PRINT OF A NEUTRON RADIOGRAPH TAKEN OF PORTION OF THE 1/2-INCH BORON/HONEYCOMB PANEL 211, CONTAINING BACKING INCLUSION AND UNDERCURE

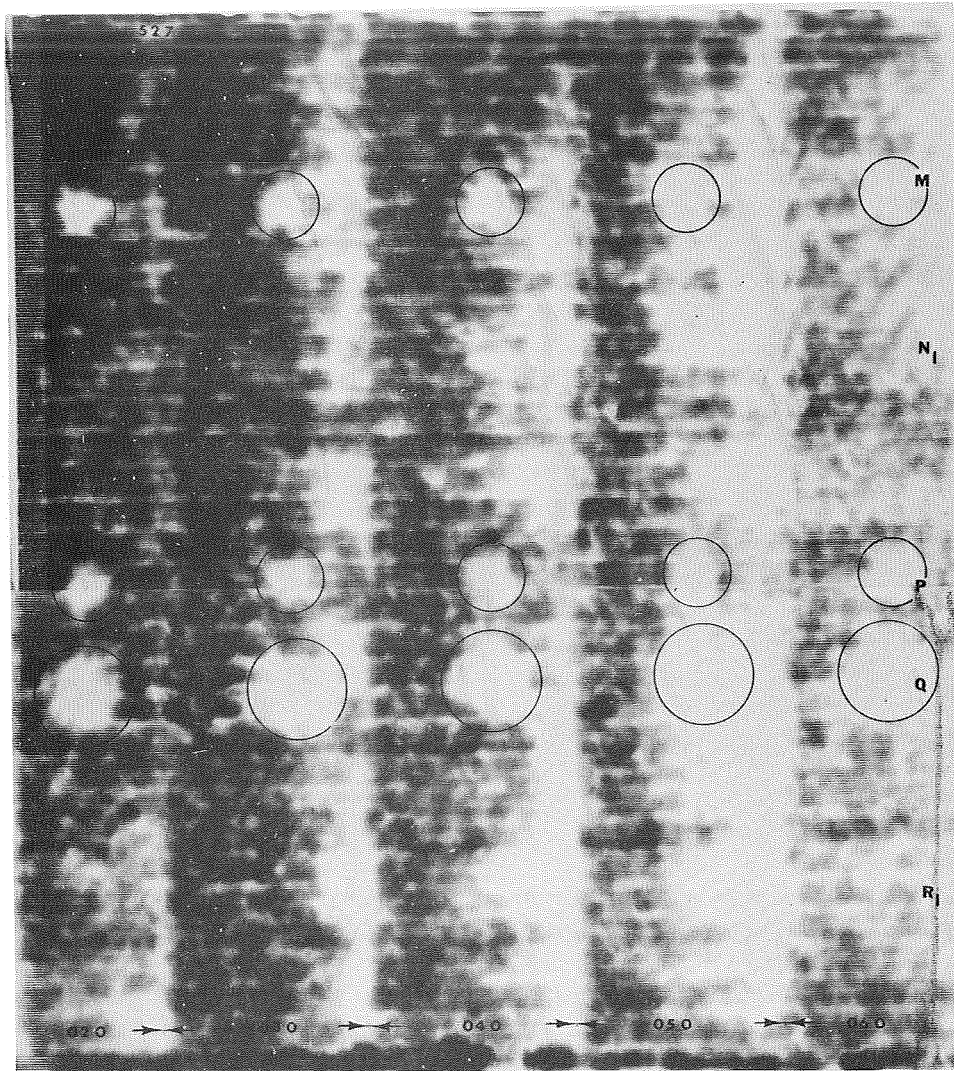
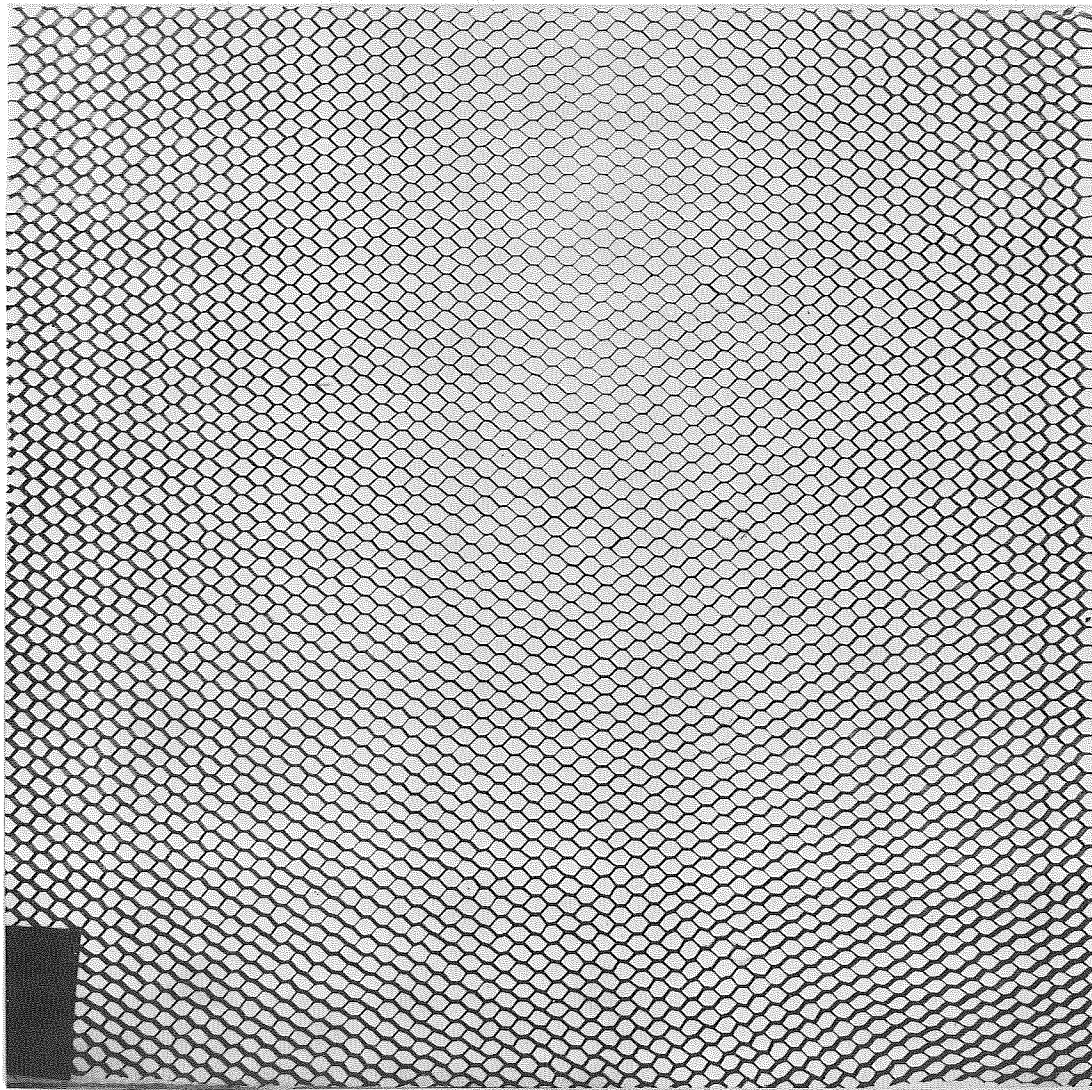


FIGURE 71. PRINT OF ULTRASONIC C-SCAN OF PANEL NO. 527(C) SHOWING INTERLAMINAR DISBONDS (N_L), NEAR-SIDE (P) AND FAR-SIDE (M) DISBONDS, CRUSHED CORE (Q), AND THE PREAGED STRIP (R_L) WHICH RESULTED IN GENERAL DISBONDING



R
L

Q

.020 .030 .040 .050 .060

FIGURE 72. REDUCED PRINT OF RADIOGRAPH OF PANEL NO. 527C CONTAINING DELAMINATIONS, NEAR-SIDE AND FAR-SIDE DISBONDS AND CRUSHED CORE (ONLY CRUSHED CORE IS VISIBLE IN RADIOGRAPH)

BIBLIOGRAPHY OF SELECTED WORKS

- Allen, J. J., and D. S. Harmer, "Selected Biomedical Applications of Thermal Neutron Radiography," Proceedings, Biomedical Sciences Instrumentation - Vol. 6, Instrument Society of America, May 1969.
- Anderson, R. T., and T. J. DeLacy, "Application of Nondestructive Testing for Advanced Composites," AFML/Aerospace/Univ. of Dayton Conference on NDT of Plastic Composite Structures, March 1969.
- A.V.C.O., "The Effect of Voids on the Mechanical Properties of High Modulus Graphite Fiber/Epoxy-Reinforced Composites," AIR-6022, U. S. Navy Air Systems Command, Contract N00019-68-C-0461.
- Blakslee, O. L., et al., "Fabrication, Testing and Design Studies with Thomei Graphite Fiber/Epoxy Resin Composites," Advances in Composites, SAMPE, Vol. 12, paper AC-6.
- Cohen, S. E., "The Design and Application of the Traversing Infrared Inspection System (TIRIS)," to be presented to the ASME Conference on Design Engineering, 22 April 1971, New York.
- Martin, G., and J. F. Moore, "Development of NDT Methods for Advanced Metallic Composite Materials," AFML-TR-69-296, July 1970.
- Martin, G., and J. F. Moore, "Research and Development of Nondestructive Testing Techniques for Composites," AFML-TR-66-270, USAF, Feb 1967, and AFML-TR-68-202, July 1968.
- McGarry, F. J., and A. M. Willner, "Microcracking in Fibrous Glass Reinforced Resin Composites, M.I.T. 23rd Annual S.P.I. Preprints, 1968.
- Perry, J. D., Viscoelastic Properties of Polymers, Wiley, 1961.
- Pether, I., "The Influence of Resin Strength and Defects on the Interlaminar Shear Strength of Filament-Wound Composites," Aerojet-General Corp., S.P.E. Transactions, January 1965.
- Pless, W. M., "Development of Nondestructive Test Techniques for Advanced Composite Materials," Lockheed-Georgia Company, ER-10012, January 1969.
- Schultz, A. W., "The Development of Nondestructive Methods for the Quantitative Evaluation of Advanced Reinforced Plastic Composites," AFML-TR-70-20, August 1970.
- Stinebring, R. C., and J. R. Zurbrick, "Properties Determination and Process Control of Boron Filament Composites Using Nondestructive Test Methods," Advanced Fibrous Reinforced Composites, SAMPE, 1966, Vol. 10.
- Zurbrick, J. R., "Nondestructive Investigation of High Modulus Graphite Fiber Composites," Union Carbide/Case Western Reserve University/Bell Aerosystems Conference on Fiber Composites, Cleveland, Ohio, Oct. 1968.

Zurbrick, J. R., "The Mystery of Reinforced Plastics Variability, Nondestructive Testing Holds the Key," Materials Research and Standards, Journal ASTM; Presentation to SPE, Detroit, May 1967.

APPENDIX

A-3

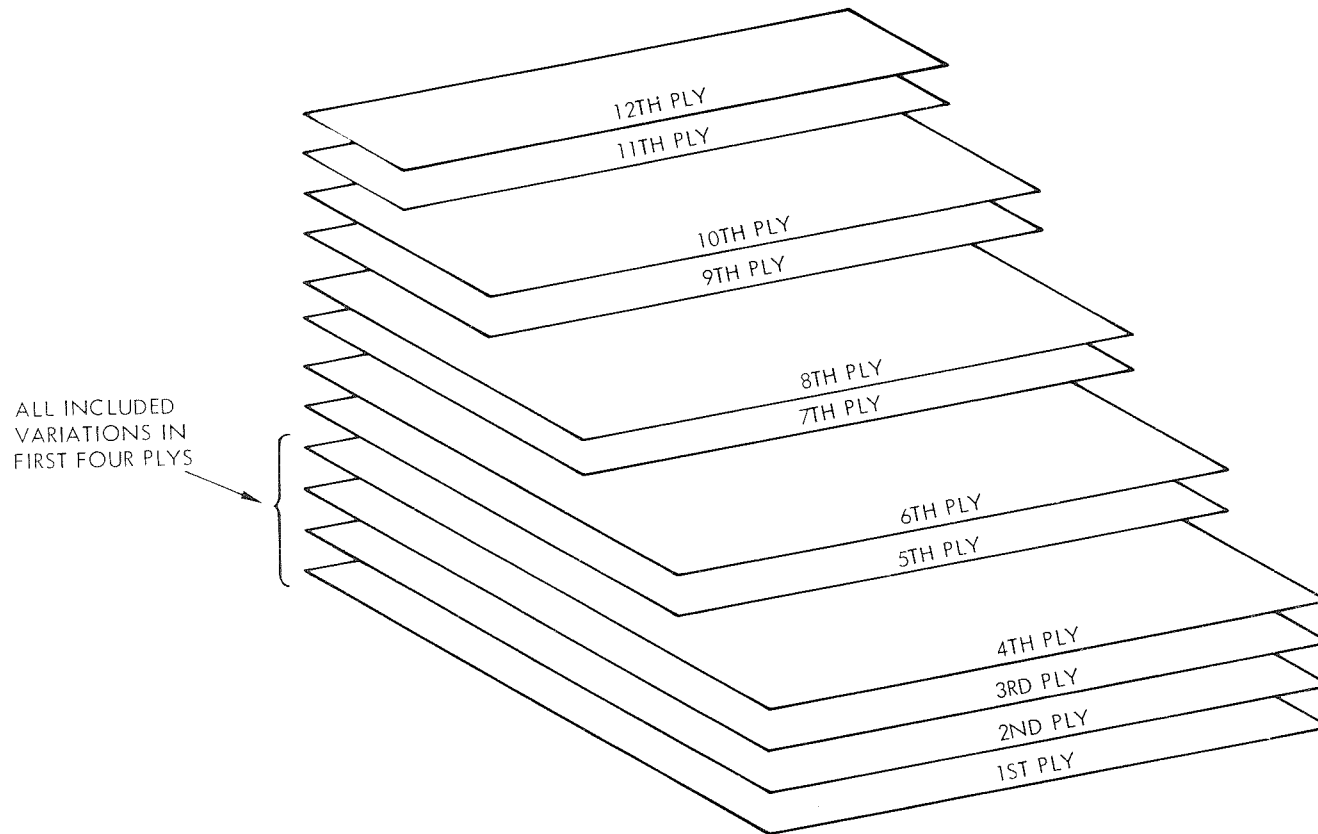
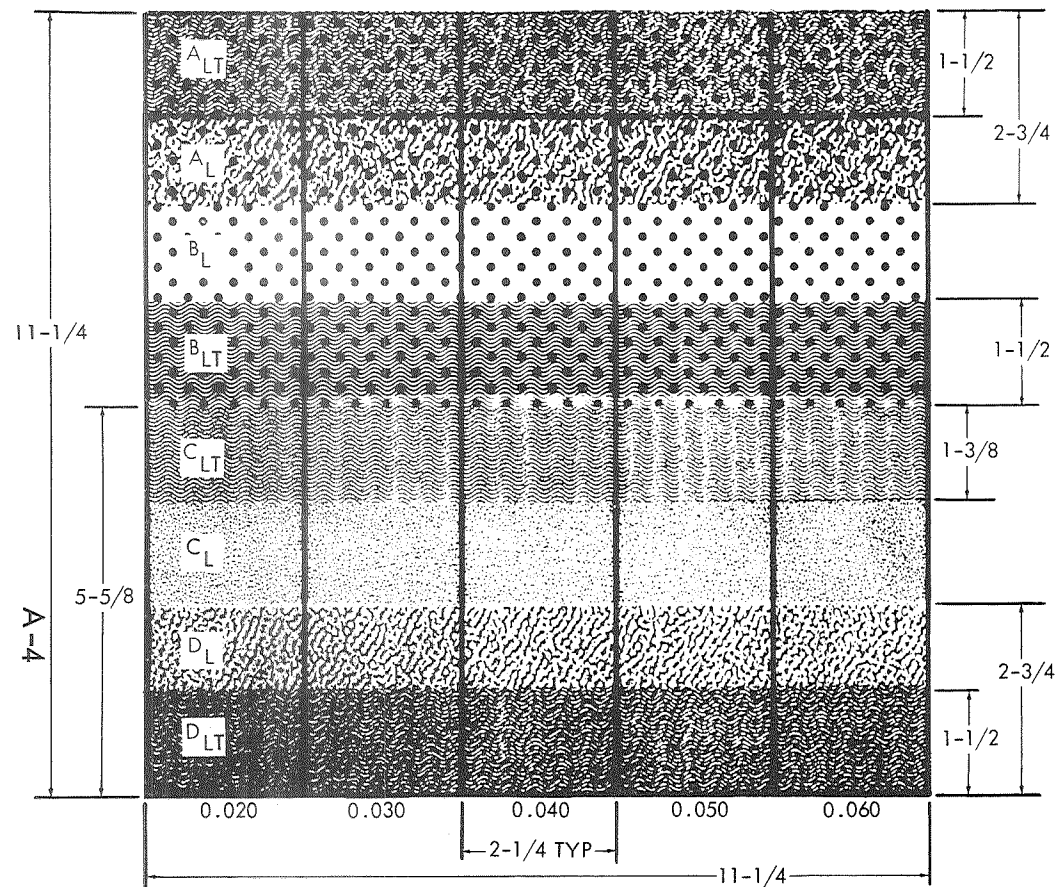
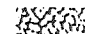


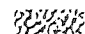



FIGURE A-1. LAMINATE ASSEMBLY



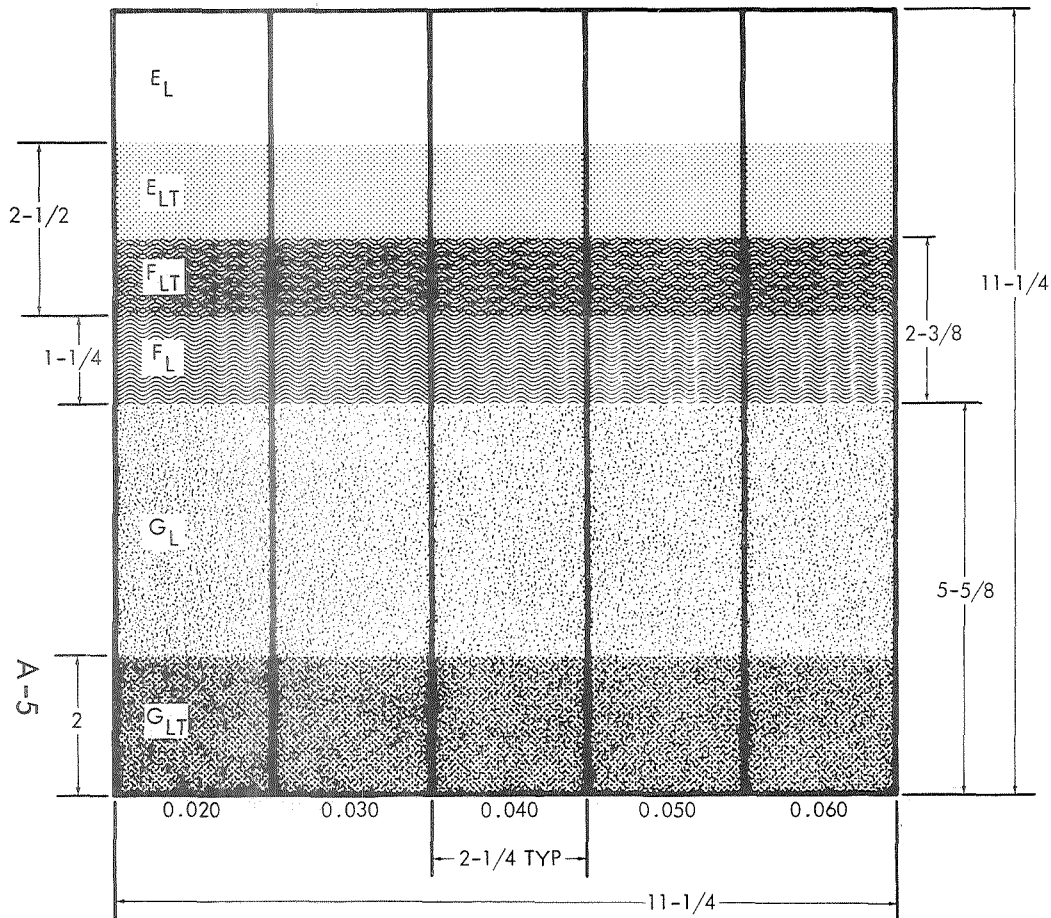
- FIBER ORIENTATION
-  MICROBALLOONS BETWEEN 2ND & 3RD PLY
 -  MYLAR
 -  ARMALON
 -  STRIP HEATING BLANKET - GROSS OVERCURE
 -  TITANIUM





Panel No.

1. Lay up three graphite-epoxy laminates, as shown. Cure. Lay up two additional laminates, defect-free. Cure.
 - 101 1a. Bond titanium strips to back of one laminate (with variations).
 - 102 1b. Bond one laminate (with variations) and one defect-free laminate to 1/2" honeycomb core.
 - 103 1c. Bond one laminate (with variations) and one defect-free laminate to 1" honeycomb core.
2. Same as above for boron-epoxy.
 - 104 2a. Bond titanium strips to back of one laminate.
 - 105 2b. Bond one laminate (with variations) and one defect-free laminate to 1/2" honeycomb core.
 - 106 2c. Same as above to 1" core.

- A_L - Plain laminate with porosity, low density, and low r/f ratio.
- A_{LT} - With titanium
- B_L - Plain laminate with low r/f ratio.
- B_{LT} - With titanium
- C_L - Plain laminate with high r/f ratio.
- C_{LT} - With titanium
- D_L - Plain laminate with porosity, low density, and high r/f ratio.
- D_{LT} - With titanium

FIGURE A-2. DENSITY/POROSITY AND RESIN VARIATIONS



 BACKING BETWEEN 2ND & 3RD PLY
 INSULATION FOR UNDERCURE
 TITANIUM
 FIBER ORIENTATION

Panel No.

1. Lay up three graphite-epoxy laminates as shown. Cure (insulated side to be placed farthest from heat). Lay up two additional laminates, defect free. Cure.
- 207 1a. Bond titanium strips to back of one laminate (with variations) (use room temperature cure adhesive).
- 208 1b. Bond one laminate (with variations) and one defect free laminate to 1/2" honeycomb core. (Use room temperature cure adhesive.)
- 209 1c. Same as 1b. above for 1" core.
2. Same as 1. above for boron-epoxy.
- 210 2a. Bond titanium strips to back of one laminate. (Use room temperature cure adhesive.)
- 211 2b. Same as 1b. above for boron-epoxy laminates to 1/2" core.
- 212 2c. Same as 1b. above for boron-epoxy laminates to 1" core.

E_L - Plain laminate, defect free.

E_{LT} - With titanium.

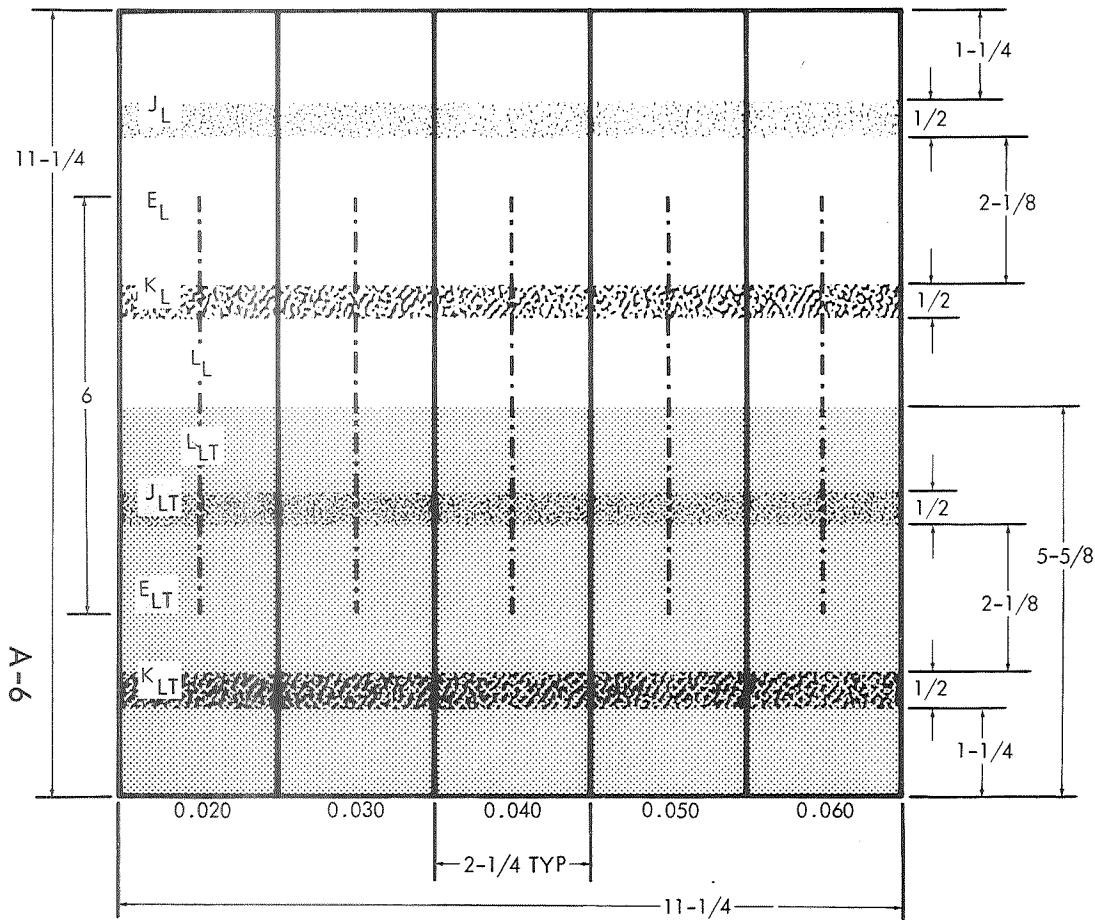
F_L - Plain laminate, with backing inclusion.

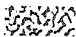




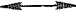
F_{LT} - With titanium.

G_L - Plain laminate, with undercure.

G_{LT} - With titanium.

FIGURE A-3. CURE VARIATIONS-INCLUSIONS



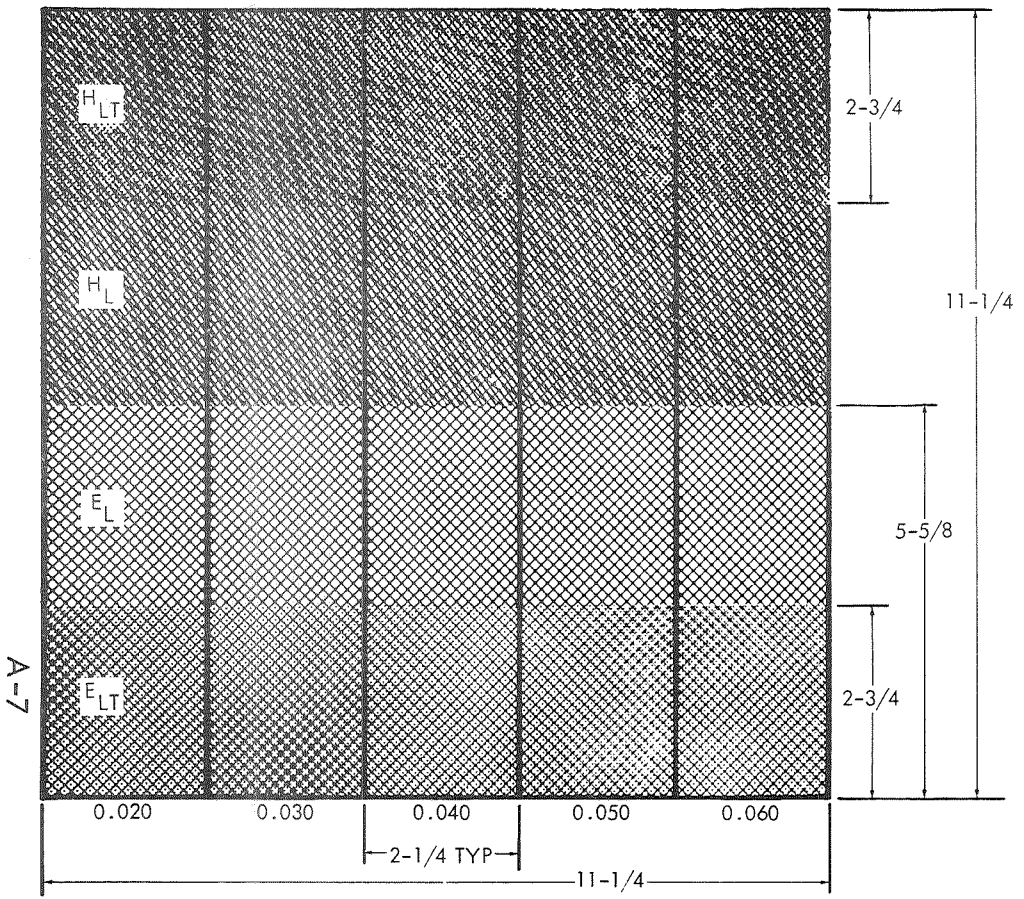
-  VOID (FIBER SPACING VARIATION) 2ND PLY
-  OVERLAP 2ND PLY
-  1/4 x 6 INCH SLOTS GRAPHITE 3RD PLY
-  6 INCH SLITS BORON 3RD PLY
-  TITANIUM
-  FIBER ORIENTATION

Panel No.

1. Lay up three graphite-epoxy laminates, as shown. Cure. Lay up two additional laminates, defect-free. Cure.
- 419 1a. Bond titanium sheet to back of one laminate (with variations) - Use room temperature cure.
- 420 1b. Bond one laminate (with variations) and one defect-free laminate to 1/2" honeycomb core.
- 421 1c. Same as 1b. above for 1" core.
2. Same as 1. above for boron-epoxy.
- 422 2a. Same as 1a. above.
- 423 2b. Same as 1b. above.
- 424 2c. Same as 1c. above.

- J_L - Plain laminate with overlap.
- K_L - Plain laminate with fiber spacing variation.
- L_L - Plain laminate with broken fibers.
- E_L - Plain laminate, defect free.
- J_{LT} - With titanium.
- K_{LT} - With titanium.
- L_{LT} - With titanium.
- E_{LT} - With titanium.

FIGURE A-4. BROKEN FIBERS, OVERLAPS, FIBER SPACING



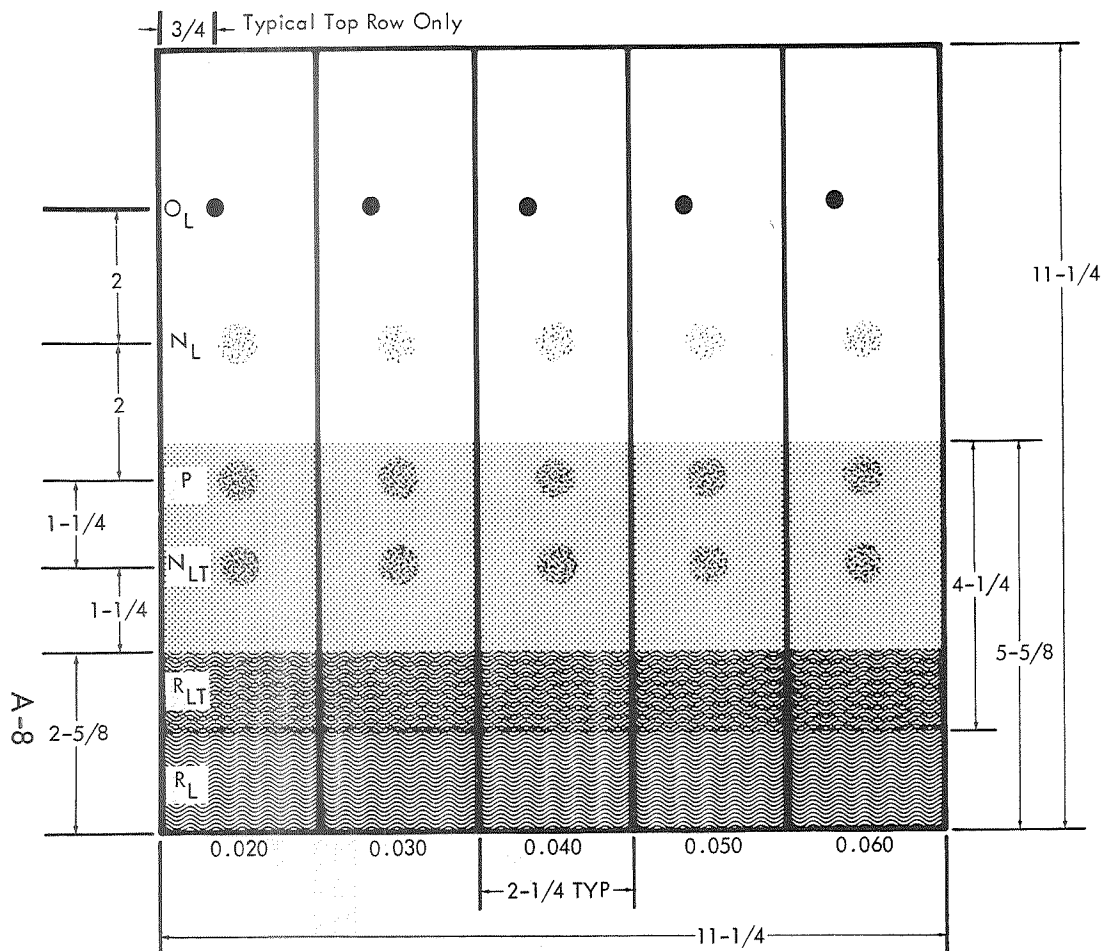
Panel No.

1. Lay up three graphite-epoxy laminates, as shown. Cure. Lay up two additional laminates, defect-free. Cure.
- 313 1a. Bond titanium strips to back of one laminate (with variations).
- 314 1b. Bond one laminate (with variation) and one defect-free laminate to 1/2" honeycomb core.
- 315 1c. Same as 1b. above for 1" core.
2. Same as 1. above for boron-epoxy.
- 316 2a. Same as 1a. above.
- 317 2b. Same as 1b. above.
- 318 2c. Same as 1c. above.

H_L - Plain laminate with 10° bias variation.
H_{LT} - Laminate with 10° bias variation with titanium substrate.
E_L - Plain laminate, defect free E_{LT} - With titanium.

- +45°, -45° BIAS
- 10° VARIATION SECOND PLY
- TITANIUM

FIGURE A-5. BIAS VARIATIONS



Panel
No.

1. Lay up one graphite-epoxy laminate, as shown. Cure.
525 1a. Bond titanium panel to back of laminate.
2. Lay up one boron-epoxy laminate, as shown. Cure.
526 2a. Same as 1a. above.

N_L - Interlaminar disbond, 1/2 inch.

N_{LT} - With titanium.

P - Disbond between titanium and laminate.

R_L - Interlaminar disbond, general.

R_{LT} - With titanium.

O_L - Interlaminar disbond, 1/4 inch.

1/2 INCH ARMALON/TEDLAR INSERTS
BETWEEN 2ND AND 3RD PLY,
BETWEEN TITANIUM AND LAMINATE

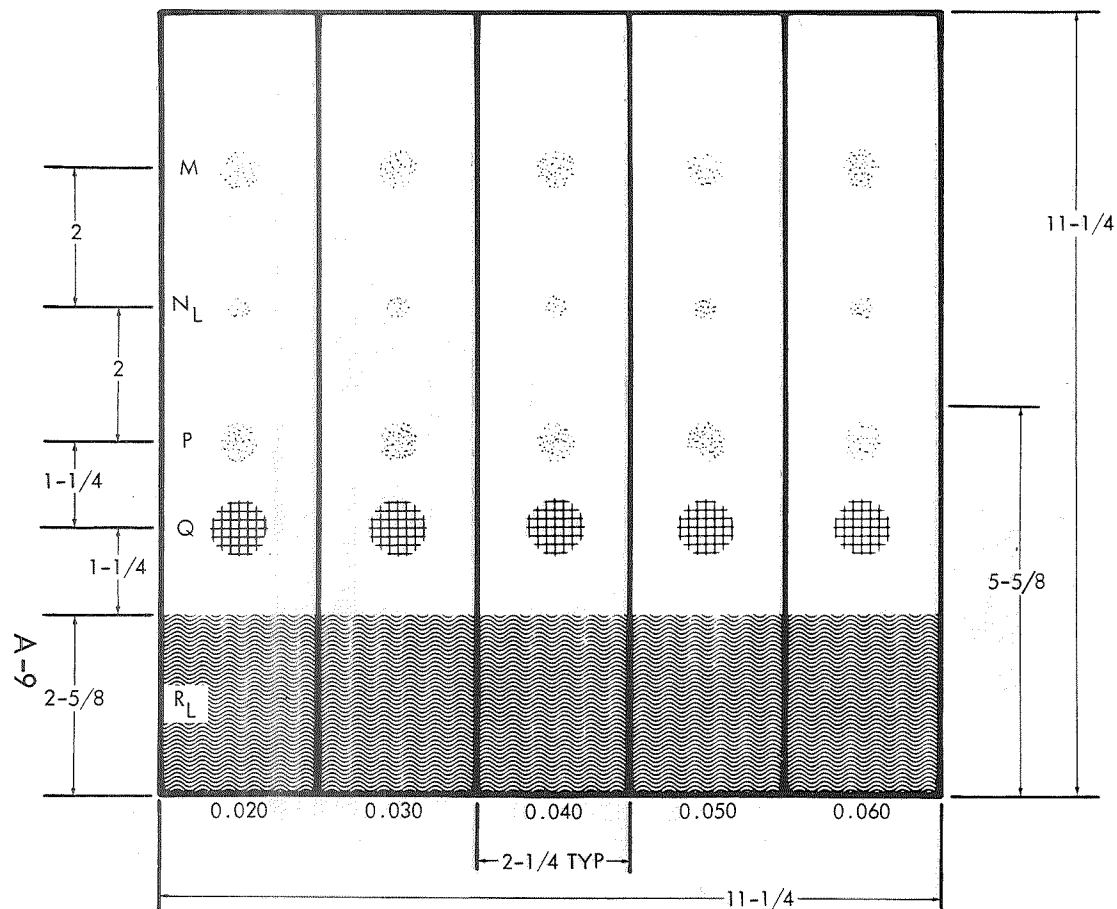
PREAGED TO SIMULATE 60 DAYS OUT OF REFRIGERATION (2ND & 3RD PLYS)

TITANIUM

FIBER ORIENTATION

1/4 INCH ARMALON/TEDLAR INSERTS
BETWEEN 2ND AND 3RD PLY

FIGURE A-6. DELAMINATIONS/DISBONDS - PLAIN AND TITANIUM



Panel No.

1. Lay up two graphite-epoxy laminates, as shown. Cure. Lay up two additional laminates, defect-free. Cure.
- 527 1a. Bond one laminate (with variations) and one defect free laminate to 1/2" honeycomb core using inserts as depicted.
- 528 1b. Same as 1a. above for 1" core.
2. Same as 1. above for boron-epoxy.
- 529 2a. Same as 1a. above for boron-epoxy.
- 530 2b. Same as 1b. above for boron-epoxy.

- M - Far side core to laminate disbond.
 N_L - Interlaminar disbond, 1/4 inch.
 P - Near side core to laminate disbond.
 Q - Crushed core.
 R - Interlaminar disbond, general.

- ARMALON/TEDLAR INSERTS
 BETWEEN 2ND AND 3RD PLY, 1/4 INCH INSERTS
 BETWEEN LAMINATE AND HONEYCOMB (FAR SIDE), 1/2 INCH INSERTS
 BETWEEN LAMINATE AND HONEYCOMB (NEAR SIDE), 1/2 INCH INSERTS
- 3/4 INCH CRUSHED CORE (IRREGULAR DEFORMATION)
- PREAGED TO SIMULATE 60 DAYS OUT OF REFRIGERATION
- FIBER ORIENTATION

FIGURE A-7. DELAMINATIONS/DISBONDS - HONEYCOMB

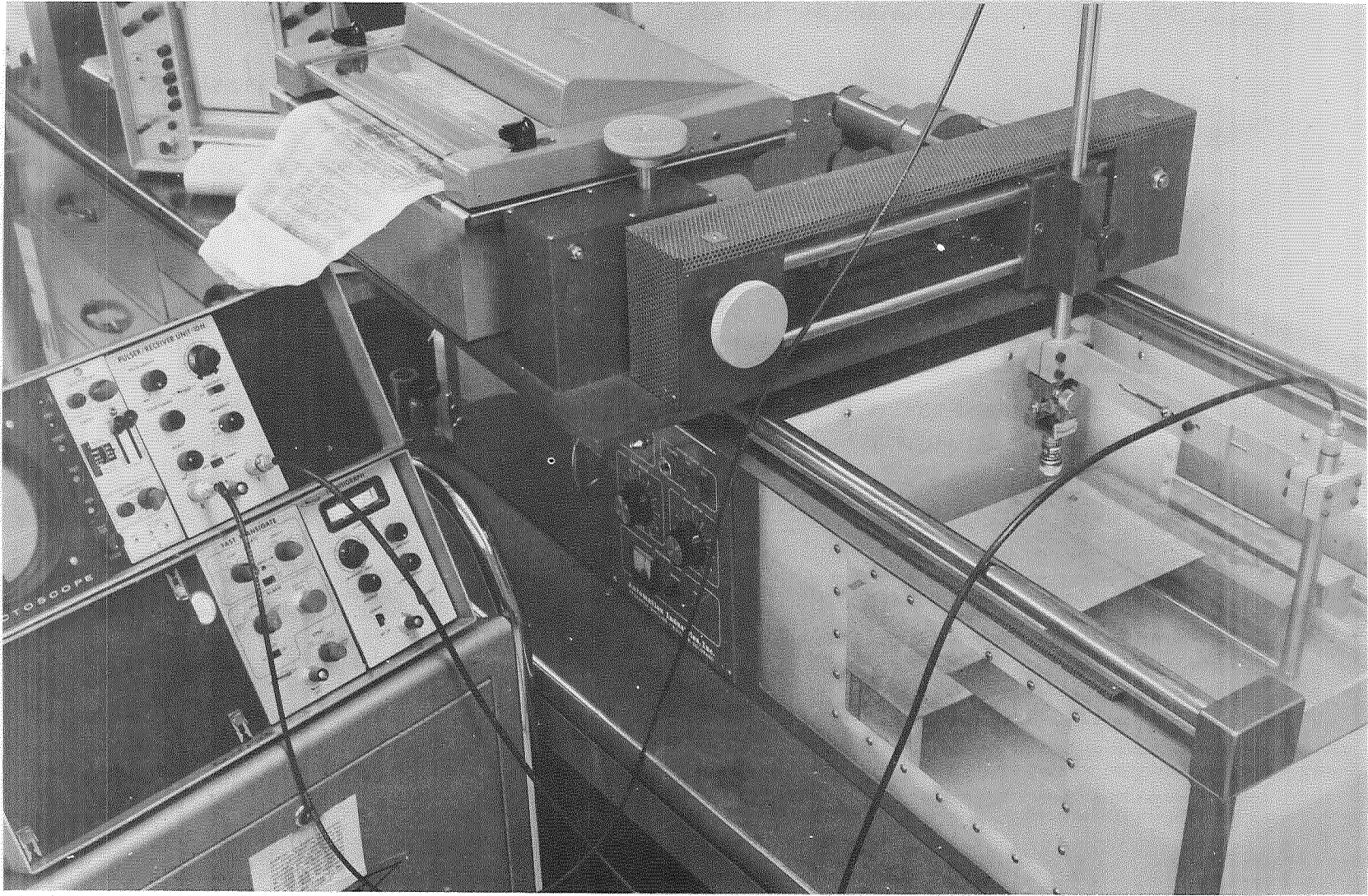


FIGURE A-8. ULTRASONIC C-SCAN APPARATUS WITH THROUGH TRANSMISSION - CALIBRATION WITH COMPOSITE STANDARD